METAL INTERACTIONS WITH NEURAL SUBSTRATES AND THEIR ROLE IN NEURODEGENERATION

A thesis submitted in fulfilment of the
requirements for the degree of

DOCTOR OF PHILOSOPHY

In the

Faculty of Science
Rhodes University

By

Barbara Anne Lack

January 2002

ABSTRACT

"Life" may be characterized as a controlled stationary flow equilibrium, maintained by energy consuming chemical reactions. The physiological functioning of these life systems include at least 28 of the elements isolated on the periodic table thus far, most of which are metals. However, as with Paracelsus Principle: "The dose makes the poison", there exists a definite link between metal levels, essential and toxic, and the onset of neurodegenerative diseases. The economic costs of brain dysfunction are enormous, but this pales in comparison to the staggering emotional toll on the victims themselves and their families. In an attempt to improve the understanding of the causes of neurodegeneration, this study focuses on one potential aspect: the possible link between metals and neurotransmitter homeostasis utilising a variety of electronanalytical techniques.

Adsorptive cathodic stripping voltammetry was employed to investigate the binding affinities and complex formation of melatonin and its precursor serotonin with calcium, potassium, sodium, lithium and aluminium. The results showed that all the metals studied formed complexes with both pineal indoleamines. However, the stability and affinity of the ligands toward the various metals varied greatly. The study suggests a further role for melatonin, that of metalloregulator and possible metal detoxifier in the brain, the *in vivo* studies which followed will further substantiate this notion.

This research additionally focused on the cholinergic system, in particular acetylcholine complex formation studies with mercury, lead, cadmium, copper and zinc using the adsorptive cathodic stripping voltammetry method. The formation and characterisation of a solid mercury-acetylcholine complex lent further strength to the *in situ* electrochemical complex formation observed. The results showed the preference of acetylcholine for environmentally toxic heavy metals (such as Cd^{2+}) over those divalent cations that occur naturally in the body.

The possible metalloregulatory role melatonin played in the three brain regions: cerebellum, cortex and corpus striatum of male Wistar rats was studied as an *in vivo*

extension of the earlier *in vitro* studies. Anodic stripping voltammetry was employed to detect metal levels present. The results showed that daily injections of melatonin was responsible for significantly decreasing copper(I), cadmium(II) and lead(II) levels in various regions of the rat brain of those animals that had undergone a pinealectomy in comparison to the saline injected group having undergone the same treatment.

Histological and electrochemical stripping techniques were applied to investigate the implications of high Al^{3+} levels in the brain regions, particularly the hippocampus. Melatonin showed signs of promise in indirect symptom alleviation and by significantly decreasing Al^{3+} levels in rats that had been dosed with melatonin prior to Al^{3+} treatments in comparison with the control groups.

Finally a preliminary study outlining a method for the production of a calcium selective microelectrode was undertaken. Further work is still needed to optimise the microelectrode production as well as its possible applications. However, whilst the overall conclusions of this entire multidisciplinary study may indeed only be in effect one piece of a very large puzzle on neurodegenerative diseases, this piece will no doubt serve as a building block for further ideas and work in this field.

TABLE OF CONTENTS

LIST OF FIGURES

LIST OF TABLES

ACKNOWLEDGEMENTS

My sincerest thanks and appreciation to Professor Nyokong for her outstanding supervision and belief in my abilities during both my Masters and Doctoral studies. Her high standards, dedication, enthusiasm and attitude towards research are an excellent example for her peers and students alike.

Professor Daya, who has co-supervised my Doctoral studies, I thank for his input in initiating this research, his friendly support and his guidance in the neuroscience field. I am immensely grateful to both supervisors for their collaborative efforts during the course of my studies.

Professor Botha I wish to thank for the skills I gained in electrophysiology and for the many patient hours spend working together on the preparation of the microelectrodes.

I acknowledge the following organisations for their financial assistance: The National Research Foundation of South Africa and Rhodes University.

My parents, Brian and Emelia, brother David and grandparents, Cecil and Murial Lack and the late Verita Allner for their love, guidance, patience, support, many sacrifices and financial assistance through all my years of study to ensure I received the best possible education.

The staff and postgraduate students of the chemistry department for their support and encouragement. Benita Tarr and Johan Buys for their helpfulness and kindness. Andre Adriaan for making the specialised glassware required. Kevin Lobb for his help with computer modeling of the compounds. Kerry McPhail, Chris Gray and Edith Beukes for their assistance in the running and analysis of certain NMR samples. Dr Watkins for his advice in the IR spectroscopy. My research groups and Dr Janice Limson for their kindness, friendship, sharing of ideas and support. Dr Cross, Purba Pal and Shirley Pinchuck for their assistance with slide preparation and microscopy. A huge thank you to Mr and Mrs Morley for all their technical assistance.

Rhodes University library staff: thank you for the friendly, supportive service you provide. In particular, Sue van der Riet and Eileen Shepherd whose tireless efforts to find those "elusive" and various internet references, are greatly appreciated.

To my friends and 'digsmates' who have encouraged, supported and beared with me through this thesis and the writing up process, my heartfelt thanks: Mez Jiwaji, Kim Wilkins, Kehan Harman, Chris Kelly, Kim Taute, Mike Ludewig, Angie Bird, Steve Robinson and Sue Cooling. A special vote of thanks to Gina Strydom and Anne Warring for going the extra mile in proof reading and supporting me through this research. Many thanks to Andrew Grant, with assistance from Emmanuel Lamprecht, for keeping my computer up and running through this stressful period. Paula Heron, my work colleague and close friend, I wish to extend my thanks to for all her help in the steriotaxic and histology work, her constant support, interest in my research, and for always being there for me. To all concerned, no matter how big or small your contribution, I would never have completed this mammoth task without your help and I am thus most grateful.

"Carpe Diem"!

ABBREVIATIONS

1D	one-dimensional
2D	two-dimensional
5-HIAA	5-hydroxyindoleacetic acid
5-HT	5-hydroxytryptophan
AChE	acetylcholinesterase
Acetyl COA	acetyl coenzyme A
AAS	atomic absorption spectroscopy
ACh	acetylcholine
AD	Alzheimer's disease
AdSV	adsorptive stripping voltammetry
ALA	γ-aminolevulinic acid
ALAD	γ-aminolevulinic acid dehydrogenase
ALS	amyotrophic lateral sclerosis
APOE4	abnormalities in the Apolipoprotein E4
APP	amyloid precursor protein
APUD	amine precursor uptake and decarboxylation
ASV	anodic stripping voltammetry
BAS	BioAnalytical Services
BBB	blood-brain barrier
CA1	*Cornu Ammonis* 1
CA3	*Cornu Ammonis* 3
c-AMP	cyclic adenosine monophosphate
CGME	controlled growth mercury electrode
ChAT	choline acetyltransferase
CJD	Creuzfeldt-Jacob disease
CNS	central nervous system
COSY	correlated spectroscopy
CPE	carbon paste electrode
CSF	cerebrospinal fluid
CSV	cathodic stripping voltammetry
DME	dropping mercury electrode
DMSO	dimethylsulphoxide
DNA	deoxyribo nucleic acid
EAA	excitatory amino acids
ER	endoplasmic reticulum
FAD	flavin adenine dinucleotide
FFI	fatal familiar insomnia
GABA	γ-aminobutyric acid
GCE	glassy carbon electrode

GSS	Gertsmann-Sträussler-Scheinker disease
HIOMT	hydroxyindole-O-methyltransferse
HDME	hanging drop mercury electrode
HSAB	hard/soft acid-base
ICP-MS	inductively coupled plasma-mass spectrometry
IHP	Inner Helmholz Plane
IR	infrared
ISE	ion selective electrode
MAO	monoamine oxidase
MEL	melatonin
MPT	mitochondrial permeability transition
NAD	nicotinamide adenine dinucleotide
NAT	N-acetyltransferase
nbM	nucleus basalis Meynert
NMDA	N-methyl-D-aspartate
NMR	nuclear magnetic resonance
OHP	Outer Helmholz Plane
OSW	Osteryoung square wave
PD	Parkinson's disease
PPD	Prion Protein disease
PSA	potentiometric stripping analysis
PVC	polyvinyl chloride
Px	pinealectomised
ROS	reactive oxygen species
RPE	rotating platinum electrode
SAD	seasonal affective disorder
SBMA	spinobulbar muscular atrophy
s.c	subcutaneously
SCE	saturated calomel electrode
SEM	standard error of the mean
SHE	standard hydrogen electrode
TBABr	tetrabutylamoniumbromide
TG	thermogravimetric
TGA	thermogravimetry analyser
WIGE	wax-impregnated graphite electrode

CHAPTER 1

A General Overview

1.1 INTRODUCTION:

The neuron, or nerve cell, from a historical standpoint has attracted more attention and caused more controversy than any other cell type. The 1990's was declared the "Decade of the Brain" and in its wake a greater understanding of the mechanisms underlying neurodegenerative diseases emerged. Further insights into the biological underpinnings of addiction and behaviour were also gained, the molecular roots of chronic pain were postulated, as well as the molecular basis of learning and memory began to unfold and hints surfaced that spinal cord injury might be reversible. However, the spate of information that gushed forward also served to underscore the complexity of the brain and the challenges that still lie ahead.

Despite the numerous advances in the 1990's, drugs that halt the progression of severely debilitating mental disorders have not progressed much beyond the drawing board. In addition, other than genetic testing for rare familial forms, ways to detect these diseases in their early stages of progression have not yet been developed. Meanwhile, the incidence of neurodegeneration is demographically programmed to soar: the 'Baby Boom' generation- the bulge of babies born in the aftermath of World War II- will soon be growing old.

However, a new decade in neuroscience has dawned, which promises the convergence of various scientific disciplines to solve the mysteries of the mind.

The key concept in neuroscience today is brain homeostasis. Neural systems are in a permanent dynamic flux and their plasticity and ability to self-adjust is well known. Responding to perturbations by establishing a new steady-state or equilibrium and even taking over functions of damaged neuronal circuits are all characteristics employed in normal brain functioning. There is also a growing appreciation that brain disorders or disease are no longer merely abnormal functioning of a normal brain, but instead are functional entities in there own right. A new trend in neuroscience is to examine these disease states as a whole, underlying any possible chemical or biochemical similarities, rather than as individual diseases pulled apart by the clinical world. Accordingly, in this study a common thread has been sought in weaving the bigger picture of related mental illnesses. The focus is on one potential aspect, which may link metals and neurotransmitter homeostasis to possible neurodegenerative avenues of disease.

Electrochemical methods, in particular stripping voltammetry, are employed in this study to investigate the interaction between metals and the neural substrates of interest, which include melatonin, serotonin and acetylcholine. The metals covered in the studied were Cu^{+}, Na^{+}, K^{+}, Li^{+}, Ca^{2+}, Cd^{2+}, Cu^{2+}, Hg^{2+}, Pb^{2+}, $Zn^{2+}$and Al^{3+}. Analytical techniques such as thermogravimetric (TG) methods, X-ray diffraction patterns (XRD), computational modeling, nuclear magnetic resonance (NMR) and infrared (IR) spectroscopy were all employed to compliment the electrochemical study. The following sections sketch the biological and analytical chemistry background needed for understanding the metal-ligand interactions and proposed implications presented in this work.

1.2 THE PINEAL GLAND AND ITS METABOLITES:

A holistic view of brain functioning cannot ignore the growing awareness of the role of the epiphysis cerebri, or pineal gland as it is more commonly known. The word 'pineal' is derived from the Latin *pinealis pinea* meaning 'pinecone'-like, as this is the shape it resembles in humans. The term epiphysis implies 'what is grown on something'.[1] The discovery of this gland is most likely to be accredited to Herophilos (325-280 B.C), the "father of anatomy".[2] Rene` Descartes (1596-1650) is commonly cited as stating that the pineal gland is the seat of the soul.[2]

Further studies were, however, neglected on the pineal gland until the nineteenth century, after the discovery of endocrine glands by Bernard (1818-1878), Brown-Sequard (1817-1894) and their co-workers.[3] Medical professionals continued to believe that the pineal gland was only a vestigial organ with no functional significance, whereas neuropathologists were aware of the clinical importance of pineal tumours.[3] However, it was not until the isolation of melatonin (MEL, or 5-methoxy-N-acteyltryptamine) from the bovine pineal gland by Lerner *et al.* in 1958 that the current explosion in pineal research began.[4] Neuroscientists, or pineal researchers at least, have now gone as far as saying that the pineal may indeed be a "master gland" or the principle homeostatic regulator.[4]

The pineal gland is an endocrine gland ideally situated anatomically to receive, integrate and compare information from both the external environment and internal milieu. In particular, the pineal gland is situated outside the blood-brain barrier (BBB) and its glandular structure is derived as an evagination of the neural tube.[5] In mammals, the pineal gland is considered to be an active neuroendocrine transducer, converting a neural

input, namely a neurotransmitter released at a synapse, to a hormonal output, such as methoxyindoles and polypeptides.[6] In addition, it appears that the pineal may itself be subjected to other hormonal signals, suggesting an endocrine-endocrine and endocrine-neuronal transduction mechanism.[7]

In the animal model chosen for this study, the rat, the pineal is known to consist of the superficial pineal gland and the deep pineal. The superficial pineal gland is located on the surface of the brain at the junction of the cerebellum and cerebral hemispheres in close association with the third ventricular region. The deep pineal is located in the diencephalon on the dorsal part of the brain stem between the habenular complex and the posterior commissural areas. The two components are connected via a pineal stalk or peduncle.[8,9] Unless otherwise stated, the term pineal gland will refer to the superficial pineal.

1.2.1 MELATONIN (MEL):

The principle pineal hormone, melatonin, is secreted in a rhythmic fashion.[10] The lipophilic nature of this hormone allows it to distribute itself through the tissues of the body with relative ease, exerting some or other action on most organs of the body. The primary role of melatonin is thought to be the chemical expression of darkness, since it is the only hormone in the body capable of 'informing' the organs of the body about the length of the day. In doing so, it is not surprising that MEL has been implicated in affective disorders which are related to the seasons such as seasonal affective disorder (SAD) and sleep disorders.[11-13]

Suitably timed doses of MEL have also shown to be beneficial in improving jet-lag symptoms and day time sleeping patterns of night shift workers.[13] Furthermore, recent findings that MEL could play a neuroprotective role against the neurological insults of stress and the finding that MEL levels decline significantly with age could elevate the status of melatonin to that of a possible anti-aging drug, should research substantiate this.[11,14]

Current investigations have focussed on the powerful antioxidant capacity of MEL. This hormone is a potent scavenger of the cytotoxic hydroxyl radicals and other reactive oxygen species (ROS), influencing numerous enzymes and factors associated with intracellular antioxidative defence systems.[15,16] In summary, MEL is a ubiquitous hormone displaying a distinct functional pleiotropy and multiple sites of action.

Biosynthesis and metabolic fate:

The biosynthesis of melatonin, is represented in Figure 1.1. The synthesis commences with the uptake of tryptophan from the circulation system where the enzyme tryptophan-5-hydroxylase governs the conversion of tryptophan to 5-hydroxytryptophan.[11] The 5-hydroxytryptophan is then transformed to 5-hydroxytryptamine (serotonin) by L-amino acid decarboxylase. Serotonin is allowed to accumulate in the pineal gland, before it is converted to N-acetylserotonin, by N-acetyltransferase (NAT), at night during the hours of darkness.[17] N-acetyltransferase is the rate-limiting enzyme in melatonin synthesis, with its function in the pineal gland being regulated by the release of noradrenaline by the postganglionic synaptic fibers.[18-20] The final step in melatonin synthesis, involves the conversion of N-acetylserotonin to N-acetyl-5-methoxytryptamine (MEL). The conversion

is achieved by hydroxyindole-O-methyltransferase (HIOMT) using S-adenosylmethionine as a methyl donor.[17,20,21]

MEL is not stored in the pineal gland, but is rapidly secreted directly into the bloodstream.[18] The normal route of melatonin secretion comprises of the pineal capillaries draining into the surrounding venous sinuses.[20] Melatonin is transported in the blood non-covalently bound to high-capacity, low-affinity binding sites on plasma albumin, while in cerebrospinal fluid, melatonin is present in its free form.[22,23]

In addition to the pineal gland, several other organs have the capacity to produce melatonin, including the retina, Harderian gland and lacrimal gland.[24,25] It appears, however, that these organs lack the ability to secrete melatonin, thus under normal circumstances the blood melatonin concentrations almost exclusively reflect that of the pineal gland. On a day-to-day basis, under specific photoperiodic conditions, the circadian MEL rhythm is very reproducible and is thus, a reliable index of pineal MEL synthesis.[26]

The half-life of melatonin in rats and sheep is only about 20 minutes.[27,28] The major site of melatonin metabolism is the liver, where melatonin is converted to 6-hydroxymelatonin by the cytochrome P-450-dependent microsomal mixed-function oxidize enzyme system.[29] Most of the 6-hydroxymelatonin is further conjugated to sulphate, rendering 6-sulphatoxymelatonin as the major urinary metabolite, although 6-hydroxymelatonin can also be conjugated to glucuronic acid.[18,29-33] The metabolic pathway of melatonin in the central nervous system is different from that in the liver.[33] In the brain, indoleamine-2,3-dioxygenase cleaves the pyrrole ring to form N-acetyl-5-methoxykenurenamine, which is then excreted in the urine.[17]

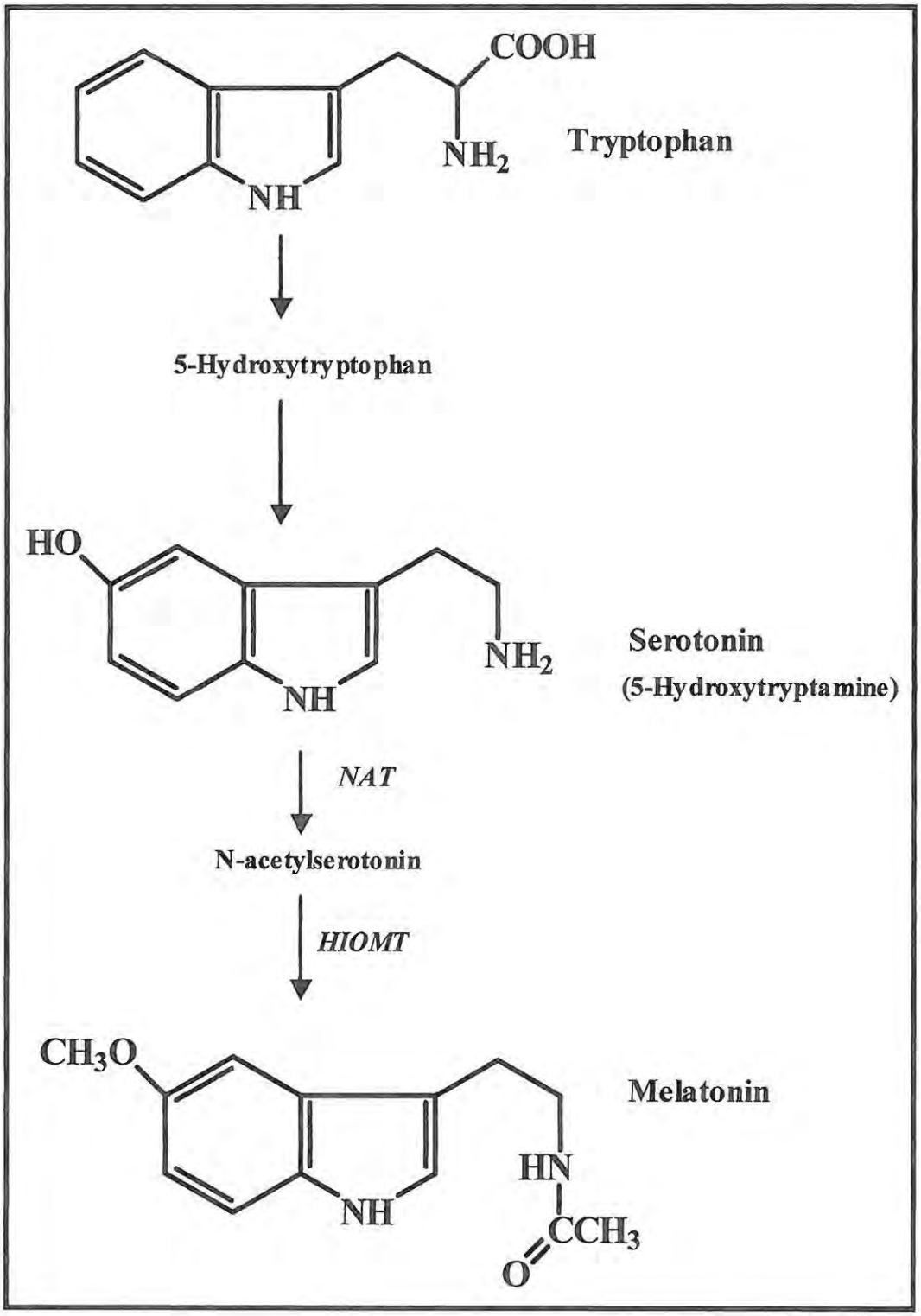

Figure 1.1 A brief biosynthetic pathway of melatonin.

NAT = N-acetyltransferase, HIOMT = Hydroxyindole-O-methyltransferase

1.2.2 SEROTONIN:

Serotonin, 5-hydroxytryptamine (5-HT), structure illustrated in Figure 1.1, derives its name from the observation in 1868 that after blood clots, the resultant serum increases in vascular tone. Classified as a monoamine type neurotransmitter, this pineal indoleamine, 5-HT, is widely distributed in nature, including neuronal structures of many vertebrates and invertebrate species. The serotonin neurons originate in several brainstem nuclei, most notably the dorsal and median raphe and its axons diffusely supply the forebrain. The diffuse nature of brain 5-HT innervation suggests that this neurotransmitter is involved in the coordination of brain functions. Many functionalities have been assigned to serotonin including: sleep, impulse control and personality, mood and psychosis.[35,36]

A role in depression is strongly suspected, on the grounds that 5-HT depletion has been shown to worsen symptoms. Along with a link to alcoholism, similar arguments have been put forward to suggest a role for serotonin in anxiety attacks and obsessional disorders, but the case is weaker in the latter. Depletions of 5-HT levels has been shown to lead to insomnia and aggressive behaviour in animal models, whilst increased levels of this neurotransmitter produces a range of bizarre stereotyped behaviours and locomotion activation, known as the 5-HT syndrome.[36]

Biosynthesis and metabolic fate:

The synthesis is a two-step process from the dietary amino acid, L-tryptophan, as depicted in Figure 1.2. Neither of the two enzymes involved is saturated, therefore the supply of L-tryptophan, which cannot be synthesized *de nova*, is the rate-limiting step. Transport of tryptophan into the brain competes with the transport of some other amino acids. Increased levels of brain tryptophan has been linked to enhanced serotonin production. The enzyme governing the conversion of 5-hydroxytryptophan to 5-hydroxytryptamine is known as tryptophan-5-monooxygenase or tryptophan-5-hydroxylase and its distribution in the brain parallels that of serotonin. Endogenous 5-HT in the brain is then decarboxylated via a nonspecific aromatic L-amino acid decarboxylase resulting in serotonin formation, which is stored in neuronal synaptosomes.[36,37]

Serotonin is released by stimulation of its cell bodies in the raphe nuclei. In some neurons, serotonin may coexist with other neuroregulators, whilst numerous other neuroregulators have been implicated in its release, including dopamine, norepinephrine and acetylcholine. The uptake system for 5-HT in nerve terminals, like the uptake system for some other biogenic amines, has high affinity, low capacity and high specificity. The effects of serotonin are terminated by reuptake into the presynaptic terminals and this process is sodium concentration- and temperature dependent.

The breakdown process of 5-HT occurs via the conversion of 5-hydroxyindole acetaldehyde by monoamine oxidase (MAO) to either the dehydrogenated 5-hydroxyindoleacetic acid (5-HIAA) or its reduced alcohol form, 5-hydroxytryptanol. Both products occur in the liver. In the brain, however, 5-HIAA is the end product. The

regional distribution of 5-HIAA is similar to that of serotonin. In fact, its levels in cerebrospinal fluid (CSF) are often taken as an index of the rate of serotonin turnover in the central nervous system (CNS).[37]

Further pathways for the metabolism of serotonin have been put forward. These pathways include the sulphate ester formation by peripheral tissues, or enzymatic methylation of the side-chain amino group. The latter is known to occur in the brain to form N^{α} - methylserotonin and N^{α}, N^{α}-dimethylserotonin. However, in the pineal gland the synthesis of serotonin is chiefly for the conversion into melatonin,

5-methoxy-N^{α}-acetylserotonin.

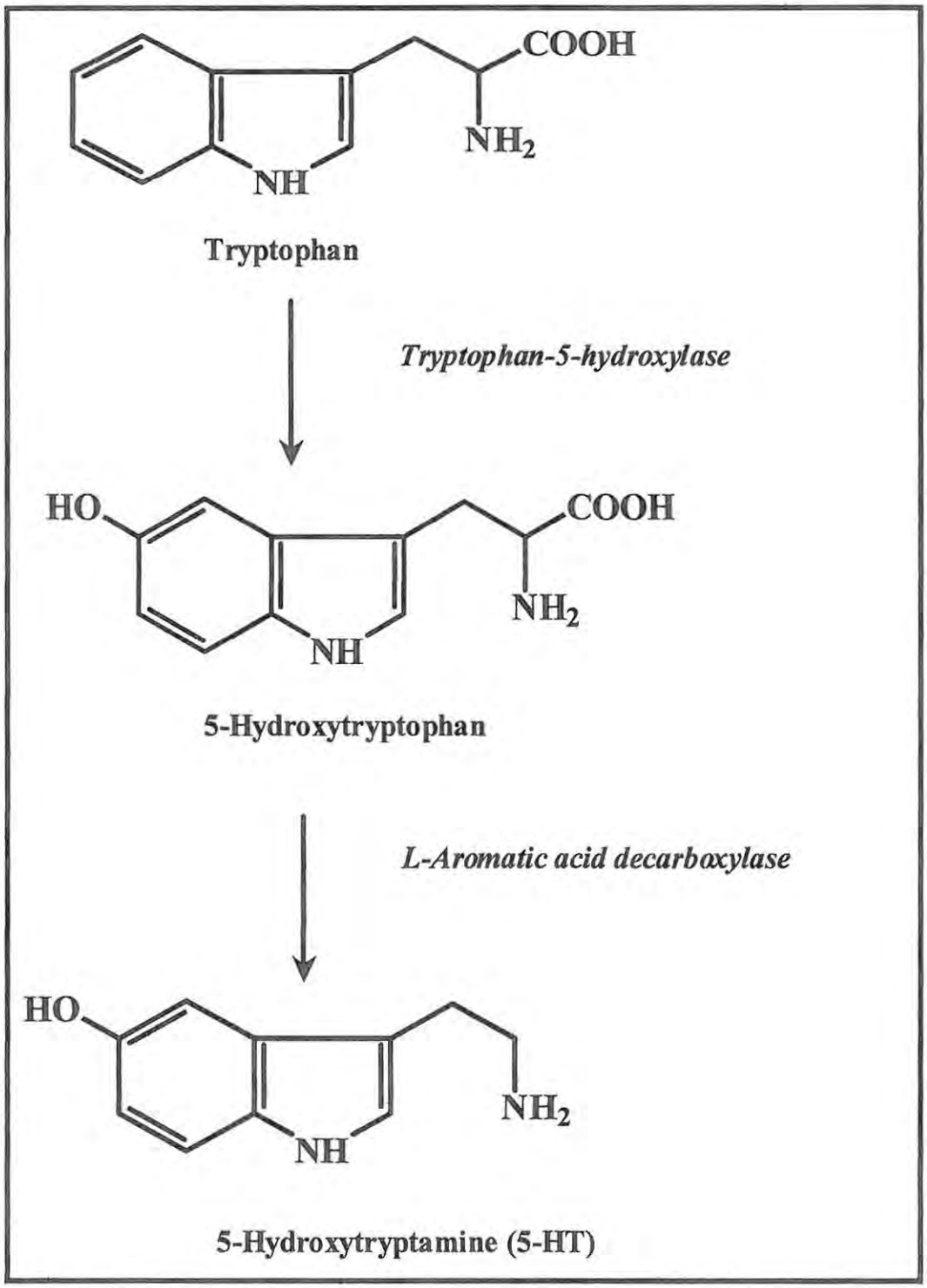

Figure 1.2. Enzymatic synthesis of 5-Hydroxytryptamine (serotonin).

1.3 THE CHOLINERGIC TRANSMISSION SYSTEM:

The basic sequence of events in neurotransmission is synthesis, storage, release, postsynaptic reception and breakdown of the neurotransmitter. Acetylcholine (ACh), Figure 1.3, was the first of the neurotransmitters to be identified as a possible mediator of cellular function by Hunt in 1907 and in 1914 Dale pointed out that its action closely mimicked the response of parasympathetic nerve simulation.[39] Loewi, in 1921, provided clear evidence for ACh release by nerve simulation.[38] All neural pathways that use ACh as their neurotransmitter are referred to as cholinergic and since ACh was the first neurotransmitter to be characterized in both function and structure many basic neurotransmitter systems have been modelled on the cholinergic systems.[38, 39]

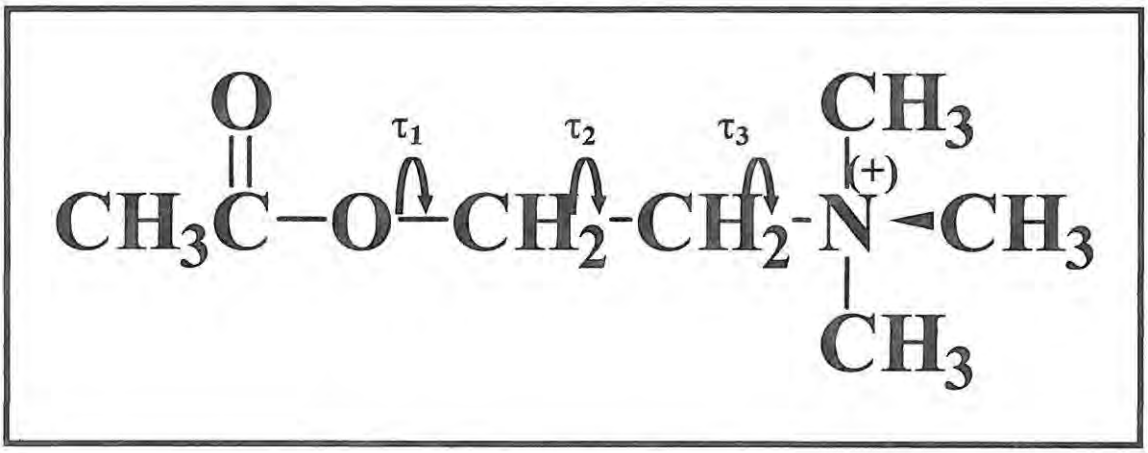

Figure 1.3 The structure of acetylcholine.

Free rotation in the ACh molecule can occur around bond τ_1, τ_2 and τ_3 as seen in Figure 1.3. Since the methyl groups are symmetrically disposed around τ_3 and constraints may be placed on τ_1 by the planar acetoxy group, the most important torsion angle determining ACh conformation in solution is τ_2.[35] The molecular structure of ACh consists of three planes: (1) the ester oxygen carboxyl group, (2) the plane of one methyl carbon atom, the nitrogen atom and the two carbon atoms from the CH_2 group and (3) the plane of the ester oxygen-CH_2 bond and one methyl carbon-nitrogen bond.[40] The bound conformations of this flexible molecule appear to differ substantially, as can be seen from the different conformers attached to the various receptor subtypes.[39]

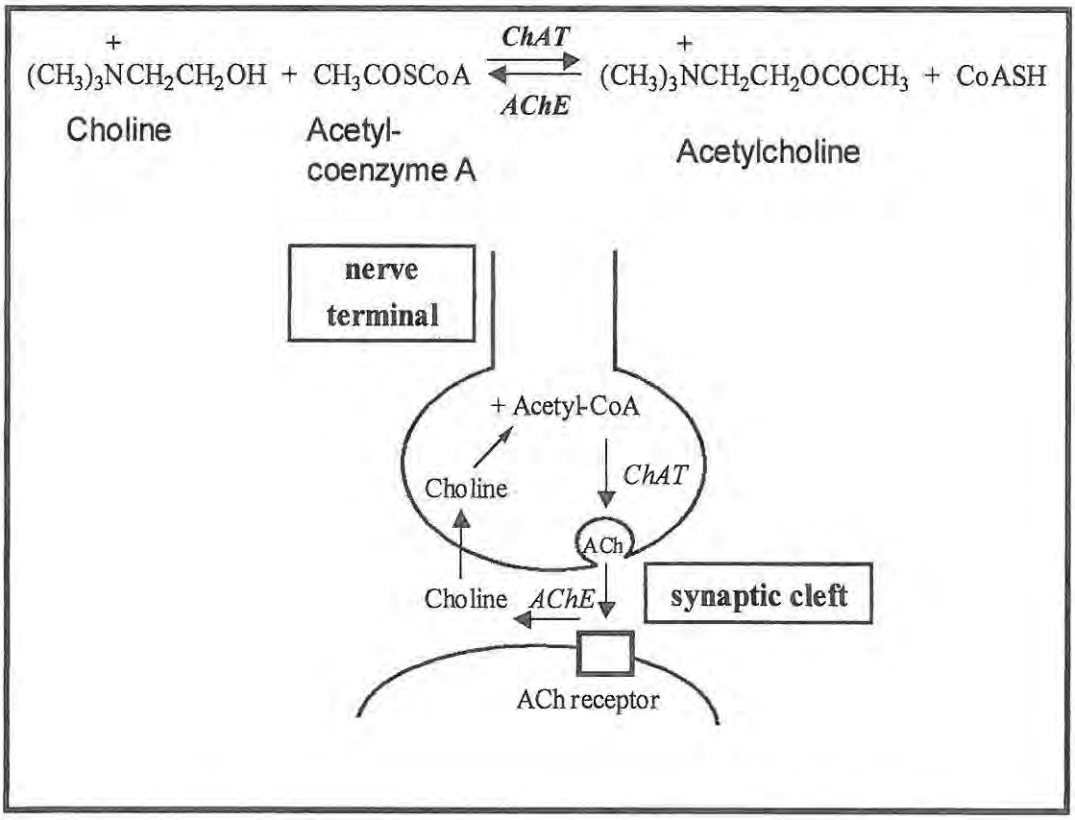

Figure 1.4 The synthesis and degradation of acetylcholine.[36]

ACh is synthesized in cholinergic nerve terminals following the uptake of the precursor choline, as seen in Figure 1.4. Choline, also derived from dietary sources, is primarily manufactured in the liver and is transported to the brain by the blood.[36,37] The ACh biosynthesis is catalyzed by the acetyltransferase (ChAT) enzyme, which employs acetyl coenzyme A (acetyl CoA) and choline as substrates as illustrated in Figure 1.4.[41] ACh levels in intact nervous structures are generally well maintained during any one physiological activity. The mechanism for this constancy may be that the release of the neurotransmitter triggers an increase in the rate of synthesis by ChAT.

Synthesized ACh is stored in synaptic vesicles that possess a carrier substance for ACh. In the vesicle the protein vesiculin helps to stabilize and store ACh, such that high concentrations of the neurotransmitter may be obtained. Stored ACh in vesicles is known as "stable" or "bound", whereas ACh found in the cytoplasm is referred to as being "labile" or "available". Whether synthesis occurs in the synaptoplasm before transfer to vesicles or whether ChAT bound to vesicles fill these directly, is not clear. What is consistent is the finding that "newly synthesized" ACh is always the first to be released during nerve activity.[37]

After ACh has been released and has acted on the postsynaptic membrane receptors, it is rapidly dissociated from the receptor. ACh is broken down by the enzyme acetylcholinesterase (AChE) to produce choline and acetate,[41] as depicted in Figure 1.4. A number of things can then happen to the choline, but the greater part is taken up into the presynaptic neuron to be reutilized in the synthesis of ACh. AChE is nature's most active enzyme and the hydrolysis of ACh occurs within seconds.[37] Vesicle bound ACh is not accessible to attack by AChE.

ACh plays a role in psychological processes such as memory, learning, attention and motivation. Each movement made, for example walking or talking, depends on the secretion of ACh from the motorneurons and its subsequent effect on muscle cells. In addition, calcium fluxes across the cell membrane and the mobilization of intracellular calcium from the endoplasmic or sarcoplasmic reticulum appear to be elicited by ACh action.[39] However, the main function of ACh appears to be in modulating cerebral activity of ascending primary inputs.[36]

1.4 NEURODEGENERATIVE DISEASES:

Health and illness are relative, falling along a continuum of bodily function. The same may be said for mental health and illness. While we all have our odd traits, the point at which an individual is said to be "mentally ill", is when the person has a diagnosable disorder of thought, mood or behaviour that causes distress or impairment of function. The economic costs of brain dysfunction are enormous. In fact more Americans are hospitalised each year with neurological and mental disorders than with any other major disease group including heart disease and cancer.[43] The cost in terms of treatment, lost wages and other consequence approaches reaches the billion dollar mark annually, however, this pales in comparison to the staggering emotional toll on the victims themselves and their families.

Neurodegenerative diseases are characterized by histological changes that are often non-specific in nature. Interpretations of findings with regards to these disease states are difficult. Researchers are forced to speculate on the basis of common background information to postulate possible mechanisms of pathogenesis. However, the theoretical choices are diverse:

(1) Toxic Damage: Neurodegenerative disease have arguably been linked to two types of toxins, namely the extrinsic and the intrinsic toxins. Studies regarding the ability of individuals to detoxify noxious agents, such as the extrinsic toxins, indicate that the disease-state might be derived from exceptional vulnerability to a variety of widespread substances. However, it is substance dependent whether or not acute, subacute or chronic exposure might have a greater effect and whether the damage is immediate or delayed. Furthermore, there is no evidence to suggest whether organic or inorganic toxins are more likely to have an aetiological role in neurodegenerative diseases. The second type of toxin, the intrinsic toxin, occurs normally within the central nervous system (CNS). Two classes of endogenous agents have been implicated in playing a part in pathogenesis-free radicals and excitatory amino acids (EAA). Although intrinsic toxins appear to play a role in neuronal death, their investigation is not within the scope of this study.

(2) Infective damage: Certain viruses have been linked to Parkisonism, dementia and motorneuron death. Specific neuronal pathways undergo progressive degeneration after bacterial infection. There is, however, no evidence of past infection as a cause of neurodegenerative diseases.

(3) Failure of deoxyribo nucleic acid (DNA) repair: Errors are known to occur when DNA replicates, but central neurons do not undergo this process. Therefore, failure to replicate correctly cannot be seen to attribute to neurodegenerative disease.

(4) Autoimmunity: Studies have shown that immunologically active cells mounting an attack on tissue components, for example attacking thyroid cells in Hashimoto's thyroiditis, may destroy cholinergic receptors of the neuromuscular junction. Activated microglia are known to accumulate at sites of nerve attrition in neurodegenerative disorders. There is nevertheless no known method, as yet, of distinguishing whether the activated microglia present kill the nerve cells or simply remove the dead cells.

(5) Failure of vital function: The theory encompasses the range of possible cellular disturbances that follow changes such as defective nutrient supply or waste removal, impaired activity of organelles such as the mitochondria and faulty production of a 'growth hormone'. The evidence supporting this possibility is the decrease in mitochondrial complex 1 reported in diseases such as Huntington's and Leber's afflictions.

(6) Late expression of a lethal gene: There are several examples of programmed cell death and the possibility that late gene expression of a gene responsible for this action cannot be ruled out.[44,45]

The modern neuropsychiatric therapeutic armamentarium contains some powerful, selective and highly effective drugs that often save lives and restore function. The most effective of these drugs (like those for complex diseases of thinking, emotion or motoric

and appetite functions) work for reasons still not clearly understood and in which the nature of the illness still drives research in the field. The corollary is that the disease that are understood most clearly in terms of causative mechanisms are not yet very treatable. Brain diseases are amongst the most elusive of targets because often there are no pertinent animal models in which to evaluate new drugs based on far more insightful views of pathogenesis.[46]

1.4.1 ALZHEIMER'S DISEASE (AD):

A chronic, progressive, degenerative disorder, which is in some rare cases familial, AD was first described by Alois Alzheimer in 1907.[47] Increasingly the disease is becoming a greater and greater health care problem as the population survives to older ages. The near linear incidence of Alzheimer's detection with age, makes this a very prevalent disorder, perhaps being detected in as many as 50% of those older than age 85. AD is characterized behaviourally by a severe impairment in cognitive function, including memory and the ability to recognize objects and orient oneself in time and space.[46,47]

Various neuropathological hallmarks of the AD sufferer's brain include: (1) senile plaques enriched in β-amyloid (Aβ) deposits, (2) neurofibrillary tangles composed of phosphorylated tau proteins, (3) abnormalities in the apolipoprotein E_4 ($APOE_4$) gene as well as (4) the two presenilin genes, (5) defects in the immune defence system and (6) deficits in cholinergic innervation with acetylcholine being a key neurotransmitter involved in cognitive processes, have all been implicated in leading to the defects of the disorder. Aβ, derived from amyloid precursor protein, has been implicated in neurotoxicity via induction of free radical formation [48-50] and the disruption of calcium homeostasis.[51]

Bioenergetic defects, of Aβ deposition, could be the final common pathway in neuronal death for this disease.

The neurofibrillary tangles, readily observed under a light microscope after silver impregnation staining, form within nerve cell bodies, particularly in the pyramidal cells of the hippocampus as a result of abnormal tau phosphorylation.[36] However, the tangles are also seen in the substantia nigra region and have been linked to certain forms of Parkinson's disease, particularly those forms that develop after encephalitis which encompasses about a quarter of the known cases.[37] The neurofibrillary tangle distribution appears to be linked to the cytoarchitectural fields or lamina of the brain, whilst the occurrence of the plaques, although more prevalent in certain areas, is less defined.[52] The number and extent of neocortical plaques and tangles are greater in AD disorders than in the 'normal' age-matched control cases.

The genetic disposition of AD towards susceptible genes, such as $APOE_4$, has left neurobiologists still struggling to identify environmental factors that could protect those who carry these defects or for factors which switch the genes on. Further controversy surrounds the APOE gene in that people who carry it will not invariably develop AD, but if they do, their brains appear to be more riddled with plaques and tangles than those AD patients who carry slightly different versions of the same gene. The analogy of these genes is paralleled with aging, since neither on their own accord is responsible for AD, both may only be regarded as high risk factors.[52]

The linking of AD to a cholinergic dysfunction appears to be an example of a unitary hypothesis. However, alternative relationships are now thought to be the case as little success has been achieved by treating patients with choline, lecithin, physostigmine or the muscarinic agonist arecholine. Current efforts have also focussed on the development of drugs that can block acetylcholinesterase centrally without hepatotoxicity and peripheral autonomic side effects, yet these drugs only appear to delay the onset of the disease.[46,53] Whilst significant advances have been made over the past decade on the respective relevance of each of these systems in the symptomatology of AD, very little attention has been given to their possible interrelationships in the aetiology of the disorder.[54,55]

Melatonin appears to have the properties to be a neuroprotective agent against Alzheimer's disease. Discoveries that melatonin prevents the death of neuroblastoma cells exposed to amyloid β-protein and amyloid peptide fragment [56,57] have been reported. Furthermore, old people and patients with AD [58] appear to suffer from a decrease in the amplitude of the melatonin acrophase.[59] Daniels *et al.* (1998) have demonstrated that prior administration of melatonin decreases lipid peroxidation induced by Aβ and aluminium in a dose-dependent manner, suggesting that melatonin may be beneficial for AD patients by reducing lipid peroxidation formation.[60] Experiments with rodents have demonstrated that pharmacological treatment with melatonin can increase life span, prevent premature aging and delay the onset of neurological disease.[61] The main thrust of research in this field now, however, is to develop drugs that could alter the course of AD or slow the progression of the disease, since the socio-economic benefits are large.

1.4.2. CEREBRAL ISCHAEMIA:

Numerous situations give rise to cerebral ischaemia including cardiac arrest, thrombotic stroke and asphyxia. Although all these conditions involve very different pathophysiologies, they are all thought to contribute to the neural degradation that occurs following cerebral ischaemia.[62] The ischaemic brain damage that occurs can take on several distinct morphological patterns, depending on the particular conditions of the ischaemia. Cerebral infarction, which is typically associated with prolonged, focal brain ischaemia, is characterized by irreversible damage to neurons, glia, and other supporting cell types in the brain.

In contrast, transient global ischaemia, such as that accompanying cardiac arrest and resuscitation or carbon monoxide poisoning, principlely injures specific populations of neurons known to be highly vulnerable to ischaemia.[63,64] Transient ischaemic attacks last less than 24 hours. Brief loss of consciousness is followed by several hours of confusion, difficulty in finding words and weakness of an affected limb.[64] The pyramidal cells in the *cornu ammonis* 1 (CA1) zone of the hippocampus, small and medium sized neurons in the striatum, non-cortical neurons in certain layers and the cerebellar Punkinje cells are among those neurons most susceptible to ischaemic injury.[65] The same pattern of 'selective vulnerability' is seen in epilepsy and hypoglycaemia.[64]

Within three minutes of disruption to cerebral circulation, the extracellular K^+ concentration around neurons rises from ±3 mM to as high as 80 mM.[66] At the same time, astrocytes and neurons can become swollen. The swelling is reversible if the period of ischaemia is brief. The reversibility depends on the CNS region and the age of the

animal. If the period of ischaemia lasts longer than three minutes, necrosis of the neurons may occur. However, neurons that are restored to normal function after a period of ischaemia, also succumb to delayed neuronal degradation. The condition may only occur a few hours to several days after the insult.[62,67]

Following transient global ischaemia, glucocorticoid levels rise. Therefore what is viewed as "expected" neuronal damage in response to focal or global ischaemia, may in fact, represent ischaemic damage worsened by the acute hypersecretion of glucocorticoids.[65] Melatonin has, however, been found to protect against ischaemia induced neurotoxicity. Recent research has demonstrated that melatonin protects the CA1 hippocampal neurons when administered during, or at least 2 hours following transient forebrain ischaemia in rats.[68] Greater neurodegeneration has also been shown to occur in pinealectomised (Px) rats following middle artery occlusion and glutamate receptor mediated, epilepsy-like seizures.[69]

1.4.3 EPILEPSY:

The pathology of this disease may be divided into changes 'causing' epilepsy and those said to arise from it, but the boundary line in these cases is diffuse. Almost any insult to the nervous system may lower the threshold for seizures. Apart from metabolic abnormalities, structural lesions are particularly likely to be associated with fits if they are (a) cortical, (b) close to the motor strip or (c) slow growing/evolving (such as tumours) in nature. Some individuals appear to have a genetic predisposition to have seizures in response to structural lesions.[37,64]

Most patients with epilepsy show no changes that could be considered a consequence of repeated fits. Following prolonged status epilepticus, however, there may be diffuse brain swelling and in some individuals chronic changes are found. At the most dramatic, in children, there may be atrophy of an entire cerebral hemisphere. More commonly medial temporal structures, including the hippocampus, amygdala and parahippocampal gyrus, may show loss of nerve cells. Abnormal electrical activity *per se* as well as secondary factors such as global cerebral ischaemia, hyperthermia and acidosis contribute to seizure-induced nerve cell death.[64]

1.4.4 HUNTINGTON'S DISEASE:

Huntington's disease is an autosomal dominant neurodegenerative disorder that is caused by a genetic defect localized on chromosome 4 with an onset at about 40 years of age.[70-73] The disease is characterized by disturbances in movement, psychiatric symptoms and a progressive dementia that leads to severe debilitation and usually death within 15-20 years.[70] Destruction of the brain is also noted with the autopsy brain weight of Huntington's disease patients normally about 20% less than average brain weight of a control group.[72,74]

The excitotoxic model has been proposed as a possible cause of Huntington's disease. Although there are other factors playing a part in the neurodegeneration that takes place in this disease, it appears that excitotoxic injury plays an important part in a more complicated array of neuropathological events, but none the less an important function in the disease process.[70] Several investigators have also explored the biochemical alterations in the processes mediating synaptic neurotransmission in the brains of Huntington's

patients, with amongst other inactivities, a severe but patchy reduction in ChAT is noted. A reduction of between 73 - 99% in striatal tissue of ChAT activity, responsible for ACh synthesis, has been reported for certain cases of this disease.[75] However the clinical diagnosis of the disease may only be confirmed by the detection of an abnormally expanded trinucleotide repeat sequence on chromosome 4.[76]

1.4.5 PARKINSON'S DISEASE (PD):

Characterized by tremor, muscular rigidity, difficulty in initiating motor activity and loss of postural reflexes, this progressive neurodegenerative disease is observed in approximately 1% of the population above 55 years of age.[46] In PD there is a selective degradation of neuromelanin-containing neurons, especially the nigral dopaminergic neurons.[77] The metabolism of dopamine by monoamine oxidase can yield 6-hydroxydopamine, which is known to yield reactive oxygen species.[78] Although proof that ROS stress actively causes the loss of monoaminergic neurons in PD is lacking, there is considerable evidence in animals and humans to support the concept.[70]

An additional hallmark of PD pathology is a deficiency of specialized amine precursor uptake and decarboxylation (APUD) system cells in the hypothalamus.[79] Interestingly the pineal gland forms part of APUD system and may actually be the 'master gland'.[80] Furthermore, most if not all chronobiological and neuroendocrine disturbances observed in Parkinson's patients are known to be regulated by both dopamine and melatonin. Arguably the progressive nature of the disease is paralleled by the well-established age-dependent decrease in MEL biosynthesis and plasma levels. In this regard, one hypothesis claims that neuronal cell death is a consequence of oxidative stress by free radicals, whilst

the potent radical scavenging and antioxidant properties of MEL have been documented, suggesting that age-related decreases in MEL levels may contribute to the aetiology of PD.[81]

1.4.6 PICK'S DISEASE:

Macroscopically, cases of Pick's disease show dramatic frontal or temporal atrophy or both. Microscopically, round argyrophilic intraneuronal inclusions (Pick bodies) and swollen cortical pyramidal cells (Pick cells) are seen together with nerve cell loss and gliosis. Some cases are familial, but little is known about the possible pathogenesis. Pick bodies are known to stain with the same antibodies as those of the neurofibrillary tangles, but they do not contain the paired helical filaments.[64]

1.4.7 PRION PROTEIN DISEASE (PPD):

The main claim to fame of the PPD's is the transmission of these neurodegenerative disorders through the prion protein in the absence of any nucleic acid. Human forms of the disease may be acquired genetically, iatrogenically or sporadically and most are transmissible. The recent studies of prion protein and PPD's are relinquishing some of the mysteries associated with the prion protein, but as of yet there is no complete understanding of this protein.[54]

Prion disease is characterized clinically by motor and cognitive abnormalities that progressively lead to dementia and provoke death within months to 15 years depending on the individual concerned. There are three main forms of the PPD's that are easily

recognizable are: Creutzfeldt-Jakob disease (CJD), Gerstmann-Sträussler-Scheinker disease (GSS) and fatal familial insomnia (FFI). However, several variants are constantly being identified and thus broaden the spectrum of these PPD's. The pathological features of PPD include variable degrees and region-specific cerebral and cerebellar spongiform change, neuronal loss, gliosis and prion amyloid plaques. Tubulovesicular structures are observed by electron microscopy, however, different forms of PPD do not necessarily exhibit each of these pathological features.[54]

1.4.8 SEASONAL AFFECTIVE DISORDER (SAD):

A strong causal relationship with seasonal changes in the prevailing photoperiod (light:dark cycle), with diminished light exposure in winter has been suggested in SAD. The disease is characterized by regularly occurring depression in autumn and winter, alternating with non-depressed periods observed in spring and summer.[82] Indeed phototherapy, by employing controlled light exposure regimes, does improve the clinical picture of SAD sufferers and other forms of depression.[83] There is also considerable indirect or ancedotal evidence for a role of MEL in winter SAD cases and the major depression syndrome. A suppression or phase-shift of MEL biosynthesis may well be involved in the therapeutic effects of light treatment.

1.5 METAL CHEMISTRY AND NEUROTOXICITY:

1.5.1 INTRODUCTION:

"Life" may be characterized as a controlled stationary flow equilibrium, maintained by energy consuming chemical reactions.[84] The physiological functioning of these life systems include at least 28 of the elements isolated on the periodic table thus far; most of which are metals.[85,86] However, as with Paracelsus Principle: "The dose makes the poison", there exists a definite link between metal levels, essential and toxic, and the onset of neurodegenerative diseases. The brain itself concentrates metals better than any other tissue in the body, but cannot function adequately without optimum levels of these elements.[87] Causal or symptomatic, metal concentration fluctuations within the central nervous system suggest an importance in understanding their role in neurodegeneration. Concentration fluctuations of these metals may potentially act as indicators to predisease states and could lead towards possible treatment measures.

However, unlike many other toxic substances, which have been created and distributed throughout the environment by man, metals are natural and have been important and useful to man since the beginning of civilization. Despite the increasing awareness of the negative effects of pollution to mankind over the past twenty years and the considerable progress been made in reducing pollution discharges in developed countries, the problems relating to metal neurotoxicity have not been abated. Primarily because metals are persistent and once they have been scattered throughout the human habitat, they remain there.[88]

Increasingly it has become clear that metal neurotoxicity is likely to be the most important environmental hazard in the contemporary world, in that all of us are exposed to toxic metals and the levels of exposure of average individuals are not much above levels known to cause disease.[88] Metals within the body exist freely in the cytosol, in storage vesicles, at active sites of enzymes or proteins or bound to ligands which facilitate their transport. The reasons for their imbalances may thus be due to displacement by other metals, toxic or essential, inhibition of the enzyme or protein, rupture of the storage vesicles, dietary deficiency or a breakdown in their transport mechanism within the central nervous system.[89, 90] Furthermore, unlike most organic pollutants, metals are neither degraded in the environment nor metabolised by the body and as a result of both synthetic and natural processes, metals have been attached to organic chemicals, often increasing their bioavailability and neurotoxicity.

Cells normally regulate the intracellular concentrations of essential metals via transport mechanisms. However, metals that lack a normal biological function may not come under the control of the cell's regulatory machinery, for example the so-called *heavy metals* from the second and third transition series and *f*-block elements that are nonessential.[90] In addition, for some elements such as lead, mercury, arsenic or chromium, the type of compound such as the ligation or oxidation state, plays a crucial role for the toxicity.[84] Although many metals may be toxic in certain circumstances, the major metals of interest to this study, which are of significance to human neurotoxicity are discussed below:

Lead: Lead toxicity has been known since the time of the Romans and some attribute the decline of the Roman Empire to lead poisoning from lead wine goblets.[88] At high doses, often in occupational settings, lead causes abnormalities on psychometric testing, including cognitive and visumotor difficulties and may often be fatal, causing an encephalitis with progressive signs of confusion, delirium with convulsions, lethargy, coma and death.[91] Children have been shown to be more susceptible to inorganic lead poisoning, due to incompletely developed metabolic pathways and blood brain barrier (BBB), producing an acute encephalopathy. Adult inorganic lead toxicity has primarily manifested itself as motor peripheral neuropathy.[92,93]

As with many other elements, the physiological retention time of lead and its compounds depends strongly on the location in the body.[84] Lead may exert its toxicity by displacing zinc or calcium at the active site of certain enzymes, or by inhibiting the biosynthesis of δ-aminolevulinic acid dehydrogenase (ALAD), which in turn results in increased δ-aminolevulinic acid (ALA) levels which have been implicated in neurotoxicity.[84,92] The organometallic fuel additive, tetraethyl lead, reveals its toxic symptoms in the form of severe disorders of the central and peripheral nervous system, such as cramps, paralysis and loss of coordination. The toxicity results from the change in permeability of neuronal membranes towards the organometallic species, including the highly selective BBB.[94]

Cadmium: Chronic exposure to cadmium in industry has been linked to impairment on measures of attention, memory and psychomotor speed.[95] Cadmium, one of the more dangerous heavy metals, has a similar ionic radius to two biologically important metal ions namely, zinc and calcium. The interference of cadmium in calcium homeostasis is the possible cause of its toxicity, with reports of calmodulin (a calcium carrier molecule)

inhibitors protecting rodents against cadmium toxicity.[96] Cadmium, a more thiophilic metal, may displace zinc at the cysteinate-coordinated metallothioneins and related enzymes.

Furthermore, cadmium has shown an oxidative toxicity mechanism by depleting glutathione and protein-bound sulphydryl groups, resulting in an increase in the production of reactive oxygen species such as the superoxide anion, hydroxyl radicals and hydrogen peroxide. Increases in these reactive oxygen species have been linked to lipid peroxidation, membrane damage and apoptosis.[97] However, under physiological conditions bioalkylation does not occur as the organometallic compounds of this electropositive metal are not stable in aqueous media.[98-100]

Mercury: The extreme toxicity of many mercury compounds has only become apparent through worldwide-publicized incidents of mass poisoning. Examples of these tragedies include Minamata Bay in Japan (between 1948 and 1960) where mercury-containing catalysts were released and the flour contamination in Iraq (1972) after the use of organomercury fungicides.[101-103] In its usual ionic form, mercury is immediately toxic since this species is easily soluble at pH 7 and does not form insoluble compounds with anions that are abundant in body fluids. However, acute poisoning with metallic mercury is very rare, but chronic inhalation of mercury vapour has been described in detail by the scientists themselves. In particular, the neurological symptoms of mercury poisoning gradually appear when working in insufficiently ventilated rooms where spilled metallic mercury has come into contact with air, as described vividly by Mellon and Stock (1977) for the first time.[104]

Mercury poisoning results in diminished blood flow to the extremities, impaired concentration and coordination, tremors (the so-called "mad hatters" syndrome) and memory loss. Acute poisoning leads to cerebellar syndrome including ataxia.[93] The potential long-term health hazards through the additional mercury incorporation via amalgam tooth filings continues to be a controversially discussed point.[84,105]

An especially toxic form is the organometallic cations, in particular methylmercury, which can be formed from cobalamin-catalyzed biomethylation within the body. The specific toxicity is connected to the ambivalent lipophilic/hydrophilic character of such organometallic species, allowing them to penetrate very tightly constructed membrane partitions for example the nervous system or the growing fetus.[98,100] Damage to primary sensory areas, fine tremor of the limbs associated with depression and a mixed neurotic (neurasthenic) syndrome including fatigue, irritability, apprehension and headaches are all symptoms of methyl mercury poisoning.[93]

Aluminium: Undoubtedly neurotoxic, a major feature in dialysis dementia and the controversial cause/effect argument of aluminium in certain brain tissue regions of Alzheimer patients, has made this metal a topical research focus.[88,93] Although not known to be employed in any physiological processes, human brain tissue has been shown to contain a bulk aluminium concentration of around 1.4 parts per million (ppm).[89,106] Aluminium has been linked to increasing the permeability of the blood-brain barrier, neuronal dysfunction, and the Alzheimer's-Parkinson's disease: amyotrophic lateral sclerosis (ALS) syndrome seen in Guam (also referred to as the Guam parkinsonism-dementia complex).[88,89,106-108] Furthermore, aluminium has been associated with chromatin binding when cells undergo mitosis and intracellularly to the promotion of free

radical production due to releasing calcium and iron(II) from within their cellular complexes.[109,110]

Aluminium exhibits complex aqueous chemistry, with several forms of the metal being present in solution, depending upon the pH. The chemical similarity of Al^{3+} and Fe^{3+} has been demonstrated by the binding of aluminium to transferrin, an iron transport protein. However, Al^{3+} is released more rapidly from transferrin than its counterpart Fe^{3+}.[111] Interference with several calcium-dependent steps of neuronal metabolism, due to competition for extra- and intracellular binding sites, may also suggest a mechanism by which aluminium exerts its neurotoxicity.[110] The strong tendency of this ion to coordinate to deprotonated 1,2 dihydroxy aromatic systems, such as the catecholamine neurotransmitters, as well as the possible aggregation role with amyloid-β peptide leading to senile plaque formation; has subsequently affiliated aluminium to further neuropathological symptoms.[84]

Copper: Existing in two main oxidation states, namely Cu^{+} and Cu^{2+}, free copper is normally found in low concentrations in the brain and blood plasma.[112] However, at higher concentrations, free copper seems to be a potent free radical generator, causing hemolysis, formation of fluorescent lipid complexes and oxidation of low density proteins.[113,114] Excessive accumulation of copper in the putamen and substantia nigra regions in the post-mortem brains of Huntington's disease subjects has also been reported.[115] Furthermore high levels of iron and copper have also been associated with the generation of hydroxyl radicals in brain tissue through the Fenton reaction, whilst Wilson's disease is an example of a genetic alteration produced by excessive accumulation of copper in the brain and liver.[116,117] In addition, the severity of the neurological signs in

Wilson's disease appears to be related to the extent of copper accumulation in the brain.[118]

Copper has long since been known to play a role in neurodegeneration, however, more recently it has been noted that the depletion of cellular glutathione resulted in a dramatic changes of copper toxicity in neurons.[119] Analogously copper-mediated toxicity may contribute to neurodegeneration in Alzheimer's disease and has been linked to stroke and seizure conditions.[120,121] Research has shown that amyloid precursor protein (APP), in Alzheimer's disease, has the ability to reduce copper(II) to copper(I) in a cell-free system; leading to increased oxidative stress in neurons. The data further substantiates an APP copper binding domain in APP-mediated copper(I) generation and toxicity in site specific primary neurons linked to neurodegeneration.[122] Perturbations to the APP metabolism and in particular, its secretion or release from neurons may alter copper homeostasis resulting in increased amyloid beta (Abeta) production and free radical generation.[123]

Zinc: The second most prevalent trace element in the body, zinc is present in particularly large concentrations within the mammalian brain. Although Zn^{2+} is a cofactor for many enzymes in all tissues, a unique feature of brain zinc is its vesicular localization in presynaptic terminals, where its release is dependent on neuronal activity. However, upon excessive synaptic Zn^{2+} release, its accumulation in postsynaptic neurons contributes to the selective neuronal loss that is associated with certain acute conditions, including epilepsy, transient global ischaemia and brain trauma.[124-128] More speculatively, Zn^{2+}, dis-homeostasis might also contribute to some degenerative conditions such as Alzheimer type dementia, Down's syndrome, Friedreich's ataxia, retinitis pigmentosa, schizophrenia and Wernicke-Korsakoff syndrome.[129,130]

The importance of zinc in neural development can be exemplified by its role in the synthesis of pyridoxal phosphate, a precursor of the neurotransmitters: dopamine, norepinephrine, serotonin, histamine and γ-aminobutyric acid (GABA). While zinc is required for GABA synthesis, high levels of zinc can retard its release, as in Pick's disease. Here higher than normal accumulation of zinc in the hippocampus causes inhibition of GABA transmission; highlighting the requirement for a steady state zinc concentration.[130,131] Mechanisms through which intracellular Zn^{2+} promotes cell death are only beginning to be understood. Recent studies suggest that metabolic inhibition and the generation of ROS forms might be crucial to both slow and rapid zinc neurotoxicity mechanisms, particularly at the mitochondrial sites.[132]

Calcium: Besides iron, and maybe even surpassing it, calcium (in ionic form as Ca^{2+}) is the most important and most versatile "bioinorganic" element.[84] Calcium ions, themselves secondary messengers, have been linked to many forms of neurodegeneration through excessive cellular Ca^{2+} loading (the Ca^{2+} hypothesis). Contrary to the Ca^{2+} hypothesis, the relationships between Ca^{2+} load and cell survival, free Ca^{2+} concentration, and Ca^{2+}-induced morphological alterations depend primarily on the route of Ca^{2+} influx, not the Ca^{2+} load. Notably, for example, the Ca^{2+} loading via the N-methyl-D-aspartate (NMDA) receptor channels is toxic, whereas identical Ca^{2+} loads incurred through voltage-sensitive Ca^{2+} channels are completely innocuous.[133]

Ca^{2+} overload, due to abnormal voltage-dependence of transient Ca^{2+} channel activation, may also contribute to motor neuron toxicity, as observed in spinobulbar muscular atrophy (SBMA).[134] Disturbances of neuronal calcium homeostasis may be induced in three different subcellular compartments, the cytoplasm, mitochondria or the endoplasmic

reticulum (ER). The mitochondrial calcium hypothesis is based on the observation that after a severe form of stress there is a massive influx of calcium ions into mitochondria, which may lead to production of free radicals, opening of the mitochondrial permeability transition (MPT) pore and disturbances of energy metabolism.[135]

The ER calcium hypothesis arose from the observation that ER calcium stores are depleted after severe forms of stress, and that the response of cells to disturbances of ER calcium homeostasis resembles their response to a severe form of stress (e.g. transient ischaemia) implying common underlying mechanisms. Elucidating the exact mechanisms of calcium toxicity and identifying the subcellular compartment playing the most important role in this pathological process will help to evaluate strategies for specific therapeutic intervention and is an on-going area of research.[135]

Sodium and Potassium: The monovalent ions of particular importance for cellular neurophysiology are sodium (Na^+) and potassium (K^+). These electrolytes play a vital role in the normal functioning of the nervous system. The resting potential of a neuron is dependent on the ratio of the concentration of potassium inside and outside the cell, whilst the action potential is governed by the ratio of intra- and extracellular sodium concentrations.[43] Although no change in total body sodium levels has been recorded during a depression incident, evidence suggests that a redistribution occurs within the body which returns to normal after recovery. In addition, total body potassium and intracellular potassium were found to be low in depression cases, but these levels did not change with clinical recovery.[43,136-138] A depletion in intracellular potassium levels, is also a common feature of essential hypertension and type 2 diabetes.[139]

Episodic ataxia type 1, associated with epilepsy in a few patients, has been linked to mutations within the potassium voltage-gated channel.[140] Brains of depressed patients, who had committed suicide, were shown to have an increased water content and reduced sodium concentration, as compared with patients that had died of natural causes.[141] Since these electrolytes also play an important role in the synthesis, storage, release and inactivation of neurotransmitters, it is conceivable that abnormalities in electrolyte distribution and metabolism *per se* could lead to altered functioning, which may in turn underlie certain depressive disorders.[138]

Lithium: Early studies have indicated that lithium is highly effective in the treatment of manic and hypomanic states, recurrent manic-depressive disorders (bipolar) as well as recurrent depression in which no manic episodes occur (unipolar).[138,142,143] However, the use of lithium salts in the treatment of depression remains a controversial issue. Lithium has been shown to interfere with some cyclic adenosine monophosphate (c-AMP) mediated hormones, stimulating specific adenylate cyclases, which are important components of the postsynaptic receptor mechanisms.[144] Reports that chronic lithium treatment increases tryptophan uptake, but decreases the activity of membrane bound tryptophan hydroxylase has been noted in rat brain synaptosomes.[145]

In addition, lithium has been found to decrease both the synthesis and release of acetylcholine (ACh), as well as increase the synthesis of glutamate and γ-aminobutyrate (GABA).[146-148] Decreases in ACh levels have been linked to certain types of Parkinson's disease and AD, whilst changes in levels of the glutamate and GABA have been associated with Schizophrenia, neuronal swelling and death as a result of excitotoxicity.[43]

1.5.2 CLASSIFICATION OF METAL ION AND LIGAND INTERACTIONS:

Hard-Soft Acid-Base (HSAB) Theory

The interaction between a metal and a biological substrate is best described as the formation of a metal-ligand coordination complex. The complex is formed by the interaction of an unfilled orbital of a metal with the filled orbital of a ligand.[84] The type and feasibility of the metal-ligand interaction is governed by the chemistry of the metal as defined by the periodic table of the elements, their redox potentials and their properties as Lewis acids or bases.[90] The following classification of the metal ion and ligand complex formation will serve as background in this work for determining the preferred interaction site(s) in computational modeling data or NMR and IR spectra.

In 1963 Pearson coined the terms *hard* and *soft* to describe metal ions and ligands.[84] In general, hard cations form their most stable complexes with hard ligands and soft cations with soft ligands. Table 1.1 illustrates some examples.

Table 1.1 Classification of Lewis Acids and Bases by Hard/Soft Criteria:

	Acids	Bases
Hard	H^+, Li^+, Na^+, K^+, Mg^{2+}, Ca^{2+}, Mn^{2+}, Al^{3+}, Ln^{3+}, Cr^{3+}, Co^{3+}, Fe^{3+}, VO^{2+}, MoO^{3+}, So_3, CO_2	H_2O, ROH, NH_2, RNH_2, RCO_2^-, Cl^-, F^-, PO_4^{3-}, $H_2PO_4^{2-}$, SO_4^{2-}
Intermediate	Fe^{2+}, Co^{2+}, Ni^{2+}, Cu^{2+}, Zn^{2+}, Pb^{2+}, Sn^{2+}, SO_2, NO^+, Ru^{2+}	Imidazole, pyridine
Soft	Cu^+, Ag^+, Au^+, Tl^+, Hg^+, Cd^{2+}, Pt^{2+}, Hg^{2+}	RSH, R_2S, CN^-, I^-, $S_2O_3^{2-}$

Hard metal ions (characterized by small ionic radii or high charge) have little electron density to share with a ligand. Hard ligands do not readily give up their electron density and thus a combination of the two results in a complex that is stabilized by simple electrostatics; for example Mg^{2+} and HPO_3^{2-} or Na^+ and $CH_3CO_2^-$. On the other hand, soft metal ions and ligands (typically possessing polarizable electron clouds) are more prone to sharing electron density with a greater degree of covalency in the bonding and so form a mutually stable complex, examples include Cu^+ and I^- or Hg^{2+} and CH_3S.

However, combining a hard metal with a soft ligand, the metal does not readily accept the electron density being offered, hence the resulting complex is less stable since both partners are incompatible. Certain metal ions have been known to exhibit intermediate behaviour and can interact reasonably well with both hard and soft species. The affinity of

a donor atom in a ligand for a hard metal ion varies as follows: F>O>N>Cl>Br>I>C~S, whilst for soft metals this order is inverted.[84,90]

Metal ion coordination number and geometry:

Within the biological context, metals mainly appear in oxidized form as formally ionized centres, which are therefore surrounded by electron-pair donating ligands. Since the chemical elements – 'inorganic' as well as 'organic'- cannot experience a biological evolution by themselves, it is their often highly complex coordination chemistry that is biologically relevant. Relatively little is known about the relevance of metal coordination to lipids and carbohydrates and other biologically important molecules, although the potentially negatively charged oxygen functions can bind cations electrostatically and even undergo chelate coordination via polyhydroxyl groups.[85,86]

Likewise, few molecular details are known about the *in vivo* interaction of low molecular weight coenzymes, hormones or other products of the metabolism, for example citrate with metal ions. The complexes formed are frequently labile which makes detection, isolation and structural characterization very difficult. For example, the physiological function of ascorbate is connected with the Fe^{III}/Fe^{II} redox equilibrium.

Table 1.2 illustrates the coordination number (C.N.) and preferred geometries for selected metal ions. Notably the coordination number and geometries of the alkali and alkaline earth metals depend on the relative sizes of the cation and ligand concerned. Sodium and magnesium, for example, readily accommodate six ligands, whereas the larger potassium

and calcium ions may expand their coordination shells to accommodate seven or eight ligands and display flexible coordination geometry.

Coordination preferences for the transition metals again depend, in part, on the steric bulkiness of the ligands surrounding the metal ion. Small cations can accommodate fewer ligands in their inner coordination spheres and tend to adopt a tetrahedral geometry that minimizes steric and electrostatic repulsion relative to a square planar geometry. Unlike the alkali or alkaline earth metals, where the bonding is predominately electrostatic in origin, the coordination complexes of transition metals contain a substantial degree of covalency. The *d*-orbital and ligand orbital energies are comparable and may interact favourably in a bonding fashion.

Distortions from the ideal symmetries are common in biology and provide important mechanisms for fine-tuning the physicochemical properties of the metal centre. Since the architecture of ligand geometry is inherent in the design of biologically active molecules - such as proteins or a naturally binding metal antibiotic - the geometry can form the basis for selective uptake of the metal ion. Furthermore, there is a large variation in metal ion concentrations in intracellular and extracellular environments. Less abundant transition metals require ligands with large stability constants (relative to the more abundant alkali and alkaline earth metals) to promote effective uptake. However, the stability constants for the most abundant monovalent ions, K^+ and Na^+, are negligible for practically all biological ligands.[84,90]

Table 1.2 Coordination number and preferred geometry of certain metal ions:

Cation	C.N.	Geometry	Biological Ligands
Na^+	6	Octahedral	O, ether, hydroxy, carboxylate
K^+	6-8	Flexible	O, ether, hydroxy, carboxylate
Mg^{2+}	6	Octahedral	O, carboxylate, phosphate
Ca^{2+}	6-8	Flexible	O, carboxylate, carbonyl, (phosphate)
$Mn^{2+}(d^5)$	6	Octahedral	O, carboxylate, phosphate N, imidazole N
$Mn^{3+}(d^4)$	6	Tetragonal	O, carboxylate, phosphate, hydroxide
$Fe^{2+}(d^6)$	4	Tetrahedral	S, thiolate
	6	Octahedral	O, carboxylate, alkoxide, oxide, phenolate
			N, imidazole N, porphyrin
$Fe^{3+}(d^5)$	4	Tetrahedral	S, thiolate
	6	Octahedral	O, carboxylate, alkoxide, oxide, phenolate
			N, imidazole N, porphyrin
$Cu^+(d^{10})$	4	Tetrahedral	S, thiolate, thioether N, imidazole N
$Cu^{2+}(d^9)$	4	Tetrahedral	S, thiolate, thioether N, imidazole N
$Cu^{2+}(d^9)$	4	Square planar	O, carboxylate N, imidazole N
	6	Tetragonal	O, carboxylate
			N, imidazole N
$Zn^{2+}(d^{10})$	4	Tetrahedral	O, carboxylate, carbonyl
			S, thiolate N, imidazole N
	6	Square pyramidal	O, carboxylate, carbonyl N, imidazole N

1.6 AN OVERVIEW OF NON-ELECTROCHEMICAL METHODS FOR METAL ANALYSIS:

Exposure to metals occurs in a number of industries from the mining, roasting and smelting of ores, to steel and metal alloy production, the manufacture of batteries and even silicon chips. The industries themselves may be very large, such as factories producing thousands of lead batteries each day, or a small one–room electroplating shop. Even a dentist's surgery where a tooth filling is being produced exposes one to the possible harmful effects or mercury from the amalgam. The literature is replete with examples of toxic exposures in the above mentioned cases and many others.

Unfortunately, the toxic exposure is not limited to workers using metals in industry, but can occur even in homeowners growing vegetables in a backyard garden. In fact many of the metals of concern in industrial exposure, lead, cadmium, mercury *etc.* are also of concern in the environment owing to the activities of humankind throughout the course of history. However, advances in analytical chemistry are progressively playing a more substantial role in the identification and quantification of metals in the environment and biological samples.[142]

In 1966 Bowen listed 78 elements in vertebrate blood which he determined using more than 10 different procedures.[89] Since then various new techniques have been discovered. Current methods used to detect metals in biological systems include neutron activation analysis, the various forms of atomic absorptions spectroscopy and even fluorimetric analysis. In addition, emerging techniques such as extended X-ray absorption fine

structure spectroscopy are actively being used to study metals at the centre of enzyme structures.[89] Furthermore, detection/quantitation limits have continually improved along with the accuracy, sensitivity and reliability of the measurements obtainable; following instrumentation technology enhancements.[142]

Spectrophotometric methods have a fairly low detection limit and may even be useful in trace element analysis. However, to avoid interferences by other metal species, the technique often requires the extraction of the metal ions into an organic solvent. In other methods, various reagents such as Rhodanine, need to be added to the sample to form coloured complexes, which can then be viewed by visible spectroscopy. Another disadvantage of the spectrophotometric method, is that the oxidation state of the metal ion is not distinguishable.[149-151]

Emmission spectrography, atomic absorption and neutron activation instrumental techniques are all particularly useful for the determination of trace quantities of certain metal ions. The trace level detection limits, however, require the use of these techniques in conjunction with solvent extraction methods. Emission spectrography, for example, can detect small quantities of gold in a metal sample in the range of 0.5-20ppm, as well as the purity level of the gold in the sample. This technique may be adapted to biological samples, for example the detection of gold content in the Auranofin® drug for the treatment of arthritis.[89,131,152]

Atomic absorption spectroscopy (AAS) is used for the quantitative and qualitative analysis of about 70 elements. There are different types of AAS based on the excitation source employed such as the flame or graphite furnace. AAS techniques have a detection limit in

the region of 10^{-8} mol dm^{-3} in solution and tend to obviate extensive sample preparation. AAS has been the technique of choice in the past for the environmental analysis of heavy metals in slaughtered animals, for example, as an indicator of environmental overloading.[153-155] A major advantage of AAS is the amount of research that has gone into optimising the technique.

While the technique is useful for the quantitative and qualitative determination of a wide range of elements, it excludes metals that cannot be reduced to an atomic vapour, *e.g.* tungsten, elements emitting in a vacuum and artificial elements. Flame AAS suffers from impaired sensitivity and precision at concentrations below the mg/ml range, whilst furnace AAS is essentially a single element technique and may therefore be time-consuming. Further disadvantages of the atomic absorption technique include the susceptibility of the technique to the presence of other interfering ions, sensitivity to pH and rigid experimental parameters (which may be overcome with the use of the solvent extraction technique) and the inability to determine the oxidation state of the metal ion in solution.

Neutron activation is another popular technique for heavy metal analysis. The sensitivity arises from the high-neutron capture cross sections of the naturally occurring metal isotopes. An advantage of this technique in biomedical applications is that no pre-treatment of the sample is required. However, disadvantages of this technique include the cost of the sophisticated equipment required for irradiation and analysis and the resulting β and γ emmisions. Time is also a constraint with long delays after analysis especially of the elements with long half-lives, where delays of up to two weeks may be experienced.[156] The neutron activation technique is not suited for studying fast interaction of metal ions within biological substrates.[149,150,157]

Inductively Coupled Plasma-Mass Spectrometry (ICP-MS) offers another alternative to the determination of metal ions in solution. The technique has been used in a wide variety of applications, including biological fields and is useful in speciation detection. The ICP-MS technique is a combinatorial technique and thus, posses enhanced sensitivity, accuracy and selectivity in comparison to any of the single techniques mentioned above.

However, the compromise for the advantages of the ICP-MS technique is in the form of the sharp increased cost, the need for a higher skilled operator and the lack of portability of the equipment. Detection limits tend to vary depending on the sample and the context (typically around 10^{-9} mol dm^{-3}), however, a limitation of the ICP-MS technique is that the sample must contain less than 0.2 % total dissolved solids, since the nebulizer becomes blocked easily. Dilution of the sample may overcome this problem, but a loss in sensitivity is then experienced.[158,159]

Electrochemistry on the other hand, a single technique, offers the advantages of high sensitivity, selectivity toward electroactive species, portability and fairly low cost instrumentation, speciation capability, rapid multi-component determinations without requiring metal enrichment techniques and a wide range of electrodes that allow assays of unusual environments.[160,161]

Extremely low (nanomolar) detection limits can be achieved with very small (5-20 ml) sample volumes, thereby allowing for the determination of analyte amounts in the order of 10^{-13} - 10^{-15} mol dm^{-3} on a routine basis. Electrochemical metal ion speciation is unique for that ion and its oxidation number, since there is only one assigned redox peak potential for a redox couple. The simultaneous detection of other metal ions in solution is possible,

provided the metal ions do not posses overlapping peak potentials. Electrochemistry, stripping voltammetry in particular, depends on the electrolytic deposition step for the preconcentration of trace components and thus has the advantage of minimizing the risk of contamination, since little or no reagent has been added. A further advantage of this technique is the flexibility of combinations with other detection techniques, such as the chromatographic or optical procedures, resulting in even further enhanced sensitivities.[149,160,162-164]

1.7 FUNDAMENTAL CONCEPTS IN ELECTROCHEMISTRY:

Faraday's discovery of the one-to-one equivalence that exists between chemistry and electricity provides the basis for all electroanalytical techniques, namely the measurement of electrical quantities, such as current, potential and charge and their relationship to chemical parameters. In general the electrochemists apply an electrical *excitation* signal (often the independent variable) to some *system* (particular electrode-solution composition and geometry) and then monitor a *response* signal (dependent variable), which together with the excitation allows some description of the properties of the system at hand.

The species being measured can either bring about a direct electrochemical response that can be detected or measured, or can be induced to bring about such a response, resulting in a process that can be detected electrochemically.[160,165] In both cases an interface is required between the chemical or biochemical species being measured and the electrochemical system performing the measurement. Electrochemical analysis is in contrast to many chemical measurements in this manner, since conventional chemical

measurements involve homogenous bulk solutions whilst the electrochemical processes take place at the electrode solution interface.[160,165] The role of the electrode may be either to monitor species in solution or to generate new species that will interact with the medium in an interesting or useful manner.[164]

1.7.1 ELECTRODE SOLUTION INTERPHASE:

The electrical double layer is the array of charged particles and/or orientated dipoles which exist at an electrode interface.[160] The first double layer model, due to Helmholz, considered the ordering of positive and negative charges in a rigid fashion on the two sides of the interface, thus giving rise to the designation of a double or compact layer. Progressive models were adopted from work completed by Gouy, Chapman, Stern and Grahame.[160] The most recent of the accepted models was proposed by Bockris, Devanathan and Müller, which takes into account the physical nature of the interfacial region.[162]

In electrochemistry, such an electrical double layer reflects the ionic zones formed in the solution, to compensate for the excess of charge on the electrode (q_e). Since the interface must be neutral, $q_e + q_s = 0$ (where q_s is the charge of the ions in the nearby solution), the counterlayer is made up of ions of opposite sign to the electrode. The electrical double layer is illustrated in Figure 1.5 and is shown to be a complex structure of several distinct parts.

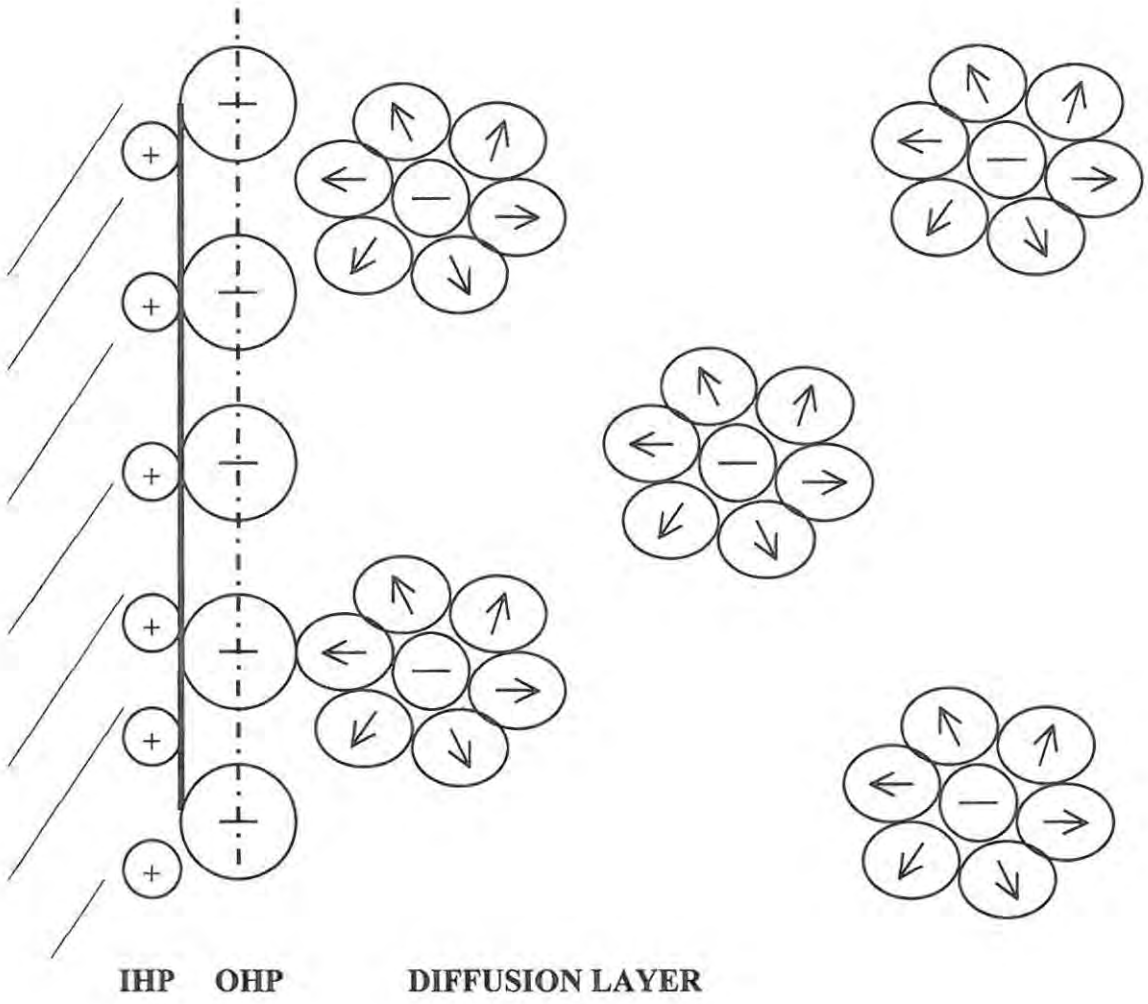

Figure 1.5 Schematic representation of the electrical double layer.

The inner layer (closest to the electrode), known as the inner Helmholz plane (IHP), contains solvent molecules and specifically adsorbed ions (which are not fully solvated). The next layer, the outer Helmholz plane (OHP), reflects the imaginary plane passing through the centre of solvated ions at their closest approach tot he surface. The solvated ions are non-specifically adsorbed and are attracted to the surface by long-range coulombic forces. Both Helmholz layers represent the compact layer and such a compact layer of charges is strongly held by the electrode, surviving even when the electrode surface is

pulled out of solution. The outer most layer, referred to as the diffuse or Gouy layer, is a three dimensional region of scattered ions, which extends from the OHP into the bulk solution. The ionic distribution illustrates the balance between ordering forces of the electronic field and the disorder caused by random thermal motion. The total charge of the compact and diffuse layers equals (and is opposite in sign to) the net charge on the electrode side. The electrical double layer can thus be compared to a parallel-plate type capacitor.[162,163]

1.7.2 TRANSPORT TO THE ELECTRODE:

Simple electrode reactions involve only mass transport of the electroactive species to the electrode surface, the electron transfer across the interface and the transport of the product back to the bulk solution. More complex reactions include additional chemical and surface processes, which precede or follow the actual electron transfer. The net rate of the reaction, and hence the measured current, may be limited either by mass transport or the reactant or by the rate of electron transfer, the slowest process being defined as the rate-determining step.[160] When three modes of transport are involved, the current response equation is complex. Contributions due to convection and migration may be minimized by utilizing quiescent solutions and strong electrolytes, respectively.[160,164]

Mass transport occurs by three different modes, as illustrated in Figure 1.6:

- *Diffusion*: the spontaneous movement under the influence of concentration gradient, *i.e.* from regions of high concentrations to regions of lower ones, aimed at minimizing concentration differences.
- *Convection*: transport to the electrode by a gross physical movement; such fluid flow occurs by stirring or flowing the solution and by rotating or vibrating the electrode (*i.e.* forced convection) or because of density gradients (*i.e.* natural convection).
- *Migration*: movement of charged particles along an electric field (*i.e.* the charge is carried through the solution by ions according to their transference number.)

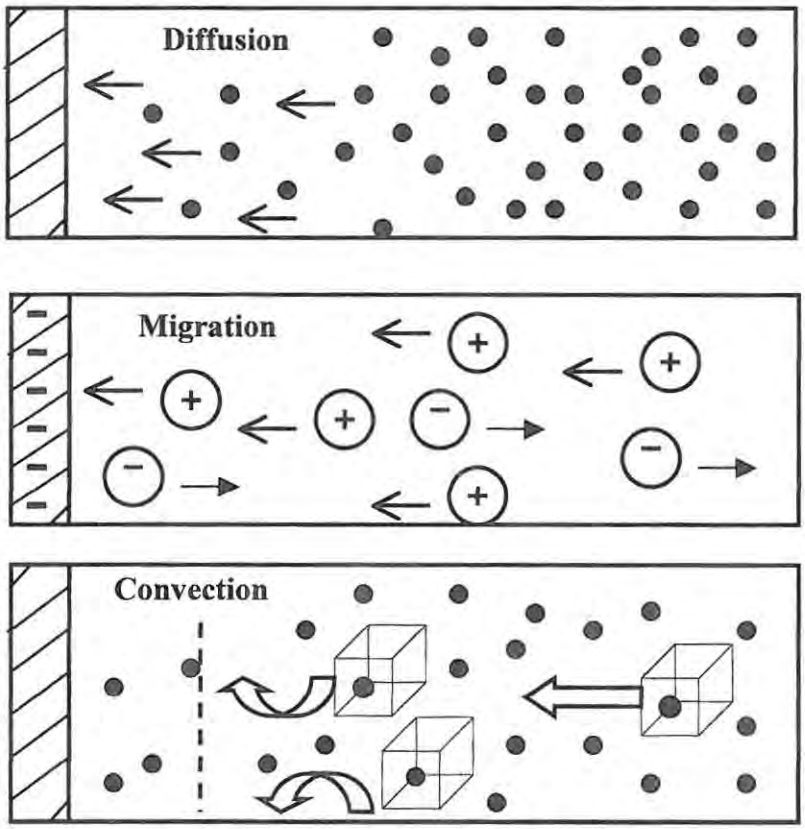

Figure 1.6 The three modes of mass transport.
(adapted from a text by Wang J.[160])

1.7.3 DEFINITION OF ELECTROANALYTICAL TECHNIQUES:

The electroanalytical techniques may be broadly defined as being either static or dynamic. Static methods entail the measurement of a potential difference at zero current, such that the system defined by the solid-solution interphase is not disturbed and the Nernstian equilibrium is maintained. Although such potentiomteric measurements are of practical importance (e.g. pH, pM), the focus of this work is on the dynamic techniques, in which a system is intentionally disturbed from equilibrium by excitation signals consisting of a wide variety of potential and current programs.

Within these broad categories, two principle classes may be distinguished, depending on whether current or voltage is the controlled parameter. The classes may then be further sub-divided by an operational nomenclature consisting of an independent-variable part followed by a dependent-variable part (i.e. volt-ammetry or chrono-potentiometry) with some system-specific modifiers (i.e. rotating disk voltammetry).[163] The family tree of electroanalytical techniques is summarized in Figure 1.7.

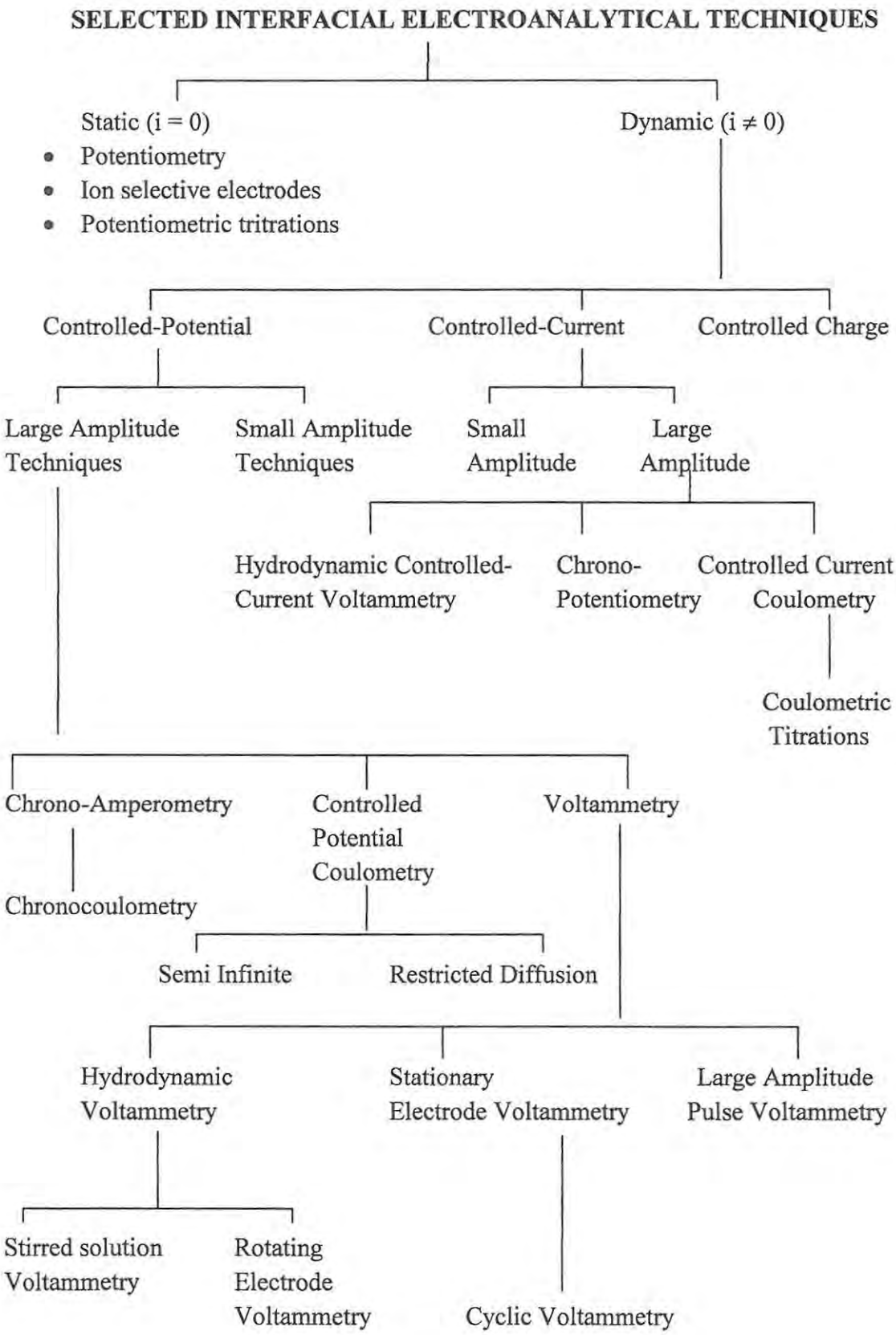

Figure 1.7 A family tree of related and important electrochemical techniques. (adapted from Kissenger P.T. *et al.*[163])

In the analytical screen, the following electrochemical techniques- voltammetry (i.e. direct-current, alternating current, fast-scan, pulse, square wave and stripping voltammetry at solid electrodes), coulometry (constant-current and –potential), potentiomteric titrations (including ion-specific electrodes) and amperometric titrations are the most commonly employed methods. Each of these electroanalytical techniques and their practical range of usefulness are presented in Figure 1.8.[163]

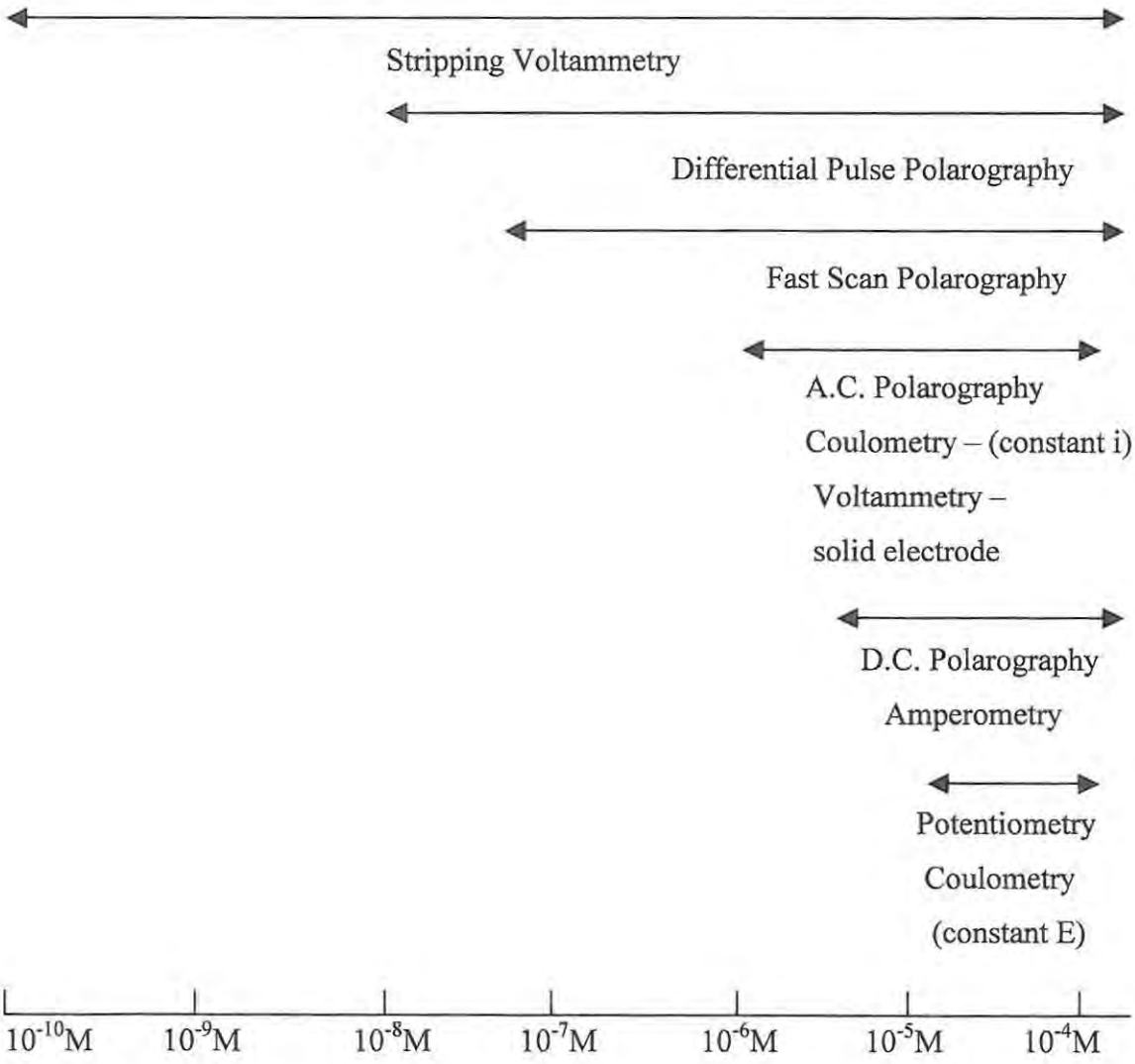

Figure 1.8 Detection range of commonly used electroanalytical techniques. (adapted from Kissenger P.T. *et al.*[163])

1.7.4 ELECTRODE REACTION:

The measurement of a species in solution using electroanalytical methods is as a result of either a spontaneous oxidation/reduction (redox) reaction between the species and the electrode, or a redox reaction induced by an applied potential, or the movement of charged ions. Redox reactions at the electrode surface resulting in electron transfer occurring are termed voltammetry (potential scan) or amperometry (constant potential) methods. When the movement of ions takes place to generate the electrochemical signal, the technique is known as potentiometry. In controlled potential techniques, for example, the role of the electrode is to monitor the current response, which is related to the concentration of the analyte. This is achieved by monitoring the transfer of electrons during the redox process:

$$O + ne^- \underset{k_r}{\overset{k_f}{\leftrightarrow}} R \qquad \textbf{Equation 1.1}$$

O refers to the oxidized species, e^- the electron and R the species in the reduced form on acceptance of the electron. The formal rate constants for the forward and reverse reactions are defined by k_f and k_r, respectively. In potentiometry the electrode responding to the analyte is termed an indicator electrode, whilst in voltammetry methods the electrode is referred to as the working electrode.[164]

The conversion of O to R by reduction results in a cathodic current, i_c. Oxidation of R to O results in an anodic current, i_a. The observed current resulting in a change of oxidation state is the faradaic current. The faradaic current is a direct measure of the rate of the

redox reaction. The resulting current potential plot is the voltammogram. For reversible systems, the net current, $i_{net} = 0$ and $k_f = k_r$. Systems such as these are controlled by the laws of thermodynamics, and the Nernst equation applies:[164]

$$E_{eq} = E^{\theta} + 2.303(RT/nF) \log C_0/C_R \qquad \text{Equation 1.2}$$

where E_{eq} = potential applied to cell, $E_{eq} = 0$ at equilibrium and E^{θ} is the standard potential for the redox reaction *vs* a standard hydrogen electrode. The R term is the universal gas constant (8.314 $J.K.mol^{-1}$), T is the temperature in Kelvin, n the number of electrons transferred in the reaction, F is the Faraday constant (96487 coulombs per mole of electrons). The C_0 and C_R terms are defined as the concentrations of O and R, respectively in mol cm^{-3}. The resulting current-potential plot, known as the voltammogram, is a display of current signal (vertical axis) *vs.* the applied potential (horizontal axis).

The overall rate of the reaction and the current observed is in general affected by the rates of mass transfer of reactant and product; electron transfer at the electrode surface; chemical reactions preceding or following electron transfer, and other surface reactions such as adsorption, desorption or electrodeposition. When any of these steps are rate limiting, the potential applied to the system will no longer be the same as the thermodynamically determined value at equilibrium. This is due to overpotential or overvoltage, the sum of the different overpotential terms associated with the different reaction steps.[166]

Overpotential is thus the difference between the equilibrium (reversible) potential of an electrode and the voltage which must be applied in order for current to flow. Alternatively, overpotential may be viewed as an activation barrier to the reaction. The total potential applied (V) is then given by:

$$V = -E + Ri + \eta \qquad \textbf{Equation 1.3}$$

Where E (V) is the reversible thermodynamic electromotive force (emf)

R (Ω) is the sum of ohmic resistance in the circuit

i (A) is the total current passed and

η (V) is the overpotential.

Ohmic resistances are introduced by voltage drops across the electrical leads, electrodes and electrolyte and may be reduced by improved conductivity of the electrolyte or reducing the distance between the electrodes.[165]

When the overall reaction rate is controlled solely by mass transport, a Nernstian response, obeying thermodynamic relationships, applies. Here k_f and k_r are sufficiently fast and are equivalent. Overpotentials due to mass transport can be simplified by controlling the contribution of convection and migration, so that diffusion is the limiting factor. The current response is thus a function of diffusion.[160] When mass transport is sufficiently fast the reaction may be limited by the reaction rate at the electrode, this then being the significant contribution to the observed overpotential. Hence $k_f \neq k_r$ and the current response is thus a function of the rate of electron transfer.[165]

1.7.5 THE ELECTROCHEMICAL CELL:

Electrode Choice:

The potential across a single electrode interface cannot be ascertained. A second electrode is thus employed, known as the reference electrode. The reference electrode is of constant potential, independent of the properties of the solution, with other potentials of the system being referred to in terms of a potential difference with respect to the chosen reference. Requirements of this electrode include a stable potential with respect to time and temperature and the potential should not be altered by small perturbations in the system, that is by the passage of a small current for example.[162,165,167]

The standard hydrogen electrode (SHE) is known as the primary reference. However, it is difficult to set up and maintain. The saturated calomel electrode (SCE) has since been introduced, but the silver | silver chloride (Ag | AgCl) electrode is by far the most commonly used reference electrode to date and consists of a silver wire anodised with silver chloride in a glass tube.[165,168] The wire is in direct contact with saturated or concentrated solutions of AgCl and either KCl or NaCl. The reference electrode is protected from the solution of analysis by a semi-permeable salt bridge.

At equilibrium the two-electrode system mentioned above is suitable for potentiometric measurements. Since there is no current passage between the electrodes, in this sense, the positioning of the electrodes relative to each other is not of importance. However, it should be noted that the larger the distance between electrodes the greater the electrical noise, which in turns leads to a lack of stable readings.

Despite the adequacy of the two electrode system, outside equilibrium conditions there is a passage of current between the two electrodes.[162] A three electrode approach is hence preferred since a major portion of the cell resistance is compensated for by the presence of an auxiliary (or sacrificial) electrode and a series of operational amplifiers and current loops. The auxiliary electrode is the current-carrying electrode and is placed in solution to complete the current path. Current flow has now been removed from the reference electrode which has been placed closer to the working or indicator electrode, causing a potential drop to be minimized and hence decrease the cell resistance.[160,162,163] The three electrode system is depicted in Figure 1.9.

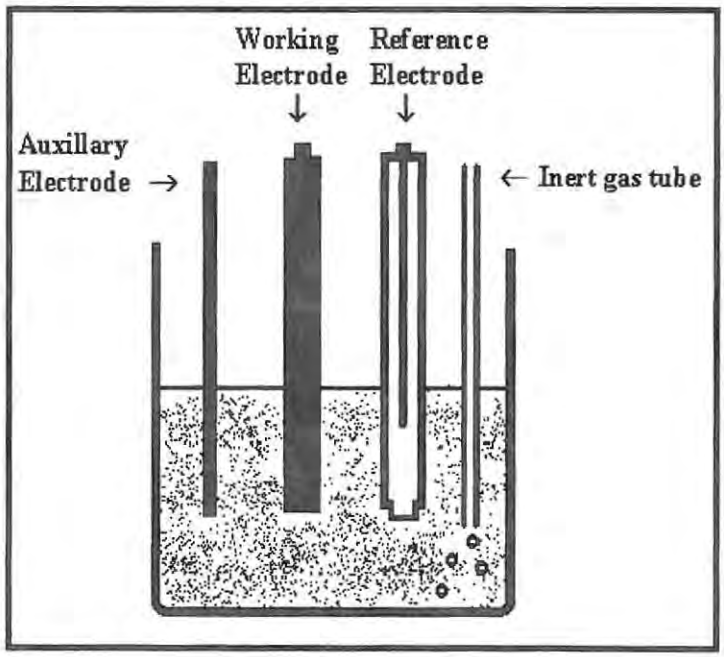

Figure 1.9 A simplified diagram of the three electrode electrochemical cell. (adapted from a text by J.Wang[160])

A suitable working or indicator electrode should provide high signal-to-noise ratio characteristics, as well as a reproducible response. Further requirements imposed on the working electrode are as follows: electrochemical inertness over a broad potential interval, high hydrogen and oxygen evolution over-voltage, low residual current (absence of pores and pronounced roughness of the surface), low ohmic resistance and the possibility of a sufficiently simple surface regeneration.

The most utilized working electrodes are those of metallic origin. Platinum, gold, mercury and carbon electrodes have been of most use, with carbon electrodes the material of choice for many electrochemical applications. Mercury electrodes have varied designs: static, the hanging mercury drop (HMDE), dropping (where the reaction is monitored at a new surface by releasing a fresh drop of mercury) or a mercury film on a support such as carbon. Benefits of the mercury drop electrodes, include a renewable electrode surface and a high cathodic potential window while the limited anodic range and toxicity are a disadvantage.

Among the most utilized of the solid carbon electrodes are carbon paste electrodes, pyrolytic graphite (ordinary or stress-annealed) and glassy carbon electrodes. Carbon paste electrodes are constructed by mixing graphite powder with a liquid, *e.g.* Nujol® into a glass tube. The other two electrodes are commercially available. Glassy carbon has excellent mechanical and electrical properties, a wide potential window and is chemically inert, exhibiting reproducible performance. Electron transfer rates at carbon electrodes are, however, slower than at metal electrodes. Electrode pre-treatment procedures can increase the electron-transfer rates.[160]

Present at carbon electrode surfaces, are surface confined species, hydroxyl and carboxyl groups, which are presumed to be involved in electrode processes. These surface functionalities provide a means of chemically modifying glassy carbon electrodes by binding redox active reagents at these sites thereby creating new electrode surfaces.[169]

At the electrode surface, the reactions are monitored via a range of electrochemical techniques. Briefly, electrochemistry, or rather voltammetry, comprises of a group of electrochemical procedures based on the potential-current behaviour of a polarizable electrode in a supporting electrolyte. Theoretically any species can be analysed if it undergoes oxidation or reduction within the working potential range of the electrode system employed. The redox reaction taking place at the electrode is therefore controlled by variation in the applied electrode potential.[170]

Solvents and Electrolytes:

Almost every electrochemical experiment is carried out in a medium consisting of a solvent and supporting electrolyte. The electrochemical reactions are thus unavoidably influenced by their nature. The solvent and electrolyte can affect an electrode process in a number of ways other than by reacting chemically with the electrolysis intermediates or products. The rate of heterogeneous electron transfer from the electrode to the electroactive substance can be affected by the structure of the electrical double layer at the electrode surface, which in turn is dependent upon the nature of the solvent and supporting electrolyte. The most common electrochemical effects exerted in the bulk solution are related to association (solvation, ion-pairing, complex formation, etc.) with the electroactive substance or electrochemically generated intermediates.[160,162]

The most important properties that the ideal solvent system ought to possess are: electrochemical inertness, high electrical conductivity, good solvent power, chemical inertness, availability in pure form or ease of purification, and low cost. The electrochemical inertness requires the solvent system not to undergo any electrochemical reaction over a wide range of potentials from very positive (strongly oxidizing) to very negative (strongly reducing). A high electrical conductivity is required in order to support passage of an electric current and the solvent system should exhibit low electrical resistance. Good solvent power implies the solvent must be able to dissolve a wide range of substances at acceptable concentrations. The chemical inertness property suggests that the solvent or electrolyte does not react with the electroactive material nor with its intermediates or products of the electrode reaction under investigation. Solvents and electrolytes should also be inexpensive, non-toxic and non-flammable; exhibiting a convenient liquid range.

1.8 VOLTAMMETRIC METHODS:

Voltammetric techniques are limited to easily reducible or oxidizable compounds and are most useful for low-level quantitation, having a wide linear dynamic range (in the order of 10^{-3} to 10^{-8}M). Voltammetry is defined as an electrolysis process that is limited by the mass transport rate at which molecules move from the body of the solution to the electrode. The current is followed as a function of the potential applied using a three-electrode cell of 1-50ml working volume. The working electrode is customarily a hanging mercury drop electrode (HMDE) or solid electrode. The latter is typically employed for anodic (oxidation) processes, utilising the any one of the following: a rotating platinum electrode

(RPE), a wax-impregnated graphite electrode (WIGE), a carbon paste (CPE) or a glassy carbon electrode (GCE).

The commonly used voltammetric methods are polarography (dc, fast-scan and differential pulse), linear sweep-, cyclic-, hydronamic-, differential pulse-, square-wave- and stripping voltammetry. The last mentioned technique involves a preconcentration step followed by a voltammetric measurement. The appeal of voltammetric methods, for the analysis of organic and pharmaceutical compounds, is attributed to its simplicity and rapidity. An extremely large number of organic compounds are either directly reducible at the DME or oxidizable at a solid electrode. The functional groups that show excellent voltammetric responses include the nitro, nitroso, quinone, azo, azoxy, azomethine, activated carbonyls and activated double bonds.

1.8.1 STRIPPING ANALYSIS:

The quantitation of trace and ultratrace components in complex samples of environmental, clinical or industrial origin represent an important task of modern analytical chemistry. In the analysis of such dilute samples, the employment of some type of preconcentration step, prior to actual quantitation, is required. The main objective of the preconcentration step is enrichment of the sample, however, the step may also serve to isolate the analyte from a complex matrix and hence result in improved selectivity and stability.

Electrolytic deposition represents an efficient method for the enrichment and isolation of trace components. Stripping analysis is the best-known analytical technique that incorporates an electrolytic preconcentration step. The technique couples the advantages

of extremely low detection limits (~10^{-10} - 10^{-11} mol dm^{-3}), multi-element and speciation capabilities, suitability for on-line and *in situ* measurements and a low cost factor.[160,162]

Stripping techniques involve two discrete steps: a preconcentration step and a stripping step. In the preconcentration step, the target analyte is accumulated onto or into the working electrode. In the stripping step, the accumulated material is oxidized or reduced back into the solution. The response recorded during this step, is proportional to the concentration of that analyte in or on the electrode, and thus, in the sample solution. There are different versions of stripping analysis, each dependent upon the nature of its preconcentration and stripping steps, which include: Anodic Stripping Voltammetry (ASV), Potentiometric Stripping Analysis (PSA), Cathodic Stripping Voltammetry (CSV) and Adsorptive Stripping Voltammetry (AdSV).[171] A detailed discussion of the relevant stripping techniques used will follow:

Anodic Stripping Voltammetry:

ASV (linear sweep form) is the most common version of stripping analysis. The preconcentration step involves the reduction of a metal ion to the metal, which usually dissolves in mercury, resulting in amalgam formation.

$$M^{n+} + Hg + ne^- \rightarrow M(Hg) \qquad \textbf{Equation 1.4}$$

Preconcentration (or deposition) is followed by a positive-going potential scan to cause re-oxidation of the species in the amalgam:

$$M(Hg) \rightarrow M^{n+} + Hg + ne^- \qquad \textbf{Equation 1.5}$$

The amalgamated metals are thus stripped out of the electrode in an order that is a function of each individual metal's standard potential, giving rise to measurable anodic peak currents. For the deposition step, the working electrode is maintained at a potential cathodic (by at least 0.4V) of the standard potential of the least easily reducible ion to be determined in solution. Forced convection (via rotation, stirring or flow) is usually used to facilitate the deposition step. The deposition time required is dependent on the sample concentration, with 1 to 10 minute periods typically sufficing for measurements in the range of 10^{-7}M to 10^{-9}M. All experimental parameters are required to be reproducible because only a small fraction of the metal ion is deposited during each measurement.

Figure 1.10 displays the potential-time sequence used in ASV. The concentration of the metal in the mercury electrode after a given preconcentration period is given by Faraday's law:

$$C_{Hg} = \frac{i_l\, t_d}{nFV_{Hg}} \qquad \textbf{Equation 1.6}$$

where I_l is the limiting current for the deposition of the metal, t_d the deposition period and V_{Hg} the volume of the mercury electrode. However, in practice the preconcentration period results in a nonuniform (parabolic) distribution of the metal concentration within the mercury electrode. The preconcentration step is hence followed by a rest period of at least ten seconds, after the forced convection is stopped, to establish a uniformed concentration

within the mercury; ensuring that the stripping step is performed under quiescent conditions.

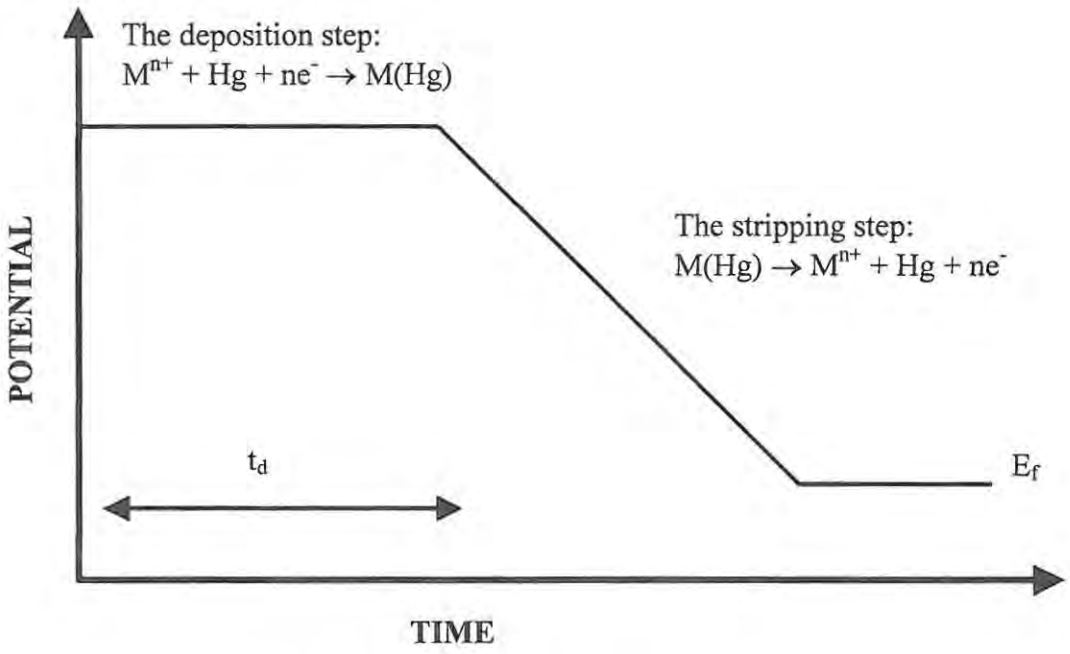

Figure 1.10 The potential-time sequence in ASV.

Cathodic Stripping Voltammetry:

Cathodic stripping voltammetry (CSV) may be viewed as the "mirror image" of ASV and involves anodic (oxidative) deposition of an insoluble film of material on the electrode; which is subsequently stripped off during a negative-going potential sweep. Most CSV applications rely on the anodic accumulation of sparingly soluble mercury compounds on a mercury surface:

$$A^{n-} + Hg \underset{\text{Stripping}}{\overset{\text{Deposition}}{\rightleftharpoons}} HgA + ne^- \qquad \textbf{Equation 1.7}$$

CSV is best suited for the determination of inorganic anions (*e.g.* halides, cyanide) or organic sulphur compounds (*e.g.* penicillins, thiols) that form insoluble salts with the electrode material. In addition to mercury, silver electrodes may be advantageous for the determination of anions that form insoluble silver salts.

Adsorptive Cathodic Stripping Voltammetry (AdCSV):

Adsorptive stripping analysis greatly enhances the scope of stripping measurements toward numerous trace elements. The strategy is relatively new and involves the formation, adsorptive accumulation and reduction of a surface active complex of the metal. A negative-going potential scan or a constant cathodic current can be employed for measuring the adsorbed complex.

Reduction of the metal species in the adsorbed complex is most common, however, the possibility of reduction of the ligand may also be exploited.[160] Redox speciation may also be obtained from the adsorptive stripping voltammetry experiments, since any oxidation state can be accumulated unlike the metallic state in the case of anodic stripping voltammetry.[171] The AdCSV process is illustrated in Figure 1.11 and the stripping step is depicted in the square wave potential scan format.

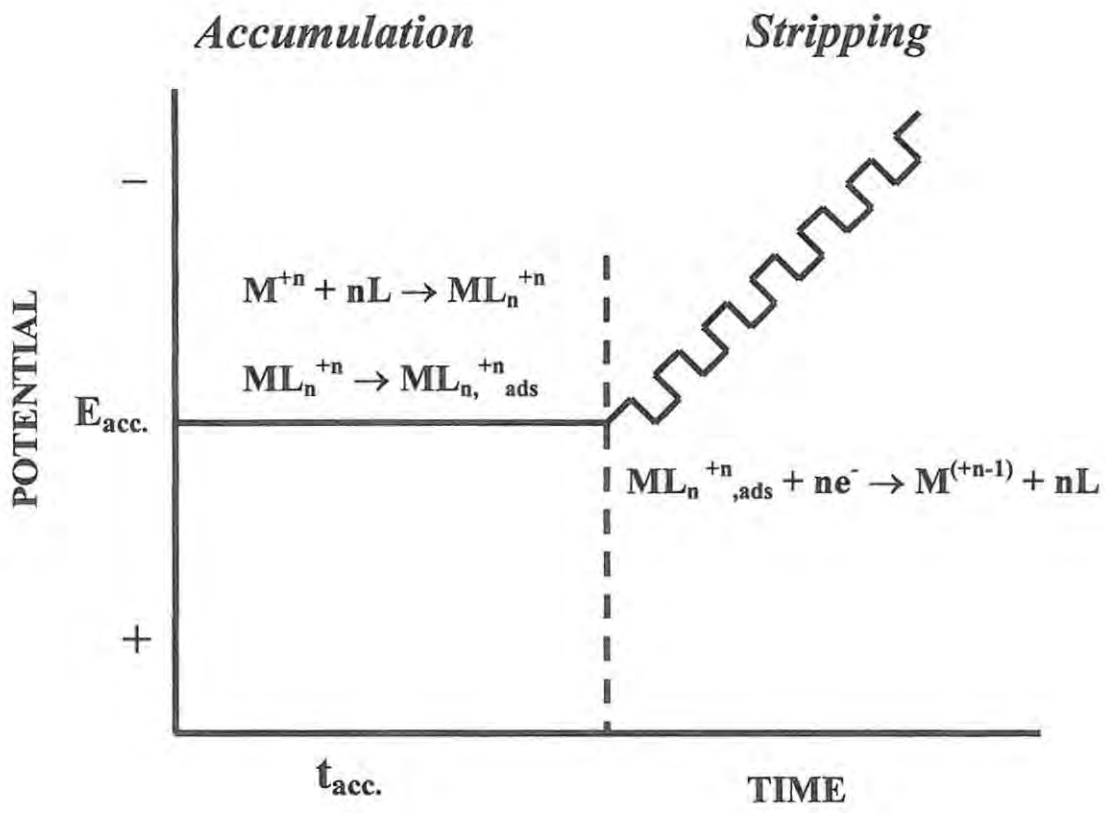

Figure 1.11 The accumulation and stripping steps in the adsorptive cathodic stripping measurements of a metal ion (M^{+n}) in the presence of a ligand (L). (From: 'Analytical Electrochemistry', by Wang J.[160])

The selectivity of the chemical step (complex formation) can be used to increase the overall selectivity of the analysis. A ligand capable of binding only a few metals should make possible the formulation of a highly selective scheme, whilst controlled adsorptive accumulation at stationery electrodes permits substantial enhancements of the electrode surface concentration of the complex.

Apart from extending the scope of stripping voltammetry, the metal complex adsorption approach offers alternative, and often improved, schemes for measuring 'difficult' metals. The term "difficult' metals refers to the group of metals that have extreme redox potentials, may form inter-metallic compounds or that suffer from poor selectivity.[162,172] A need to develop ligands that may increase the sensitivity and selectivity of metal ion determination has been expressed.[172] Ligands such as catechol and oxine have been documented for the detection of a wide range of metal ions including copper, iron, molybdenum, uranium and tin.[160,172]

Square Wave Stripping Voltammetry:

Square wave voltammetry was invented in 1952 by Barker, but little use was made of this technique at the time owing to difficulties with the controlling electronics. Advances in instrumentation has allowed this technique to become an important tool in analysis.[31] Square wave voltammetry is defined as a large-amplitude differential technique in which a wave form composed of a symmetrical square wave, superimposed on a base staircase potential, is applied to the electrode.[160,173]

A variety of square wave forms exist and this has lead to a fair amount of confusion, since the wave forms employed have simply been described as square waves. There are in fact three main types of square wave formats namely: Barker, Kalousek and Osteryoung employed in square wave voltammetry.

The Barker format is the simplest to visualise since the wave form is a direct analog to the sinusoidal ac voltammetry form. The format employs a symmetric square wave of

frequency 'f' and amplitude 'dE' riding on either a ramp or slow staircase wave form. Barker square wave methods are characteristically employed in conjunction with mercury drop electrodes and multiple cycles of this type of square wave is applied to each drop of mercury.

The Kalousek method is characteristically employed in square wave polarography and is termed the Kalousek Type III. Kalousek formats employ a lower frequency method, which measures the current only on the reverse half wave cycle of the square wave. Extreme sensitivity to the electrochemical reversibility of the couple and the chemical stability of the product of the forward step are known characteristics of the Kalousek Type III form.[174]

The most common form of square wave today was first proposed by Ramaley and Krause, however, this form is most closely associated with the Osteryoungs as a result of their many publications in this field.[175,176] The Osteryoung wave form, as it is now termed, differs from the other two formats in that the base potential (potential of the staircase) increases by 'dE' for each full cycle of the square wave whose half height is 'E_{sw}' and whose period is 'τ'. The Osteryoung wave format may be applied to stationery, as well as drop electrodes.[177]

The general response obtained from square wave formats is the difference between the current sampled at the end of the forward pulse and the current sampled at the end of the reverse pulse within a given wave form cycle. The diagrammatic representation of the square wave voltammetry technique is illustrated in Figure 1.12.

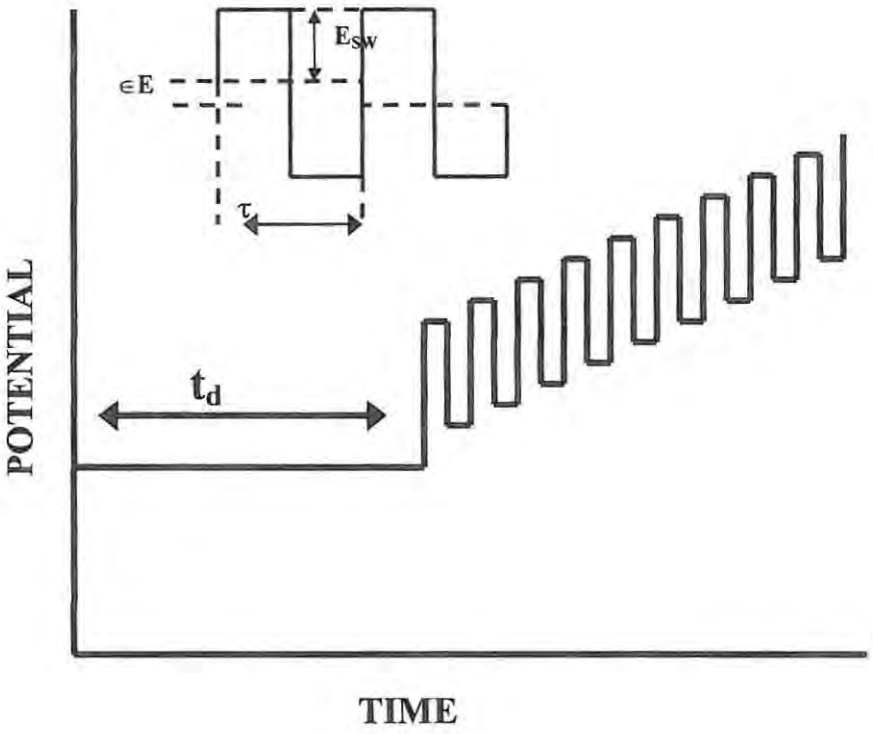

Figure 1.12 Excitation signal for square wave potential scan voltammetry. (Adapted from: 'Analytical Electrochemistry', by Wang J.[160])

Advantages of the square wave technique include: enhanced sensitivity over linear sweep potential scan forms, greater speed in analysis and reduced problems with the blocking of the electrode surface compared to the differential pulsed techniques.[162]

Osteryoung square wave potential scan stripping voltammetry in this work was employed for metal analysis and metal ligand interactions. However, unless otherwise stated, the linear sweep form was utilised in anodic and cathodic stripping voltammetry methods.

1.9 COMPUTER MODELING, NUCLEAR MAGNETIC RESONANCE AND INFRARED SPECTROSCOPY AS ALTERNATE TECHNIQUES FOR METAL LIGAND INTERATIONS STUDIES:

1.9.1 COMPUTER MODELING:

Advances in computing, in particular the ready availability of high-resolution graphics, have greatly increased the interest in computer-based molecular modeling. Molecular modeling is now widely used as an aid in the interpretation of experimental results and in the design of new materials including the study of the interaction of metal ions with biological substrates. The fundamental assumption underlying the molecular mechanics method, is that the positions of the atoms of a molecule, ion, solvate or crystal lattice are determined by forces between pairs of atoms, (bonds, van der Waals interactions, hydrogen bonding and electrostatic interactions) and between groups of three (valence angles) and groups of four (torsional angles, planes) atoms.[178]

Two types of information are obtained from any molecular mechanics experiment: the minimum value of the strain energy and the structure associated with that minimum. However, the modeling of large biomolecules, and their interactions with metals, is fraught with difficulties. The major problem arises from the flexibility of the molecules, resulting in a manifold of adopted conformational geometries.

However, despite the difficulties with biological models, when no unequivocal determination of a structure is available by experimental methods, then structure prediction may be the only means of obtaining a three-dimensional model of the molecule. In metal-macromolecule adducts this is often the case and structures obtained by molecular modeling can be a genuine aid in the visualization of these interactions.[178]

The computational study aims at a graphical representation of the molecule with a minimized energy configuration. Full-scale molecular modeling of melatonin and serotonin as well as their respective metal complexes was not attempted. A visual picture of the energy minimized metal-melatonin/serotonin complex and the type of metal co-ordination to the ligand was obtained. This research thus contains the first known visual images of a metal-melatonin or serotonin complex.

1.9.2 NUCLEAR MAGNETIC RESONANCE SPECTROSCOPY:

Nuclear magnetic resonance (NMR) spectroscopy over the past few decades has become a very powerful tool for the organic chemist and additionally revolutionized the study of natural products. The careful choice of one- and two- dimensional experiments has efficiently elucidated the structure of several complex biological molecules. However, the technique is only applicable to those nuclei which possess a spin quantum number, *I*, greater than zero. The most important of such nuclei are the ^{1}H and ^{13}C nuclei, although, ^{31}P and ^{14}N have become increasingly important as more biological-type experiments are being performed.[179,180]

The basis of the NMR experiment is to subject the nuclei to radiation, which will result in a transition from the lower energy state to a higher level. The precise difference in energy levels between the two spin orientations is dependent on the particular location of the atom of the molecule, since each nucleus is affected by the differing effects of the magnetic fields of neighboring nuclei. Only nuclei, which are in exactly, the same magnetic environment will have exactly the same energy difference between spin orientations, when placed in a magnetic field. In NMR spectroscopy these differences in energy are detected and provide information on the variety of locations of the nuclei in the molecule.[179]

By convention, frequency, and therefore magnetic field strength, increase from left to right in the NMR spectrum. Tracing the spectrum from left to right is referred to as moving upfield, whilst moving from right to left is a downfield shift. Upfield absorptions are said to be more shielded and the downfield absorptions are the result of deshielding. The position of an absorption peak in the NMR spectrum may be represented either on a frequency scale (Hz), or on the scale of magnetic field (tesla) and by convention the frequency scale is used. However, in order to make direct and rapid comparisons between spectra recorded on instruments operating at different frequencies, the positions of absorptions are normally quoted on the σ scale, which is independent of the instrument operating frequency. The σ value is obtained by dividing the position in Hz by the instrument frequency (in MHz) and is expressed in parts per million (ppm).[180]

The study of molecular structure, conformational changes, interactions of biological molecules with various substrates and certain types of kinetic investigations, are the primary uses of NMR in the biological field. The studies are carried out in solution and at present there appears to be an upper molecular mass limitation of 20 000 Daltons in the

study of biological macromolecules. The major reason for the limitation is the large number of protons in similar structural environments, resulting in numerous absorption peaks in a similar region.[181]

NMR spectroscopy is a non-destructive technique and structural determinations may be carried out on less than 1 mg of sample. Developments in the field of NMR spectroscopy over the last two decades have completely altered the approach towards structural elucidation. The applications of this technique are numerous and advantageous, especially when studying interactions of biologically active molecules and metals.

The one-dimensional (1D) experiment involves the excitation of a single type of nucleus, ^{1}H and ^{13}C being the most common. However, despite the complexity of the ^{1}H NMR spectrum, a great deal of preliminary information may still be obtained. Two-dimensional (2D) experiments are more efficient for the simultaneous determination of a large number of spin correlations. All 2D experiments involve the use of a multiple pulse sequence containing a variable delay t, between pulses in which free induction decays $S(t_2)$ are measured for an evenly spaced series of values of t_1 to build up a matrix of data $S(t_1.t_2)$. The most commonly used 2D experiment is ^{1}H-^{1}H homonuclear shift correlated spectroscopy (COSY), which is frequently used for polysaccharide determination.

In the COSY experiment the basic pulse sequence involves the application of a 90° pulse to the sample, followed by a delay period (t_1), during which the spin system evolves as it would in a normal free induction decay. A second 90° pulse, the mixing pulse, interrupts the evolution, followed by a second time period t_2, which allows the evolution of the spin system resulting in a detected and recorded free induction decay signal.[152,180] Double

Fourier transformation results in two 1D spectra, which can be plotted at right angles to each other resulting in a COSY contour plot. The diagonal of this plot represents the 1D spectrum.[180,181]

The aim of the NMR experiments in this study is to obtain a defined structure of melatonin and serotonin and to substantiate any electrochemical data obtained for the metal-melatonin or serotonin interactions.

1.9.3 INFRARED SPECTROSCOPY:

Infrared (IR) spectroscopy can be described as the use of instrumentation in measuring a physical property of matter, and the relating of the data to chemical composition. The instruments used are called infrared spectrophotometers, and the physical property measured is the ability of matter to absorb, transmit, or reflect infrared radiation.

Infrared spectroscopy is a non-destructive type of analysis (the sample can normally be recovered for other use), and is useful for microsamples.[182] The region of infrared spectrum which is of greatest importance to the organic chemist is that which lies between 4000 and 660 cm^{-1}. Metal complexes may be studied in the lower region of the spectrum. Absorption bands in the spectrum result from energy changes arising as a consequence of molecular vibrations of the bond *stretching* and *bending* (*deformation*) type. The positions of atoms in the molecule may be viewed as the mean equilibrium positions of atoms in molecules, whilst the bonds between atoms are analogous of springs, subject to stretching and bending.

Hydrogen or carbon bonded to oxygen or nitrogen, for example, give rise to strong infrared absorption patterns because of the polarity of these particular bonds. In contrast, no absorption results from stretching vibrations in a homonuclear double or triple bond which is symmetrically substituted; such vibrations are termed *infrared inactive*. The recognition of such bonds is possible by an examination of the Raman spectra of these molecules.[89,180]

Infrared spectroscopy is thus used in this research to further investigate metal-ligand interactions, in particular metal-melatonin, -serotonin or -acetylcholine complexes.

1.10 OVERALL RESEARCH AIMS:

The toxicity of the heavy metals and fact that the brain itself, concentrates metals better than any other tissue in the body, but cannot function adequately without optimum levels of certain metals,[87] has prompted research into the possible regulatory role of melatonin and its precursor serotonin. An earlier electrochemical study in our laboratory has shown that melatonin binds, cadmium, copper(II), iron(III), lead and zinc in a concentration dependent manner in pH 4.4 buffered solutions.[131] Melatonin, serotonin and trytophan have also been shown to exhibit an affinity for aluminium, but could not be compared with the other metals studied, as the reaction was completed under non-aqueous conditions.[131] However, to date very few publications have been cited utilising electrochemical methods to study metal-ligand interactions with neural substrates.

The first part of this study thus aims to electrochemically detect any possible interactions of melatonin and serotonin with metals that are essential for normal neuronal transmission *i.e.* sodium, potassium and calcium. The effects of lithium and aluminium, under pH 7,

were also investigated as a further route for melatonin's metalloregulatory ability and to provide possible insight into the link between serotonin levels and lithium treatment in depression.

Along similar lines, the interaction of acetylcholine with the heavy metals mercury, lead and cadmium, as well as the biologically important zinc and copper ions were investigated. Depletion of acetylcholine levels has been implicated in a number of neurodegenerative disorders, whilst concerns about the effects of mercury from tooth amalgams have also been voiced.[84,46,105] The aim of this section of the study was to explore the option that levels of acetylcholine may be directly linked to complex formation between this neurotransmitter and potentially toxic heavy metals, cadmium, lead and mercury, or quintessentially toxic metals in the body: *viz.* copper and zinc.

An *in vivo* study was then performed on an animal model to assay metal levels in pinealectomised rats of the Wistar strain. The pinealectomised animals have lost the chief melatonin and serotonin producing organelle and the nature of this procedure was to analyse the pineal indoleamines regulatory ability towards metals levels in the brain. After surgery and sufficient recovery time, the brain was then divided into three major regions, namely cerebellum, cortex and striatum. The metal levels of each region was assessed with the aim of ascertaining which region accumulated the most metal toxicity in the absence of a possible metalloregulatory system.

The following chapter of this study aimed for clarity on the aluminium link to aged-related neurodegenerative damage as well as any possible protective effects melatonin may posses in counteracting such effects. The chosen animal model, male rats of the Wistar strain,

where subcutaneously injected daily for a fairly lengthy period of time with a dose of aluminium or a combination of aluminium and melatonin, after which the animals were sacrificed. Histological and electrochemical methods were employed to examine the extend of, and melatonin's possible protective nature against, aluminium toxicity.

A preliminary study in calcium ion sensing was also undertaken. The aims of the work included the production of a calcium selective microelectrode for insertion into a cell and the application of the probe to measure Ca^{2+} levels within a specific brain region. The importance of which can be noted from the role of calcium in excitotoxicity and neuronal damage, as discussed in Section 1.5.1.

CHAPTER 2

Pineal Indoleamine Metal-Ligand Interactions

2.1 INTRODUCTION:

Melatonin, the chief product of the pineal gland,[183] and its precursor serotonin, the "mood molecule",[184] have been shown to interact with a number of metal ions either by altering their actions or by altering their conductance through biological membranes. Such interactions have been shown to have possible biological significance, particularly with reference to melatonin's ability to protect against tissue damage.[185] Furthermore, decreases in melatonin levels may be a factor in the increasing oxidative damage observed in the elderly.[186]

The resting potential in neurons is dependent upon the ratio of the concentration of the potassium inside and outside the cell, whilst the action potential is dependent upon the ratio of the concentration of intracellular and extracellular sodium. In other tissues, melatonin stimulates a voltage-dependant sodium selective current in lens epithelial cells and trabecular meshwork cells and also enhances activation and inactivation kinetics.

***This work has been published and hence is not referenced in this chapter: Lack B, Daya S and Nyokong T, Interaction of serotonin and melatonin with sodium, potassium, calcium lithium and aluminium, J. Pineal Research (2001) 31:102-108.**

It also specifically stimulates tetrodotoxin insensitive voltage-dependent sodium current by a novel mechanism.[187] Whether this is accomplished by direct interaction with the metal or by altering transport of the metal is not known. Potassium ion channels and guanylyl cyclases have also been reported to be modulated by melatonin.[188]

Melatonin has been shown to play a role in regulation of potassium, sodium and chloride in the common dentex, *Dentex dentex*.[189] The hormone also inhibits the activity of large conductance calcium-activated potassium channels,[190] suggesting that melatonin inhibits endothelial potassium channels to decrease flow-induced release of nitric oxide and blocks smooth muscle potassium channels to enhance vascular tone.

That melatonin also plays a role in insulin regulation through ion regulation, is evident in a study which demonstrates that insulin response to glucose (specific) or KCl (non-specific) is significantly and reversibly reduced when the islets are treated with melatonin. Serotonin on the other hand, considerably enhances both glucose and KCl stimulated insulin release.[191] Melatonin has further been linked to reducing the quinolinic acid-induced damage of hippocampal neurons,[192] a mechanism presumed to be due to prevention of calcium overload. Zhang and Zhang (1999) have recently shown that melatonin inhibits neuronal calcium overload in mouse brain cells.[193] The actions of serotonin also appear to modulate both calcium[194] and potassium currents.[195]

Lithium chloride, an important therapeutic agent used in the treatment of mania, causes a reduction in plasma, pineal and ocular melatonin in quail and hamster models [196] as well as altering the melatonin acrophase in chick pineal glands.[197] Aluminium, an agent postulated to have a role in the aetiology of Alzheimer's disease, has previously been

shown to form complexes with melatonin and it's precursors.[198] In the present study, we describe the interaction of melatonin and serotonin with sodium, potassium, calcium, lithium and aluminium, in aqueous media and under biological pH conditions, using adsorptive cathodic stripping voltammetry (AdCSV) methods.

The first step in AdCSV is the formation of a metal-ligand complex (in this study: metal-serotonin and metal-melatonin) during the purging step, followed by the controlled interfacial accumulation of the complex formed onto the electrode during the deposition (or pre-concentration) step at a fixed optimum deposition potential and time. The reduction of the adsorbed metal complex by application of a potential in the negative direction occurs during the stripping step, as discussed in Section 1.8.1 under adsorptive cathodic stripping voltammetry and summarised in the following equations:

$$M^{+n} + nL \rightarrow ML_n^{+n} \qquad \textbf{Equation 2.1}$$

$$ML_n^{+n} \rightarrow ML_n^{+n}{}_{,ads} \qquad \textbf{Equation 2.2}$$

$$ML_n^{+n}{}_{,ads} + xe^- \rightarrow M^{+n-x} + nL \qquad \textbf{Equation 2.3}$$

Where L = ligand and M = metal. Equation 2.3 applies in cases where reduction occurs at the metal. Reduction may also occur at the ligand. The ligand must be able to bind the metal freely in solution, and the resulting metal-ligand complex must adsorb onto the electrode. The ligand must also freely release the metal back into solution during the stripping step. The extent of the increase in current response of the metal ion on addition of the ligand is an indication of the affinity of the ligand for the metal. The extent of shift in the reduction potential for the metal ion after the formation of the metal-ligand complex has been equated to a measure of the stability of the complex.[172,199-202]

2.2 EXPERIMENTAL:

2.2.1 REAGENTS:

All reagents were of analytical grade and hence no further purification steps were employed. Triply distilled deionised water was used for all experiments. Solutions of Na^+, K^+, Ca^{2+}, Li^+ and Al^{3+} were prepared from the corresponding metal chloride salts obtained from SAARCHEM-HOLPRO Analytical (South Africa). Serotonin (creatine sulphate complex, Aldrich) and melatonin (Aldrich) solutions were prepared daily; serotonin was dissolved in distilled water, whilst melatonin was dissolved in absolute ethanol and subsequently diluted with distilled water. The final ethanol concentration in the solution was 0.2% (v/v). The nitrogen purge gas used for the electrochemical experiments was obtained from MEDGAS® and purified by being passed through a drierite self-indicating mesh (anhydrous $CaSO_4$), purchased from SAARCHEM. A solution of 0.05 mol dm^{-3} tetrabutylammoniumbromide (TBABr, Aldrich) was used as the chosen electrolyte. In the NMR and IR research conducted, the analytically pure deuterated dimethylsulphoxide (DMSO(D6)) and potassium bromide (KBr) were purchased from Aldrich.

2.2.2 APPARATUS:

Stripping voltammograms, on the linear sweep scan mode, were obtained with the BioAnalytical Services (BAS, Lafayette, Indiana, USA) CV-50W voltammetric analyser. A Controlled Growth Mercury Electrode (CGME, BAS Model MF-9058) was employed as the working electrode. A silver | silver chloride (3mol dm^{-3} KCl) and a platinum wire were

employed as the reference and auxiliary electrodes, respectively. The Viritis Freezemobile 6 was used for the freeze-drying process.

Infrared spectra were recorded with the computer interfaced Perkin Elmer Spectrum 2000 Fourier transformed spectrophotometer, utilising the KBr pressed disc technique. Nuclear Magnetic Resonance (^{1}HNMR, ^{13}CNMR and various 2D spectra) data was recorded on the Bruker AMX 400 MHz pulsed Fourier transformed NMR spectrometer. All samples were contained in stoppered analytical grade 5mm tubes throughout. The computer modeling technique was employed to obtain a visual picture of the complexes. Cerius^{2} version 4.5 software, on an O_2 Silicon Graphics machine, was run for all modeling experiments.

2.2.3 METHOD:

Clean glassware is essential for the analytical techniques. In all experiments performed in this and ensuing chapters, the glassware was washed in detergent and rinsed several times before being soaked in nitric acid for at least 24 hours. Before use, the acid washed items were further rinsed several times in triply distilled deionised water.

Electrochemical Techniques:

TBABr and appropriate concentrations of the metal ions and of the ligand (either serotonin or melatonin) were introduced into an undivided electrochemical cell to achieve a total cell volume of 15ml. The use of TBABr as an electrolyte allowed potential scans over a broad negative potential scanning window; particularly suitable for the metals studied in this experiment. The solution was then stirred and deaerated with nitrogen gas for a minimum

period of 5 min, after which a constant flow of nitrogen was maintained over the solution throughout the measurement. The metal-ligand complex is expected to have formed at this stage. An optimum deposition potential was then applied for a given period of time. The adsorption of the metal-ligand complex onto the electrode occurs at this stage.

The voltammograms were recorded in a negative direction from the accumulation potential to at least 0.2 V beyond the reduction peak of the metal complex. An optimum scan rate of 25 mV sec^{-1} was applied. During the stripping step the current response, due to the reduction of the metal complexes of melatonin or serotonin, was measured as a function of potential. AdCSV experiments were also performed for the metal ion in the absence of the ligand or for the ligand in the absence of the metal ion. The concentrations of serotonin and melatonin were varied from 1.0×10^{-8} mol dm^{-3} to 5.0×10^{-8} mol dm^{-3}, whilst the metal ion concentrations ranged from 1.0×10^{-9} mol dm^{-3} to 1.0×10^{-8} mol dm^{-3}.

Spectroscopic Techniques and Computer Modeling:

Attempts to prepare crystalline metal-ligand complexes were unsuccessful, hence the freeze-dried powder form was used for the spectroscopic studies (as discussed below). In solid infrared analysis, the pressed disc technique was applied. Pure, dry KBr was intimately ground with a known weight of sample, using an agate mortar and pestle. The mixture was then added to a manually-operated press system for the preparation of a KBr disc. The possibility of impurities in the KBr was eliminated with the use of a blank disc system.

Care should, however, be taken to ensure both discs prepared are of equal thickness, otherwise inverse peaks may occur if the potassium bromide is damp or impure and this will be particularly noticeable if the reference disc is thicker than the sample disc.[180] Dry, analytical grade KBr is crucial to the IR experiment The dried potassium bromide was prepared by placing the KBr in a shallow dish in an oven, at 120 °C, for at least 24 hours. After sufficient drying time had passed, the KBr was stored in an oven at ~ 100 °C.

Providing care has been taken in disc preparation, the final product should be slightly opaque, due to the presence of the sample (the blank disc should be transparent). Should the disc show a number of white spots, these would be a result of the mixture being unevenly ground. If the disc shows a tendency to flake, then excessive grinding of the powder is indicated. A disc changing to a cloudy colouring is indicative of water uptake by the disc and should be avoided.[180,182]

The solid sample complexes, formed between the metal ion and serotonin or melatonin, were prepared by mixing solutions of the ligands (1.0×10^{-3} mol dm^{-3}) with an excess of the metal ions (1.0×10^{-2} mol dm^{-3}) and freeze-drying the solution for an average of 24 hrs or until a powdery solid was formed. The infrared (IR) spectra of these complexes were then recorded and compared with the IR spectra of freeze-dried serotonin or melatonin alone.

All NMR samples were prepared using deuterated DMSO. Equimolar concentrations of the metal ion and serotonin or melatonin were weighed out into the NMR tubes and dissolved in the deuterated solvent. The lowest concentration required to obtain a suitable proton or carbon NMR and COSY spectrum was 20 mg ml^{-1} of the ligand substrate in

deuterated solvent. The spectra obtained were then compared to those of the ligand alone in the deuterated DMSO.

In the computer modeling experiments, pre-drawn serotonin and melatonin structures were subjected to molecular mechanics dynamic simulation runs. In these experiments a universal force field was applied in an attempt to find the global minimum energy conformation of the structure. Atomic charges of the molecules were calculated using the charge equilibrium package and the registered Hyperchem® software package provided the vehicle for further viewing of the molecule in the space-filled form. Proposed metal-ligand interaction sites were postulated for lithium and serotonin or melatonin based upon the HASB theory, Section 1.5.2, and the calculated electronic charge on the minimized ligand conformation.

2.3 RESULTS:

Electrochemical Study:

The purging time, deposition potential and deposition time were optimised for the adsorptive cathodic stripping voltammograms of each metal-ligand complex. The experiments were performed by keeping all other variables constant and only altering the parameter being optimised. As an example, Figure 2.1 (A) and (B) show the parameter optimums for the deposition potential and deposition time of the potassium-serotonin complex respectively. Optimisation of parameters was completed for serotonin in the presence of all the metal complexes investigated and then applied to the melatonin study.

The highest current response observed was used as the measure in ascertaining the optimum value of the parameter. The optimum deposition potentials were -1200 mV for Al^{3+} and Li^{+}, whilst -1400 mV for Na^{+}, Ca^{2+} and K^{+} were employed to affect the adsorption of the metal-ligand complex onto the electrode. A deposition time of 120 seconds was chosen to accommodate all metals studied. The purging time was set for 5 min. to achieve the metal-ligand complex formation.

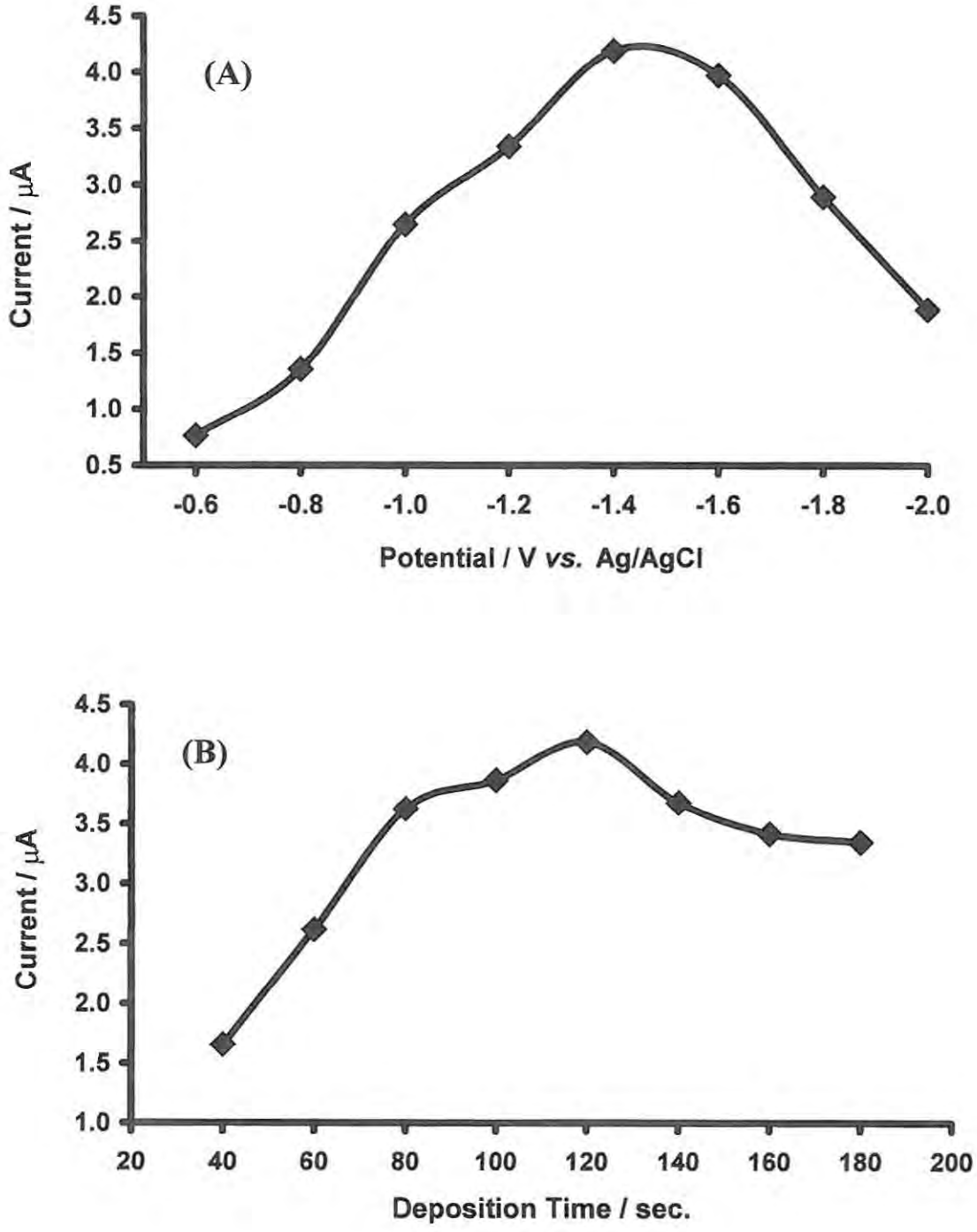

Figure 2.1 **Optimisation of (A) deposition potential and (B) deposition time for the potassium-serotonin complex. [Potassium] = 3.3 x 10^{-9} mol dm^{-3} and [Serotonin] = 6.7 x 10^{-8} mol dm^{-3}, respectively.**

Adsorptive cathodic stripping voltammograms of Na^+, K^+, Li^+, Ca^{2+} and Al^{3+} in the presence of serotonin are shown in Figure 2.2 (A-E) respectively. The AdCSV peaks of the metals in the absence of serotonin are observed at -2.20, -2.18, -2.23, -2.29 and -2.29 V *vs.* Ag | AgCl, for Na^+, K^+, Li^+, Ca^{2+} and Al^{3+}, respectively. Addition of serotonin to solutions of the metal ions resulted in the shifting of the reduction peaks of the metals to more negative potentials for Al^{3+}, Li^+, K^+ and Na^+. A positive potential shift was observed for the interaction of serotonin with Ca^{2+}, Table 2.1.

An enhancement in the reduction currents was observed for all the metals in the presence of serotonin. Addition of melatonin to solutions of the metal ions also resulted in the enhancement of the reduction currents of the metal peaks, Figure 2.3 (A-E). Shifts to more negative potentials were observed for the formation of metal-melatonin complex, for all the metals under consideration.

Electrochemistry of serotonin and melatonin in the absence of metals has been investigated. Zoulis *et al.* (1990) described the use of stripping voltammetry methods to study serotonin, melatonin and tryptophan.[200] Also Radi and Bekhiet (1998) used voltammetric methods to study melatonin on carbon electrodes.[203] The reduction peak for serotonin in the absence of metal ions was observed in this work at -1.76 V *vs.* Ag | AgCl. For melatonin, the AdCSV peak in the absence of metal ions was observed at -2.18 V *vs.* Ag | AgCl. In order to confirm that the peaks in Figure 2.2 (A-E) and 2.3 (A-E) are due to the reduction of the metal centre, the peaks were spiked with a known amount of metal ion and an enhancement in peak current was observed. On addition of serotonin or melatonin, no enhancement of these peaks was noted.

Table 2.1 AdCSV parameters for the metal-serotonin or metal-melatonin complexes:

[a]Metal	[b]E_P (mV) *vs.* Ag/AgCl[a]	ΔEp (mV)	[c]Slope (A/mol dm^{-3})
Serotonin	-1760		
Sodium	-2246	-40	1.97 (0.995)
Potassium	-2254	-77	1.04 (0.985)
Calcium	-2266	+27	0.88 (0.991)
Lithium	-2348	-123	0.59 (0.967)
Aluminium	-2360	-71	0.81 (0.955)
Melatonin	-2181		
Sodium	-2290	-85	1.39 (0.996)
Potassium	-2318	-141	1.29 (0.991)
Calcium	-2311	-18	1.02 (0.986)
Lithium	-2323	-97	0.39 (0.982)
Aluminium	-2333	-44	0.65 (0.987)

[a] lowest electrochemically detectable levels of serotonin and melatonin ligands = 6.7×10^{-8} mol dm^{-3} whilst the [Metal] = 3.3×10^{-9} mol dm^{-3} under the chosen experimental parameters.

[b]E_p = peak potentials of the metal-ligand complexes. ΔE_p is the difference between the peak potentials of the metal ions and those of the metal-ligand complexes. [c]Regression coefficients are shown in brackets.

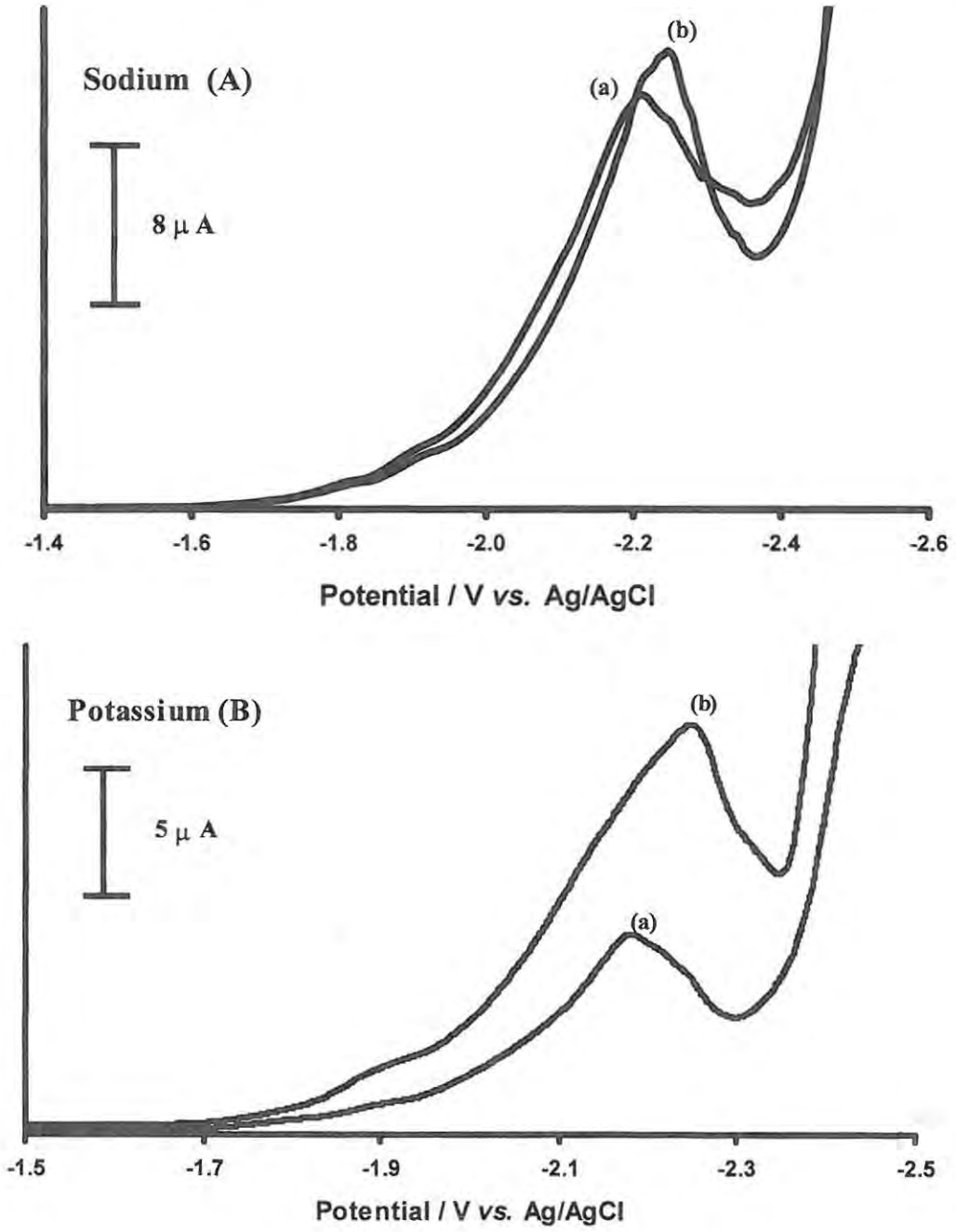

Figure 2.2 **Adsorptive cathodic stripping voltammograms obtained for 6.7×10^{-8} mol dm^{-3} serotonin in the presence of (A) Na^+ and (B) K^+. (a) Voltammograms for the metals alone and (b) in the presence of serotonin. [Metal] = 3.3×10^{-9} mol dm^{-3}, scan rate = 25 mV s^{-1}.**

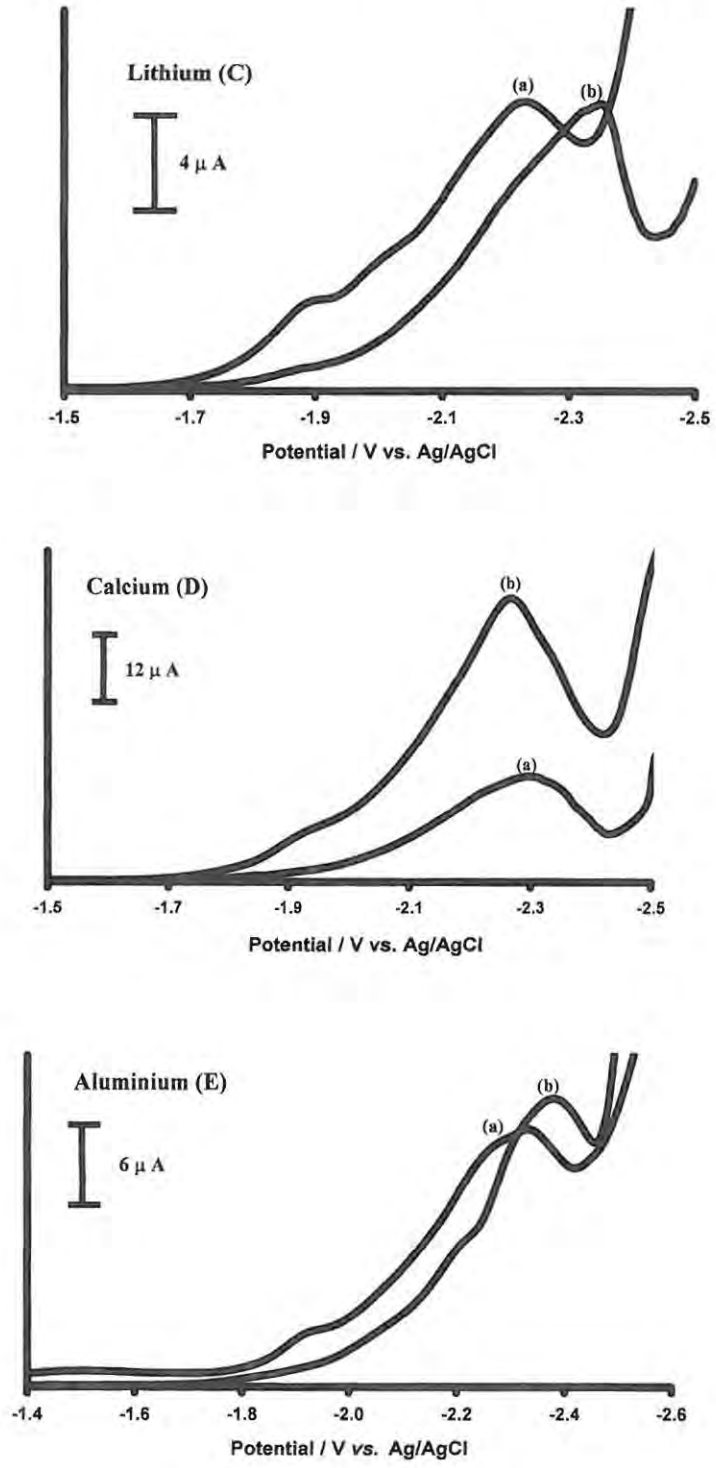

Figure 2.2 (continued) **AdCSV obtained for 6.7×10^{-8} mol dm^{-3} serotonin in the presence of (C) Li^{+}, (D) Ca^{2+} and (E) Al^{3+}. [Metal] = 3.3×10^{-9} mol dm^{-3}, scan rate = 25 mV s^{-1}.**

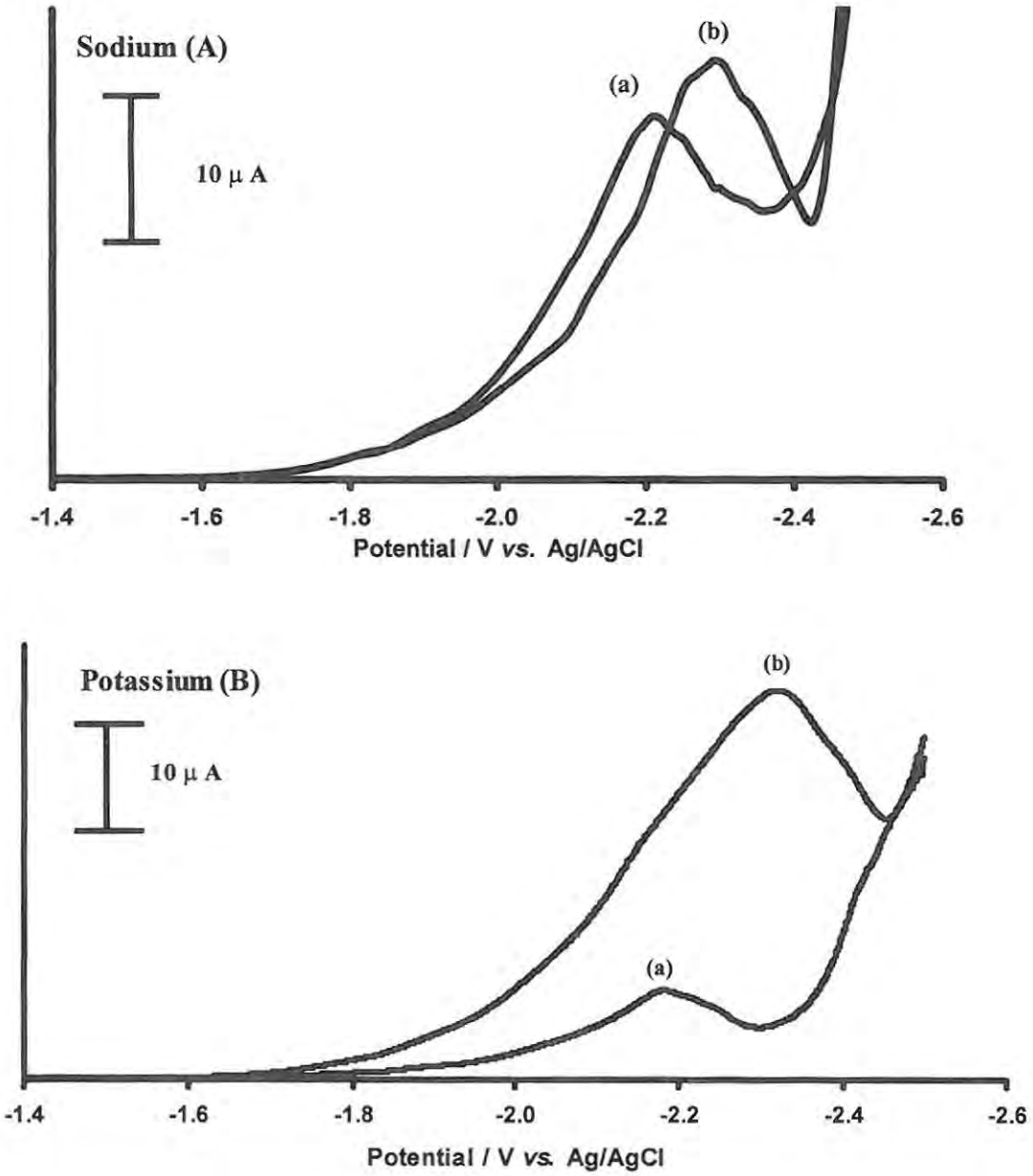

Figure 2.3 **Adsorptive cathodic stripping voltammograms obtained for 6.7×10^{-8} mol dm^{-3} melatonin in the presence of (A) Na^+ and (B) K^+. (a) Voltammograms for the metals alone and (b) in the presence of serotonin. [Metal] = 3.3×10^{-9} mol dm^{-3}, scan rate = 25 mV s^{-1}.**

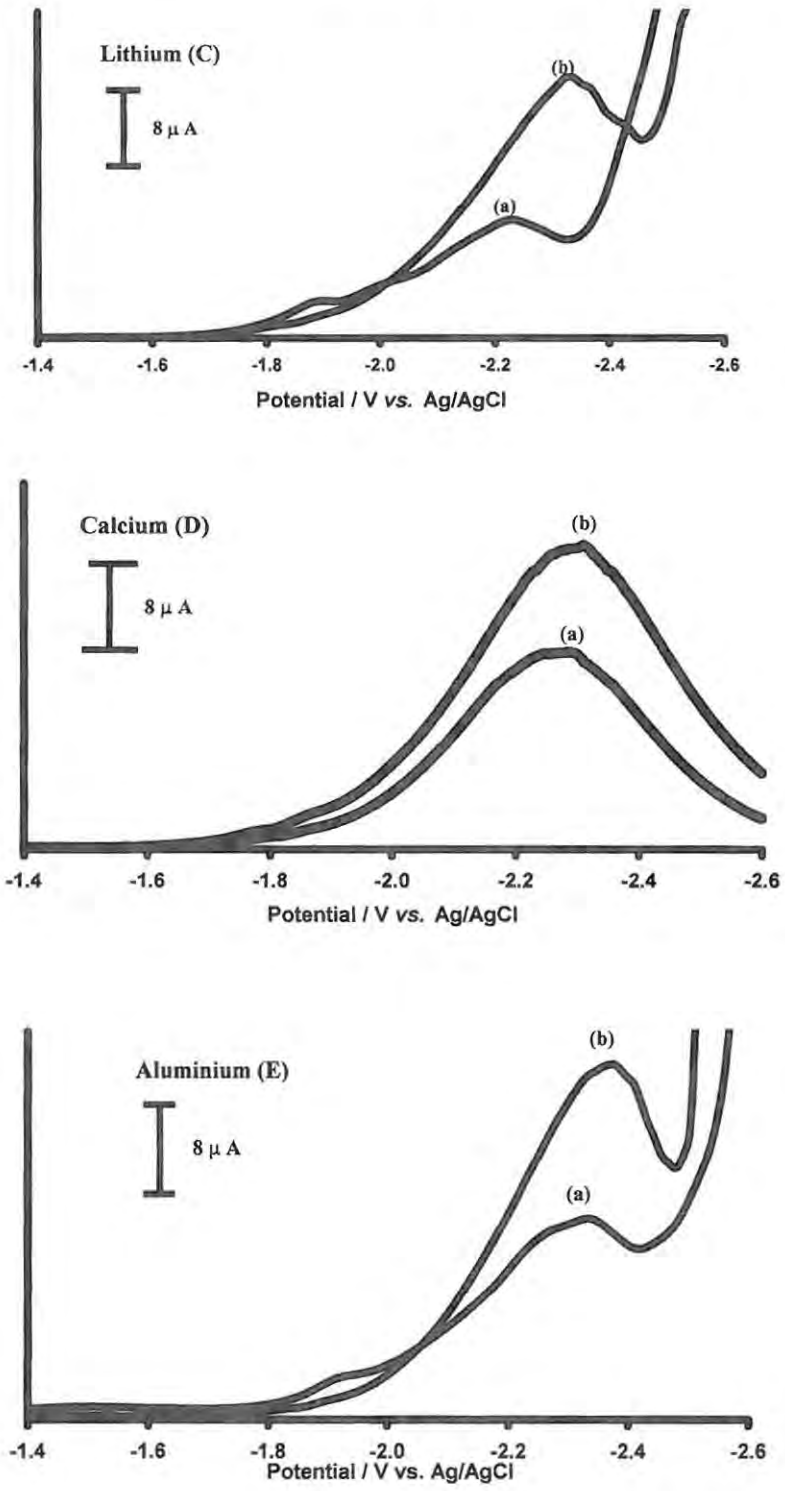

Figure 2.3 (continued) **AdCSV obtained for 6.7×10^{-8} mol dm^{-3} melatonin in the presence of (C) Li^{+}, (D) Ca^{2+} and (E) Al^{3+}. [Metal] = 3.3×10^{-9} mol dm^{-3}, scan rate = 25 mV s^{-1}.**

The shapes of the peaks shown in Figures 2.2 and 2.3 for metal-serotonin and metal-melatonin complexes, respectively are similar to those of the metal alone, confirming that reduction of the metal-serotonin or metal-melatonin complex occurs at the metal. Reduction peaks due to serotonin or melatonin alone, in the absence of metals, were not evident at the concentrations employed in Figures 2.2 and 2.3. The metal peak was thus chosen for monitoring the formation of the complex between serotonin or melatonin and the metals.

The enhancement in the reduction currents on addition of serotonin, or melatonin, to the solution containing the metal, is an indication of the *in situ* formation and accumulation of the metal-serotonin or metal-melatonin complex onto the Hg electrode. The shift in the reduction peaks to more negative potentials on addition of serotonin or melatonin to solutions containing the metal ion suggests that the metal-serotonin or metal-melatonin complexes formed are more difficult to reduce than the free metal. The extent of the shift in reduction peak potential of the metal on addition of serotonin or melatonin is a good measure of the stability of the metal-serotonin or metal-melatonin complex formed *in situ*.

Table 2.1 lists the shifts in peak potentials, ΔE_p, for the reduction of the metals on addition of serotonin or melatonin ligand species. For serotonin, the large negative shift observed (ΔE_p = -123 mV) on addition of serotonin to Li^+ solutions reflects the stability of the resulting lithium-serotonin complex when compared to the other metal-serotonin complexes. The high negative ΔE_p value also shows that the resulting complex is more difficult to reduce when compared with the reduction of the free metal and the other metal-serotonin complexes. For melatonin, a high negative ΔE_p value was observed for the

potassium-serotonin complex showing that a more stable complex is formed between potassium and melatonin when compared to the other metal-melatonin complexes.

The positive ΔE_p value, observed for the complex between serotonin and Ca^{2+}, indicates the ease of reduction of the calcium-serotonin *in situ* complex, and suggests that this complex was not stable and hence easily reduced when compared to the complexes of serotonin with Li^+, Al^{3+}, K^+ and Na^+. Based on the magnitudes of the shifts in reduction potentials of the metals on addition of serotonin, the relative stability of the *in situ* complexes formed between the metals and serotonin decreases with the metal as follows: $Li^+ > K^+ > Al^{3+} > Na^+ > Ca^{2+}$. For the complexes between melatonin and the metals, the stability of the complexes increases with the metal as follows: $K^+ > Li^+ > Na^+ > Al^{3+} > Ca^{2+}$. Thus, both Li^+ and K^+ form more stable complexes with serotonin and melatonin when compared to the other metal complexes under consideration. Melatonin favours K^+ over Li^+ and serotonin favours Li^+ over K^+. Both melatonin and serotonin do not favour coordination to Ca^{2+}.

Peak currents for the metal-serotonin or metal-melatonin complexes increased with increase in the concentration of the metal as shown in Figures 2.4 (A) and (B) for serotonin and melatonin complexes, respectively. The plots are linear, the slopes of which along with the regression coefficients are listed in Table 2.1. The magnitude of the slope is an indication of the affinity of the ligand for the metal ion. For the same concentration of serotonin, Figure 2.4 (A) shows that the highest currents were observed in the presence of calcium and the lowest currents in the presence of lithium. For melatonin, Figure 2.4 (B), there is considerable overlapping of the lines, but at concentrations of 7×10^{-9} mol dm^{-3} and less, the lowest currents were observed for Na^+ and the highest for Li^+. In contrast, at

concentrations exceeding 7 x 10^{-9} mol dm^{-3}, the lowest currents were observed for Al^{3+} and the highest for K^{+}.

The standard curves shown in Figures 2.4 (A) and (B) can be used for the determination of the metal ions in the presence of serotonin and melatonin. Concentration detection limits of the order of 10^{-10} mol dm^{-3} for serotonin and melatonin were obtained, using AdCSV, in the presence of the metals discussed in this work. AdCSV currents increased with increase in the concentrations of serotonin and melatonin as shown in Figure 2.5 at constant concentration of K^{+}.

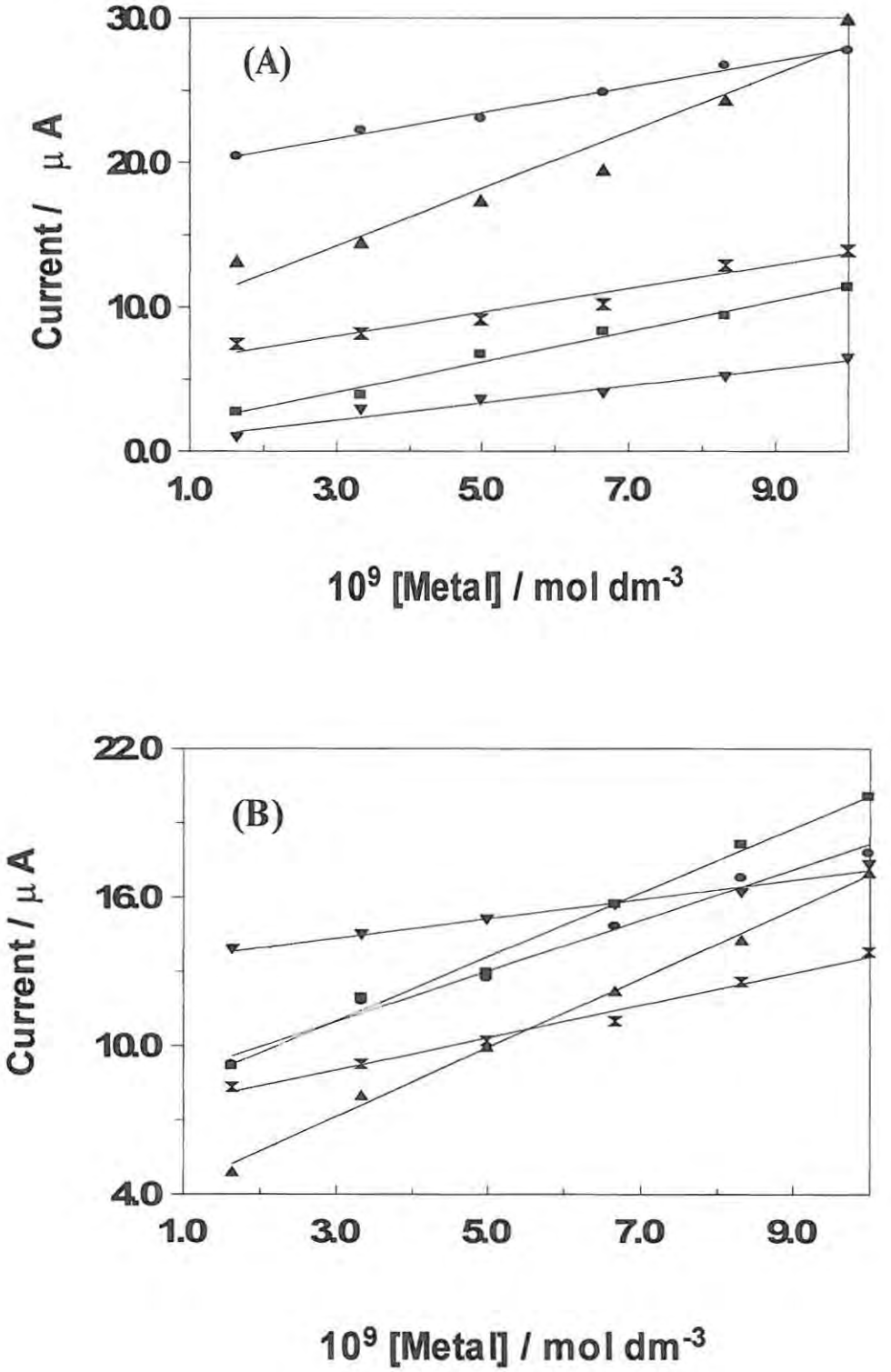

Figure 2.4 **(A) Variation of currents with metal ion concentration for 6.7×10^{-8} mol dm^{-3} serotonin and (B) for 6.7×10^{-8} mol dm^{-3} melatonin. Ca^{2+} (●), K^{+} (■), Na^{+} (▲), Li^{+} (▼) and Al^{3+} (⧗)**

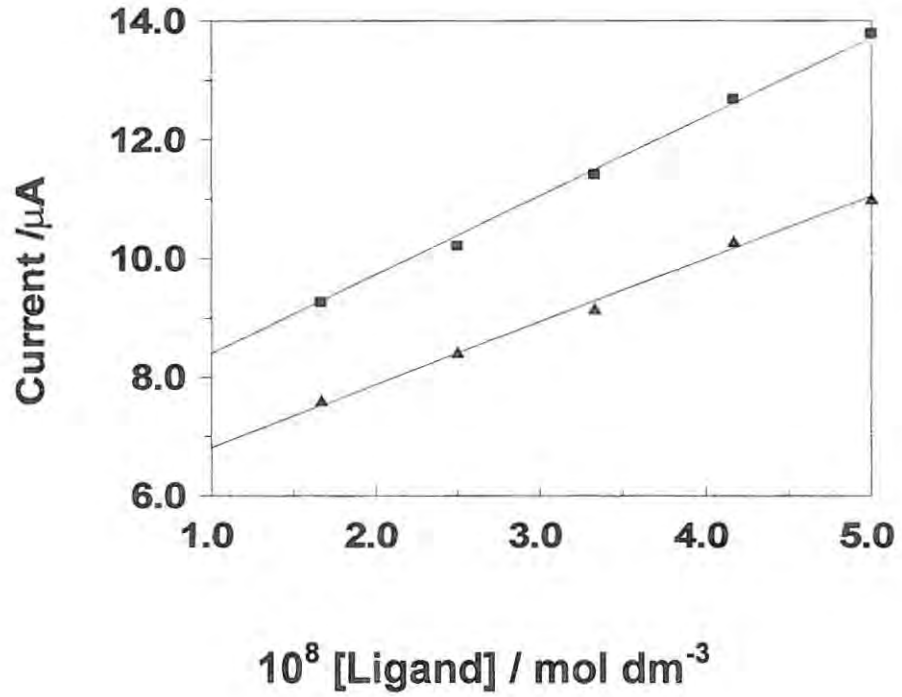

Figure 2.5 **Variation of currents with ligand concentration for serotonin (▲) and melatonin (■). $[K^+] = 3.3 \times 10^{-9}$ mol dm^{-3}, scan rate = 25mVs^{-1}.**

Spectroscopic Studies and Computer Modeling:

The IR spectra, of the solid complexes prepared by freeze-drying solutions containing serotonin or melatonin and an excess of the metal ions, were recorded and compared with the IR of the freeze-dried ligand alone, Figure 2.6. For serotonin, binding of the metal ions may occur either at the OH, NH_2 or NH positions of the ring. IR spectra of the serotonin-metal complexes showed a decrease in intensity and a small shift in the vibration band at 3414 cm^{-1}, when compared to the IR of serotonin alone, suggesting an interaction at the NH position. Further minor spectral changes were also observed throughout the IR

spectra. However, due to the overlap between OH and NH vibrations in this IR region, binding at the OH site cannot be ruled out. There were no definite differences in the spectra of the melatonin-metal complexes when compared to the IR spectra of melatonin alone.

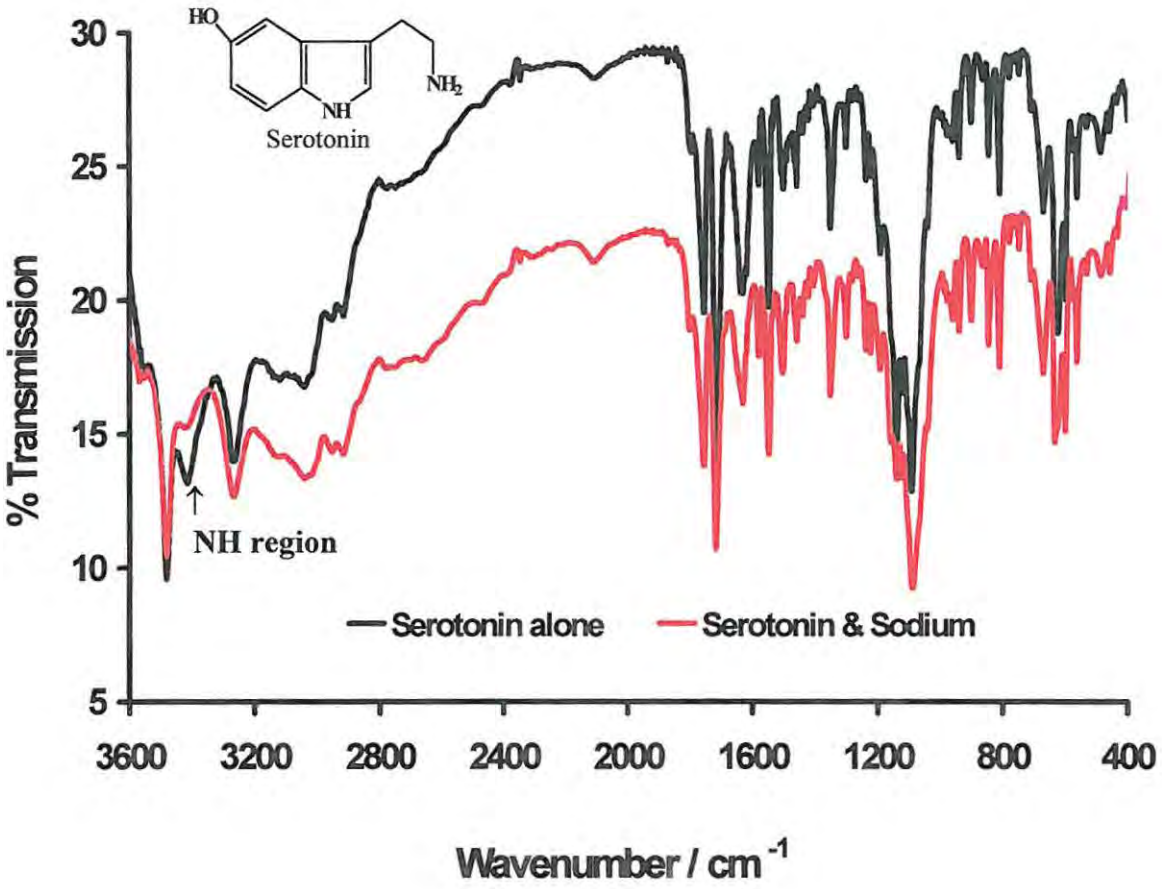

Figure 2.6 **Infrared spectra of the freeze-dried serotonin alone and in also in the presence of sodium ions.**

The binding of the metals to serotonin or melatonin was also studied by recording the ^{1}HNMR spectra of melatonin or serotonin in the presence and absence of the metal ions (examples presented in Appendix 1-4). Binding of the metals to the ligands will result in significant shifts in the NMR peaks corresponding to the atoms where binding occurs. For melatonin the NH peak on the ring, observed at 10.60 ppm, was shifted downfield in the presence of the metal ions. The shifts are listed in Table 2.2.

Table 2.2 ^{1}HNMR shifts observed for the melatonin or serotonin NH peaks following addition of the metal ions: (+ indicates a downfield shift)

	δ Shift (ppm) *Melatonin:		δ Shift (ppm) Serotonin:
Metal	**Ring (NH peak)**	**Chain (NH peak)**	**Ring (NH peak)**
Lithium	+0.241	+0.278	+0.169
Potassium	+0.144	+0.020	+0.022
Sodium	+0.084	+0.095	+0.029
Calcium	+0.030	+0.040	+0.004

* A reminder of the melatonin structure:

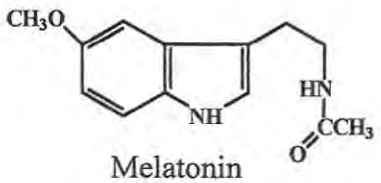

Melatonin

The largest shift was observed in the case of Li^+ and the smallest for Ca^{2+}. No significant shifts were observed for Al^{3+}, hence it is not included in Table 2.2. The NH (ring) peak shifted downfield depending on the metal as follows: $Li^+ > K^+ > Na^+ > Ca^{2+} > Al^{3+}$. For the side chain NH group, the trend was $Li^+ > Na^+ > Ca^{2+} > K^+$.

The significant shifting in the NH resonance observed, particularly for Li^+, suggests binding of the metal ions at nitrogen atoms in melatonin. Since an excess of the metal ion was employed, it is likely that binding occurs at both NH positions in melatonin.

Serotonin was only sparingly soluble in deuterated DMSO, but on addition of the metal ions to the solutions of serotonin, the solubility improves considerably. This observation does suggest interaction occurs between serotonin and the metal ions. Downfield shifts in NH peak were observed for serotonin in the presence of the metal ions, Table 2.2. The resonances shifted downfield depending on the metal ion as follows: $Li^+ > Na^+ > K^+ > Ca^{2+} > Al^{3+}$. The observation of a larger shift for Li^+ is consistent with the observation of greater stability of the serotonin-lithium complex obtained from the electrochemical studies.

The low solubility of serotonin in DMSO did not allow for the clear observation of the OH or NH_2 groups. These resonances were observed at different positions in the presence of the different metals, showing that the metals do have an effect on these groups as can be seen in Table 2.3. It is important to note the presence of creatine sulphate may affect the interactions between serotonin and the metal ions. For both serotonin and melatonin, the data presented here does not give clear evidence of the actual coordination site of the metals.

Table 2.3 ^{1}HNMR peaks observed for NH_2 and OH resonances for serotonin in the presence of metal ions:

	δ (ppm)	
Metal	OH	NH_2
Lithium	8.804	8.430
Potassium	8.638	8.261
Sodium	8.651	8.244
Calcium	8.578	-

In conclusion, all the metals investigated formed *in* situ complexes with both serotonin and melatonin. However, the stability and affinity for the ligands to the various metals varied greatly. Both Li^+ and K^+ formed more stable complexes with serotonin and melatonin when compared to the other metal complexes under consideration.

The computer modeling package was used to obtain electrostatically generated models of melatonin and serotonin alone, Figure 2.7 (A) and (B), or in combination with lithium as illustrated in Figures 2.8 (A) and (B) respectively. In the case of serotonin, the most electronegatively charged group was that of the OH with a charge of –0.68401 in comparison to the NH_2 (chain) and NH (ring) groups with values of –0.6282 and –0.5210. The electrostatic representation of melatonin afforded a slightly different picture with the O-CH_3 region displaying the highest negative charge of –0.5639. The NH (ring) group was assigned a value of –0.5298, whilst the NH (chain) and COOH regions exhibited values in the order of –0.4936 and –0.5016 respectively.

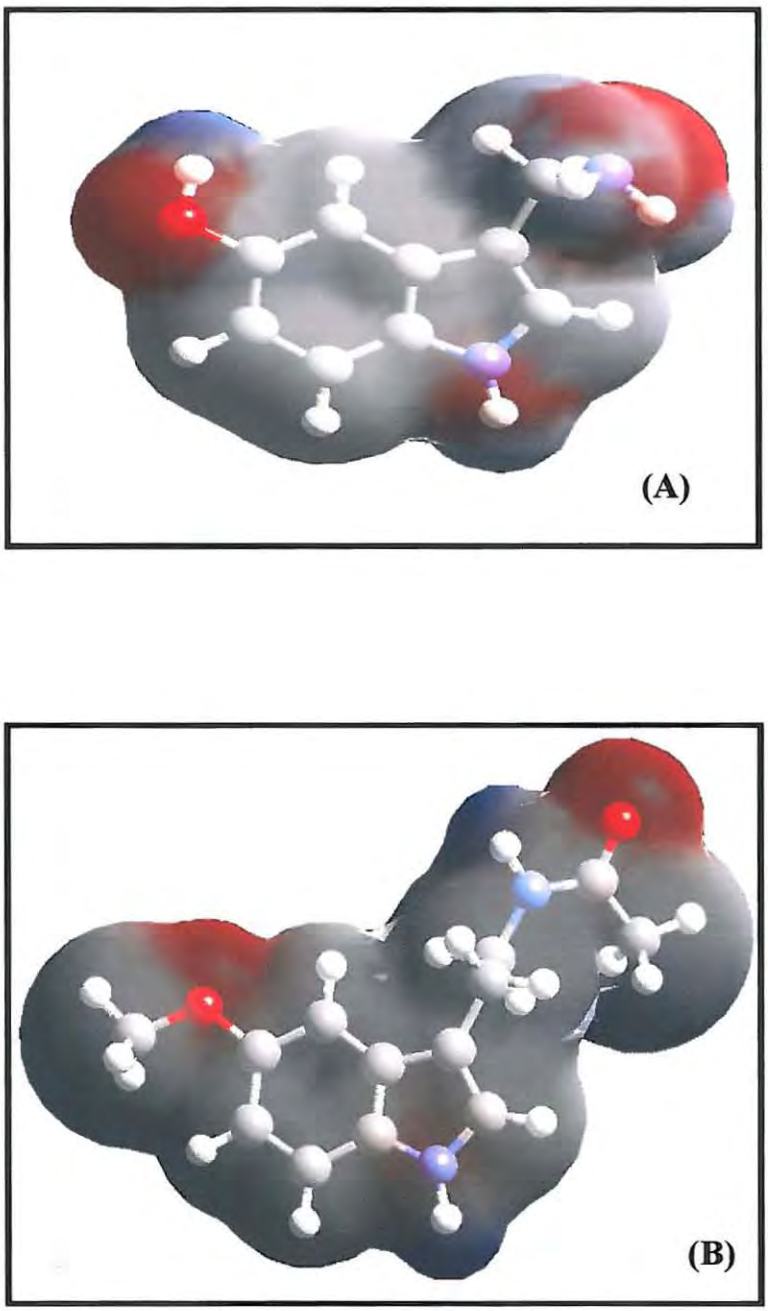

Figure 2.7 The electrostatic model of serotonin (A) and melatonin (B).

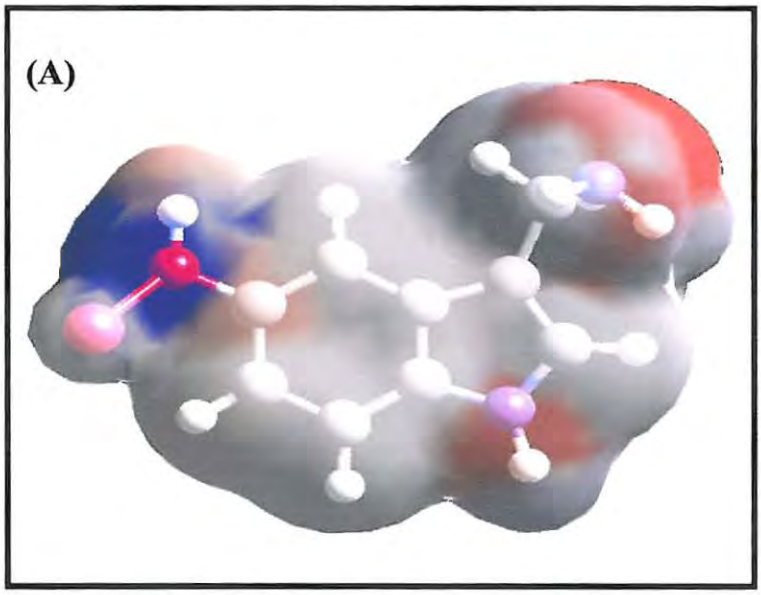

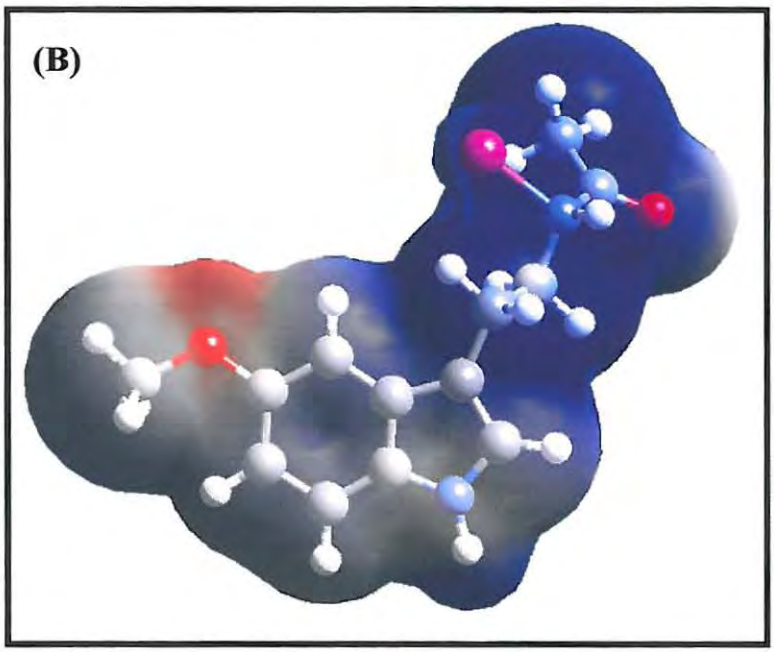

Figure 2.8 **The electrostatic model of the Li-serotonin (A) and Li-melatonin (B) complex. The Li^+ ion can been seen to be attached to the OH group.**

The highly electropositively charged lithium ion is likely to favour attack at the ROH, RNH_2 or NH_2 sites as described by the HSAB theory in Section 1.5.2. However, taking the possible steric hindrance effects into account on the serotonin molecule and comparing the electronegativity characteristics of the NH and NH_2 groups, the most feasible site for Li^+ attack was that of the OH region and hence was modeled as such.

When considering the melatonin structure the addition of the lithium ion was modeled from the $O\text{-}CH_3$ attack face. The region is the most electronegative and constitutes the least amount of steric hindrance. Furthermore the HSAB theory, Section 1.5.2, indicates the affinity of the Li^+, a hard acid, for a hard base structure as seen on melatonin in the form of the O-methyl group.

A series of energy minimised space filled models were generated for serotonin and melatonin as illustrated in Figure 2.9 (A) and (B). The colour code chosen was that of nitrogen atoms being represented in blue, oxygen atoms are red and carbon and hydrogen atoms are seen to be grey and white respectively. The minimised energy conformer was then utilised to create a graphic image of the Li-serotonin or Li–melatonin complex as depicted in Figure 2.10 (A) and (B) where the Li^+ ion is modeled in a pinky colour. Computational modeling has afforded a graphical view of possible attack sites on the ligand as well as the changes that occur, spacial and electrostatic, as a result of the metal-ligand interactions in comparison to that of the ligand alone.

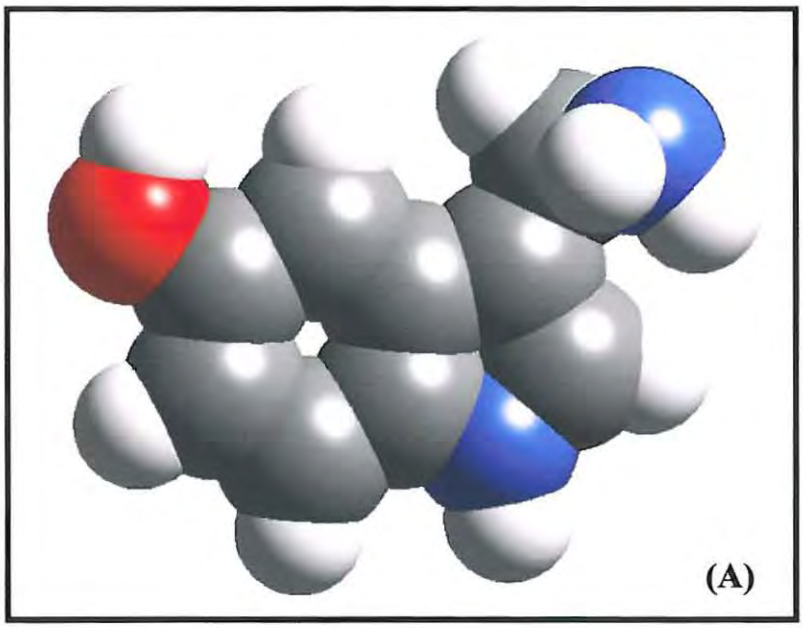

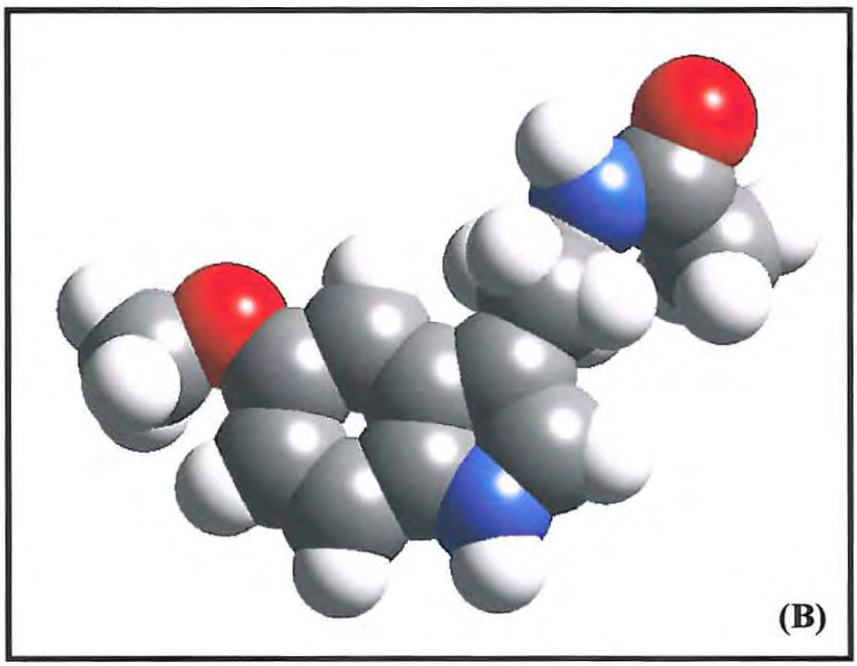

Figure 2.9 **Space-filled model of the global energy minimized serotonin (A) and melatonin (B).**

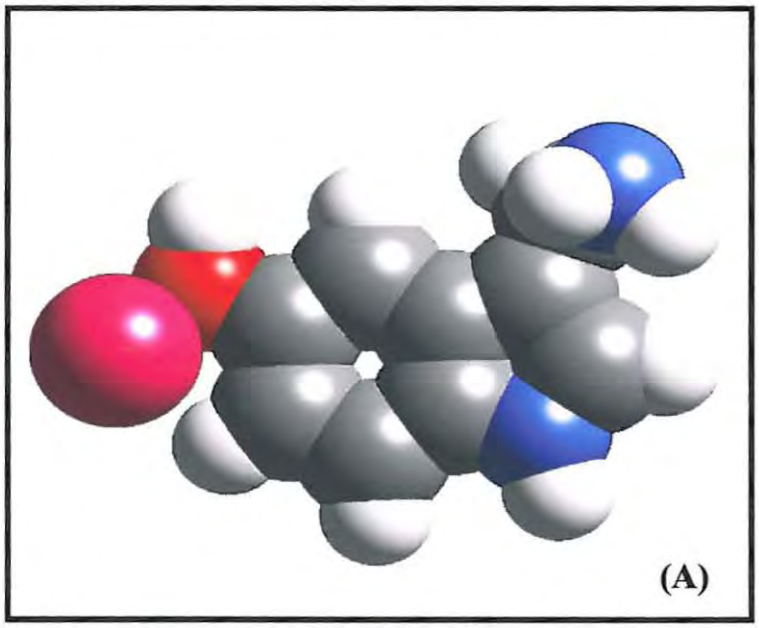

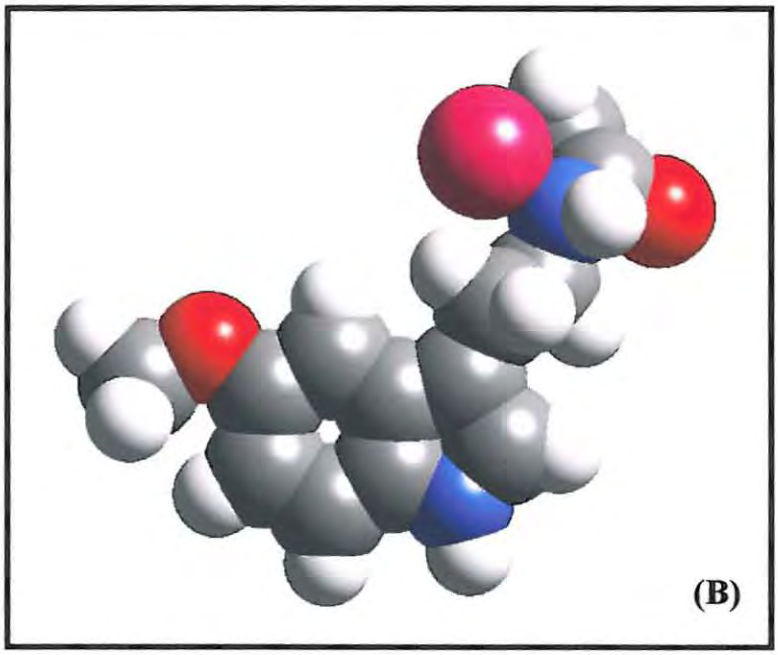

Figure 2.10 **Space-filled model of the global energy minimized Li-serotonin (A) and Li-melatonin complexes (B).**

2.4 DISCUSSION:

The binding and stable complex formation between both ligands, serotonin and melatonin, with lithium, potassium and sodium is of biological importance. It is known that melatonin inhibits the activity of large conductance calcium-activated potassium channels [190] and also reduces the KCl-induced insulin response to glucose.[191] The reason for this could be due to direct chelation of potassium by melatonin. The observed interactions may also be explained, as in Section 1.5.2, in terms of different structural and chemical aspects of the bond formation between the metals and these ligands of interest. Looking at the structural representation of melatonin and its precursor, serotonin, in Figures 1.1 and 1.2 respectively, possible binding sites of the metals may be elucidated in terms of the HSAB theory.

The monovalent cations of group 1 are accordingly classified as hard acids,[90] preferring the OH or NH_2 sites on the ring periphery in both serotonin and melatonin. The divalent and trivalent cations of Ca^{2+} and Al^{3+} respectively may also be categorized as hard acids, but the decreased atomic radii in these cases may further contribute to differences noted in binding positions for these ions.[90] The O-methyl group on melatonin is in addition a hard base and thus acts as a suitable hard acid acceptor site. The carbonyl and two NH groups, however, are soft bases thus prefer attack from soft acids such as the radical species and are unlikely sites for binding by the metals studied. However, from the IR and NMR data obtained, the NH groups on serotonin and melatonin cannot be ruled out as possible binding sites, particularly since excess metal ions were employed in both these studies. The comparative hardness or softness of the functional groups on serotonin and melatonin

may be a factor, which defines their relative particular strengths and affinities for the metal bond formation.

Although this study shows that calcium ions form a very weak and unstable complex with melatonin, in light of the findings that melatonin inhibits neuronal calcium overload in mouse brain cells,[193] chelation of potassium ions by melatonin could prevent opening of the voltage gated calcium channels. In this respect, melatonin is known to enhance activation and inactivation kinetics in lens epithelial cells and trabecular meshwork cells and to also stimulate the voltage-dependent selective currents in these tissues.[187] Whether this is due to chelation of metals is not known.

The finding that serotonin forms a strong and stable complex with Li^+ is also important in terms of the possible mode of action in the psychopharmacology of this metal. The mode of action of Li^+ in the treatment of manic-depressive disorder has not yet been characterised. One possible explanation offered by the present study is that the formation of a serotonin-Li complex could introduce an increase in the half-life of serotonin thus preventing its rapid destruction by enzymes such as monoamine-oxidase. This would allow for a greater pool of serotonin in the synaptic cleft.

The finding that melatonin also binds this metal with tenacity, but to a lesser degree than serotonin, could explain why this metal reduces plasma, pineal and ocular melatonin levels.[196] It is possible that the melatonin-Li complex is not detected as melatonin *per se*, or that the serotonin-Li complex prevents the conversion of serotonin to melatonin.

The binding of Al^{3+} by both serotonin and melatonin is of significance in Alzheimer's disease where this metal in known to accumulate in the brain.[198] Whilst it is uncertain whether Al^{3+} does indeed play a role in the aetiology of Alzheimer's disease, it's introduction into the brain can mimic many of the pathological features of Alzheimer's disease, except for the cortical somatostatin deficit.[204] It thus appears that chelation of metal ions by these indoleamines, as shown in the present study as well as the stability of the complexes formed, indicate that such complexes can have important biological and pharmacological consequences.

In conclusion, all the metals investigated formed complexes with both serotonin and melatonin. However, the stability and affinity for the ligands to the various metals varied greatly. Both Li^+ and K^+ formed more stable complexes with serotonin and melatonin when compared to the other metal complexes under consideration.

CHAPTER 3

The cholinergic metal-ligand studies

3.1 INTRODUCTION:

Cholinergic dysfunction in the brain is associated with neurodegenerative disorders such as Alzheimer's disease, as discussed in the general introduction, Chapter 1. Notably the presence of the acetylcholine synthesizing enzyme, choline acetyltransferase (ChAT), is decreased in the brains of Alzheimer's disease (AD) patients, whilst the choline levels remain indifferent.[205] However, the aetiology of AD appears to be multifactorial and mercury too may play a role in this disorder, since elevated levels of this metal ion has been detected in postmortem AD brain tissue [206,207] and in the blood of AD patients.[208]

Thompson *et al.* (1988) further observed that the elevation of mercury in the nucleus basalis of Meynert (nbM), as compared with age-matched controls, was the largest trace-element imbalance observed AD patients' brains.[207] From their studies, Wenstrup *et al.* (1990) conclude that mercury could be an important toxic element in AD,[209] but as to whether mercury deposition in AD is a primary or secondary event remains to be determined. Furthermore, as mentioned in the general introduction (Chapter 1), the long-

term effects of assimilated low levels of mercury, such as those found in teeth amalgams or in the environment, remains unclear.[105]

In addition to mercury, lead is also known to alter cholinergic function. Models for peripheral neurotoxicity have shown that lead, when added acutely to *in situ* or in vivo preparations, blocks the stimulated release of acetylcholine from preganglionic and prejunctional nerve terminals.[210] Goldstein *et al.* (1974) have demonstrated that subencephalopathic lead exposure affects the integrity of capillary endothelial cells *in vivo* and *in vitro*, thus compromising the function of cellular constituents of the blood brain barrier.[211] Added to this, or overlaid upon it, is the possibility that lead stored in the body, mostly in the mineral compartment, may be mobilized during the aging process. The efflux of lead from bone stores has been reported in postmenopausal women and in retired lead workers.[212]

Yoshida (2001) evaluated the cadmium toxicity on the mesencephalic trigeminal neurons of the adult rat.[213] The data showed that cadmium directly affects nerve cells; the toxicity of which is mediated by continuous elevation in intercellular calcium levels resulting in induced necrotic cell death. Furthermore, the cadmium neurotoxicity was antagonized by the presence of zinc ions.[213] However, zinc itself has been shown to be potently neurotoxic to neuronal cell cultures. The concentration of zinc is non-uniform in the brain, with the highest levels being recorded in the cerebellum, hippocampus (higher in the hilar region and lowest in the fimbria), retina and the pineal gland.[214]

Alzheimer's disease exhibits prominent injury in the hippocampal pyramidal neurons, acetylcholine–containing neurons in the basal forebrain and somatostatin-containing neurons in the forebrain region. These neuron populations have been shown to possess highly zinc permeable calcium channels providing a route for rapid and direct zinc entry. Indeed, given the current understanding of zinc-mediated injury mechanisms, cumulative effects of repeated zinc exposures could conceivably contribute to oxidative and mitochondrial dysfunction observed in Alzheimer's disease or amyotrophic lateral sclerosis. Further studies have suggested an alternate method in which zinc could play a role in Alzheimer's disease is by promoting the aggregated state of β-amyloid (Aβ) peptide. High concentrations of zinc have been found in mature amyloid plaques in both human tissues and in transgenic mouse models of the disease.[214]

Copper has long since been known to play a role in neurodegeneration. However, the mechanism behind the neuronal-specific toxicity of copper remains unclear. Horning *et al.* (2000) proposed that synaptically released zinc and copper probably function to modulate neuronal excitability under normal conditions.[121] However, zinc and copper can also be neurotoxic by contributing to the neuropathology associated with a variety of conditions, such as Alzheimer's disease, stroke, and seizures.[121]

Heron *et al.* (2001) investigated the effects of copper and manganese on the brain mitochondrial respiratory chain and on the flavin adenine dinucleotide (FAD) – dependent enzyme, monoamine oxidase (MAO).[215] The enzyme has been linked to the oxidative deamination of neurotransmitters such as serotonin and dopamine in the brain. The study concluded that copper and manganese influence mitochondrial function at the nicotinamide adenine dinucleotide (NAD(H)) and FAD-dependent reactions. However, copper, and not

manganese, appeared to bind to the mitochondrial suspension inducing flocculation and sedimentation. The disruption of normal mitochondrial functioning in providing the cell with energy may have detrimental effects on the survival of the cell, leading to apoptosis. Mitochondrial respiratory chain defects have been implicated in the pathogenesis of AD, whilst mitochondrial dysfunction has been associated with the neurodegenration of Parkinson's disease.[215-217]

There exists a possibility that heavy metals such as mercury, cadmium and lead might be able to bind directly to acetylcholine, rendering it inactive. In addition, imbalances of zinc and copper levels, observed in neurodegenerative disease cases, may be related to acetylcholine interactions. The present study thus aimed at examining the possibility of an interaction of cadmium, mercury, lead, zinc and copper with acetylcholine utilising the adsorptive cathodic stripping voltammetry (AdCSV) technique described in Section 1.8.1. AdCSV has been used successfully in studying the interaction between metal ions and ligands.[172,198,199,218]

Furthermore, techniques such as thermogravimetry (TG), KBr-disk IR and X-ray powder diffraction (XRD) patterns have been used in this research to characterise a freeze-dried solid sample prepared from mercury and acetylcholine, compared with that of the ligand alone. A brief discussion on these techniques will follow. From a thermal decomposition point of view, the kinetic behaviour, the rate controlling processes and the mechanisms of thermal decomposition of most coordination compounds are generally similar to those that characterize the decompositions of the simple salts. However, the increased number and variety of constituent groupings accommodated in the reactant structures introduces diversity and complications into the chemistry of the decomposition mechanisms.[219]

In thermal decomposition, ligand release, through dissociation of the coordinate linkage, may be accompanied by, or rapidly followed by, secondary reactions, so that mechanisms generally involve several different contributory processes. As a result of this complexity, relatively few detailed studies of the kinetics and mechanisms of solid state decompositions of coordination compounds have been reported. Where ligands other than water occupy the coordination shell, the complexity of the chemical changes has often made it necessary to limit the objectives of investigations to comparisons of the thermal behaviour of members of a related series.[219]

The thermogravimetric data obtained is a comparison between the ligand alone and the metal-ligand complex. However, it is worth noting that differences in behaviour resulting from ligand substitutions or variation of ion structure are small in coordination compounds.[219]

In the infrared analysis, the region of study is referred to as the high frequency range from 4000-650 cm^{-1} and in general, vibrational changes in this sector originate from the ligand component of the complex. The spectra of metal complexes are mostly obtained in the crystalline state as a Nujol® mull or in a KBr disk, however, the structure of the metal complex in the crystalline state maybe markedly different from that in solution or in the gaseous phase. In the crystalline state the configuration around the metal may be distorted or changed by coordination of neighbouring molecules.[180,182,220]

Nakamoto *et al.* (1968) have shown that the un-ionised, ionised and coordinated carboxyl groups exhibit relatively strong bands between 1750 and 1550 cm^{-1}.[220] The un-ionised carboxyl group of $R_2N\text{-}CH_2COOH$ for example, has been shown to absorb in the region

between 1730 and 1700 cm^{-1}. On the other hand, the coordinated carboxyl group absorbs between 1650 and 1590 cm^{-1}, the exact frequency of which has been shown to be dependent on the nature of the metal attached. In general the frequency is known to become higher as the metal oxygen bond becomes more covalent in nature.[220] Pouchert (1975) has reported a carbonyl stretch band of the unconjugated ester to lie close to the 1740 cm^{-1} region and it is accompanied by the stretch bands of the carbon-oxygen single bond between 1250 and 1000 cm^{-1}.[221] Furthermore, Bellamy and Branch (1954) have shown that the C=O stretching frequency is shifted linearly to lower frequency values with an increase in the stability constant for a series of divalent metal cation complexes.[222]

X-ray diffraction is a widely used experimental method for materials analysis. The X-rays are electromagnetic radiations with a specific wavelength of the order of 1 Angstrom. A property of the electromagnetic radiation is its inherent electric field, which interacts with charged particles such as the electrons in the solid. The interaction causes the electrons to emit wavelets and when these wavelets interfere with each other constructively, diffraction takes place. For a polycrystalline or powder sample, different crystallographic planes may be orientated simultaneously at their corresponding Bragg angle (θ) with respect to the incident beam, so that they may cause diffraction to occur simultaneously at different angles (2θ, the diffraction angle) from the incident beam. A number of diffracted beams may emanate from the same sample at the same time. All these diffracted beams need to be detected in order to obtain the complete diffraction pattern. Powder diffraction patterns are mainly used to identify crystalline phases, but structure determination via X-ray powder diffraction has become an important field.[223]

3.2 EXPERIMENTAL:

3.2.1 REAGENTS:

As per Chapter 2, all reagents were of analytical grade, MEDGAS® supplied the nitrogen purge gas, whilst triply distilled deionised water was used for all experiments. Hg^{2+}, Pb^{2+}, Cd^{2+}, Cu^{2+} and Zn^{2+} stock solutions were prepared from the corresponding metal chloride salts, obtained from Merck Ltd. Acetylcholine chloride (Sigma – St Louis, MO, U.S.A.) was prepared daily in triply distilled deionised water. A solution of 0.05 mol dm^{-3} tetrabutylammoniumbromide (TBABr, Sigma – St Louis, MO, U.S.A.) was used as an electrolyte for the electrochemical experiments.

3.2.2 APPARATUS:

Electrochemical Study:

Stripping voltammograms, utilising the OSW mode, were obtained with the BioAnalytical Services (BAS, Lafayette, Indiana, USA) CV-50W voltammetric analyser. Comparisons were made between the gold, platinum and glassy carbon working electrodes (BAS models MF2014, 2013 and 2012 respectively) as to their suitability as working electrodes for the study of an acetylcholine-mercury complex. The gold electrode was chosen for further experimental work, permitting a comparative study between the interaction of acetylcholine with mercury or lead. A silver|silver chloride (3 mol dm^{-3} KCl) and a platinum wire were employed as the reference and auxiliary electrodes, respectively.

A controlled growth mercury electrode (CGME) mode on the hanging drop mercury electrode (HDME) apparatus, BioAnalytical Systems model MF-9058, was chosen to study the interaction between cadmium, copper(II) or zinc complex formation with acetylcholine. This electrode was chosen for easy of use and in continuation of an earlier study in our laboratory, published by Matlaba *et al.* (2000), where complex formation between acetylcholine and aluminium, amongst other metals, was investigated.[224] Benefits of the mercury drop electrodes, include a renewable electrode surface and with the CGME function being employed as choice on the HDME apparatus, a previous disadvantage of inconsistent mercury drop sizes has been eliminated. A silver|silver chloride (3 mol dm^{-3} KCl) reference electrode was chosen, whilst a platinum wire was employed as the auxiliary electrode.

Solid complex analysis:

A Viritis Freezemobile 6 was used for freeze-drying samples. The freeze-dried acetylcholine sample was compared with the freeze-dried metal-acetylcholine complex in the presence of mercury utilising thermogravimetric analyser (TGA), IR and XRD methods. For the TGA experiments a Perkin Elmer TGA-7 Series Thermogravimetric Analyser was utilised. IR spectra were obtained on a Fourier transformed infrared apparatus, with a computerised Perkin Elmer Spectrum 2000 IR spectrophotometer. A Seifert X-ray generator made use of a copper tube to generate emissions of the k α line of the copper spectrum. A Philips PW 1965/40 proportional detector probe was coupled to a Philips PW 1050/25 diffractometer and camera to obtain the X-ray powder diffraction patterns of the freeze-dried ligand alone and in the presence of mercury.

3.2.3 METHOD:

Electrochemical Techniques:

Mercury and Lead Study:

Solutions containing the metal ion and the ligand in a 1:4 ratio (favouring acetylcholine as this was found to be the optimum metal:ligand ratio) were deaerated for a minimum period of 5 min, after which a flow of nitrogen gas was maintained over the solution throughout the measurement. The metal-ligand complex is expected to have formed at this stage. Further parameter optimisation, as demonstrated in a similar manner to Chapter 2, resulted in a deposition potential of 500 mV for Hg^{2+} and 700 mV for Pb^{2+} being applied for an optimum deposition time of 50 seconds. The adsorption of the metal-ligand complex onto the electrode occurs at this stage and the potential chosen was obtained from the optimisation of the deposition potential for the metal-ligand complex at a fixed deposition time and a constant concentration of the metal and the ligand. The deposition time was similarly optimised utilising the optimal deposition potential and a constant concentration of the metal and the ligand.

The OSW AdCSV voltammograms for mercury and lead, in the presence of acetylcholine, were recorded in a negative direction from the accumulation potential to at least 200 mV beyond the reduction peak of the metal complex. The square wave key parameters included: a step potential of 4 mV, amplitude of 25 mV and a frequency set at 15 Hz. The voltammetry experiments were also performed for the metal ion in the absence of the ligand and for the ligand in the absence of the metal ion on the gold electrode surface.

The preparation of the working electrode surface before each run was extensive to ensure reproducibility was obtained. The glassy carbon electrode preparation included dipping in nitric acid, rinsing with distilled deionised water, polishing on a Buehler felt pad with fine alumina and finally being rinsed in the electrolyte of choice several times. The platinum electrode underwent similar treatment. However, for the platinum electrode soaking in a mild hydrogen peroxide solution, before the polishing step, for 10 minutes was also employed in the regeneration of the electrode surface. The soaking step was particularly necessary in cases where the reproducibility of the stripping peak appeared problematic.

The gold electrode required the most extensive preparation of the three solid electrodes, but this is not uncommon, particularly when mercury is being investigated, as the ease of a gold-mercury amalgam formation is well documented. The residual mercury film is removed by firstly rinsing the electrode in distilled water and methanol followed by applying a few drops of 6 M nitric acid and allowing the colour to change from greyish-black to rusty yellow. The step is then repeated, but care should be taken not to use concentrated nitric acid as this will damage the plastic coating of the electrode.

A fine grit pad, whose surface has been wetted with distilled deionised water, is used to give the gold electrode an even matte finish. A diamond slurry of 3 μm is then used on a nylon polishing pad for further treatment of the surface. The polishing steps are critical to ensure the reproducibility of the electrode and thus over-polishing of the surface is preferred to under-polishing. The diamond slurry is oil-based and thus the final step in gold electrode preparation requires rinsing the surface with methanol followed by copious amounts of distilled deionised water and finally the electrolyte.

Cadmium, Copper and Zinc Study:

The AdCSV studies for cadmium, copper(II) and zinc were carried out on the CGME. The linear sweep mode of stripping voltammetry was chosen in place of the OSW format employed above for the mercury and lead study, as the focus of this study was on complex formation rather than very low detection limits. The electrolyte used was TBABr (0.05 mol dm^{-3}) and as with the mercury and lead study, the solutions containing the metal ion and the ligand were deaerated for a minimum period of 5 minutes, during which time the metal-ligand complex formation is expected to have occurred. Thereafter, a flow of nitrogen gas was maintained over the solution throughout the measurements.

Optimisation of the metal-ligand ratio, as per the mercury and lead study, resulted in a favourable ligand concentration of 4.0×10^{-4} mol dm^{-3} being used and varying metal concentrations from 6.7×10^{-6} mol dm^{-3} to 4.0×10^{-5} mol dm^{-3} to demonstrate the linear relationship between the two. The optimum deposition potentials were -350 mV, -100 mV and -400 mV for analysis of cadmium, copper(II), and zinc respectively over a period of 50 seconds, in a similar manner to Chapter 2. Voltammograms were recorded in a negative direction from the deposition potential to at least 400 mV past the reduction peak of the metal.

Solid sample analysis:

In the TGA experiment, a milligram quantity of sample was placed in a heat and acid cleaned weighing pan and scanned over a temperature range of 50-300°C. The mass loss versus temperature plots generated for the ligand alone and the proposed acetylcholine-mercury complex were compared noting any differences in mass lost and the onset temperature of the decomposition stages.

In the solid infrared analysis, the pressed disc technique was applied. Pure, dry potassium bromide was intimately ground with a small quantity of freeze-dried sample using a mortar and pestle. The mixture was then added to a manually operated press system for the preparation of the KBr disc. The possibility of impurities in the KBr was eliminated with the use of a blank disc system. A powder for the diffraction pattern analysis was obtained by coarsely grinding the sample and evenly packing it into a clean, shallow grooved aluminium sample holder, before it is mounted on the XRD machine.

3.3 RESULTS:

Electrochemical Study:

Mercury and Lead Study:

Optimisation of the metal:ligand ratio was completed for lead and used for the rest of the metals studied, see Figure 3.1. A ratio of 1:4, in favour of the ligand, was chosen.

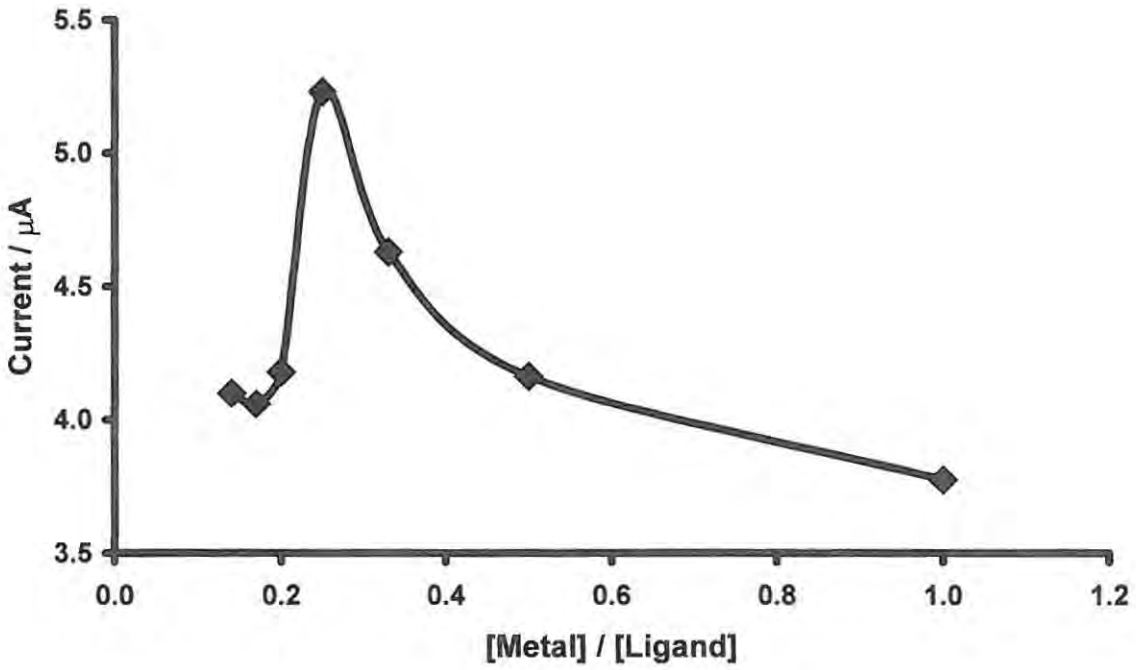

Figure 3.1 Optimisation of the metal:ligand ratio for the Pb^{2+}-ACh complex.

The comparison for the choice of working electrode for the detection of the mercury-acetylcholine complex is shown in Figure 3.2. The platinum and glassy carbon electrodes demonstrated peak currents for the detection of the proposed mercury-acetylcholine

complex, but the platinum electrode suffered from reproducibility problems, whilst the glassy carbon electrode exhibited a smaller peak current as compared with that of the gold electrode.

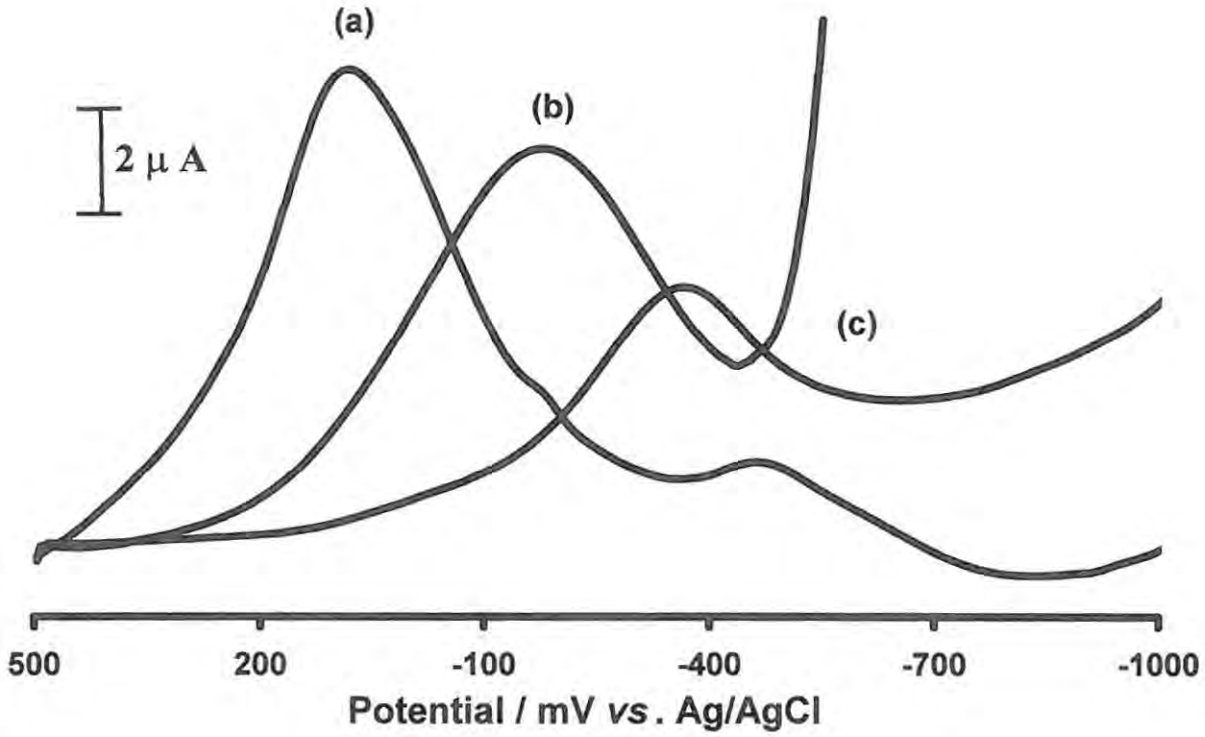

Figure 3.2 Adsorptive cathodic stripping voltammograms obtained for mercury (1.0×10^{-8} mol dm^{-3}) in the presence of acetylcholine (4.0×10^{-8} mol dm^{-3}) utilising either the gold (a), platinum (b) or glassy carbon (c) working electrode.

In this work the gold electrode proved to be the most stable electrode with the highest peak current value for a comparative analysis between the mercury- or the lead-acteylcholine complex formed, providing the methodical systematic cleaning routine was adhered to.

The choice of the gold electrode for the mercury study is in agreement with work published by Watson *et al.* (1999), where the gold electrode was the electrode of choice for the detection of aqueous mercury.[225] One reason for the use of a gold surface is its high affinity for mercury, which enhances the preconcentration effect.

The use of a gold electrode for the detection of mercury ions in solution is not a new concept, but overcoming the problems associated with mercury-gold amalgam formation at the working electrode surface is still hotly debated.[225,226] In general, solid gold electrodes are less commonly used than the fibre or plated gold surfaces since the solid electrodes were thought to undergo structural changes caused by amalgam formation and hence required time-consuming and complex electrochemical pre-treatment steps.

However, in a review by Bonfil *et al.* (2000) no surface structural changes were noted when the solid gold electrode was used in the anodic stripping voltammetric detection of mercury in comparison to the bulk electrochemical deposition experiment.[226] The reason for this is the fractional surface coverage that occurs during the deposition step, typically less than 1% in ASV. Under such experimental conditions some metal ions form a uniformed adlayer, a process referred to as underpotential deposition. Thus, during repetitive deposition and dissolution of mercury on gold electrodes, as is the case when ASV is applied under typical concentrations below 10^{-7}mol dm^{-3} and for relatively short deposition times or by deposition from higher concentrations in the underpotential deposition region, excellent reproducibility is reached starting from the first run.[226] Watson *et al.* (1999) reported that repetitive mercury measurements, typically employing up to 20 cycles, resulted in a standard deviation of below 5%.[225]

Adsorptive cathodic Osteryoung square wave stripping voltammograms of mercury chloride in the absence and presence of acetylcholine are compared in Figure 3.3 (a) and (b) respectively on a solid gold working electrode. The OSW mode was employed for the mercury and lead experiments in this chapter in order to improve on the sensitivity of the electrode and detection limits obtainable. On addition of acetylcholine there is a slight negative shift in the peak potential (16mV) and this is accompanied by an enhancement in peak current.

The reduction peak for mercury chloride in the absence of acetylcholine was observed at 94 mV *vs.* Ag | AgCl in this work. The shape of the peak shown in Figure 3.3 (b) for the mercury-acetylcholine complex is similar to that of the metal alone, thus suggesting that reduction of the metal-ligand complex occurs at the metal site. Moreover, no reduction peak is observed for acetylcholine in the absence of a metal ion.

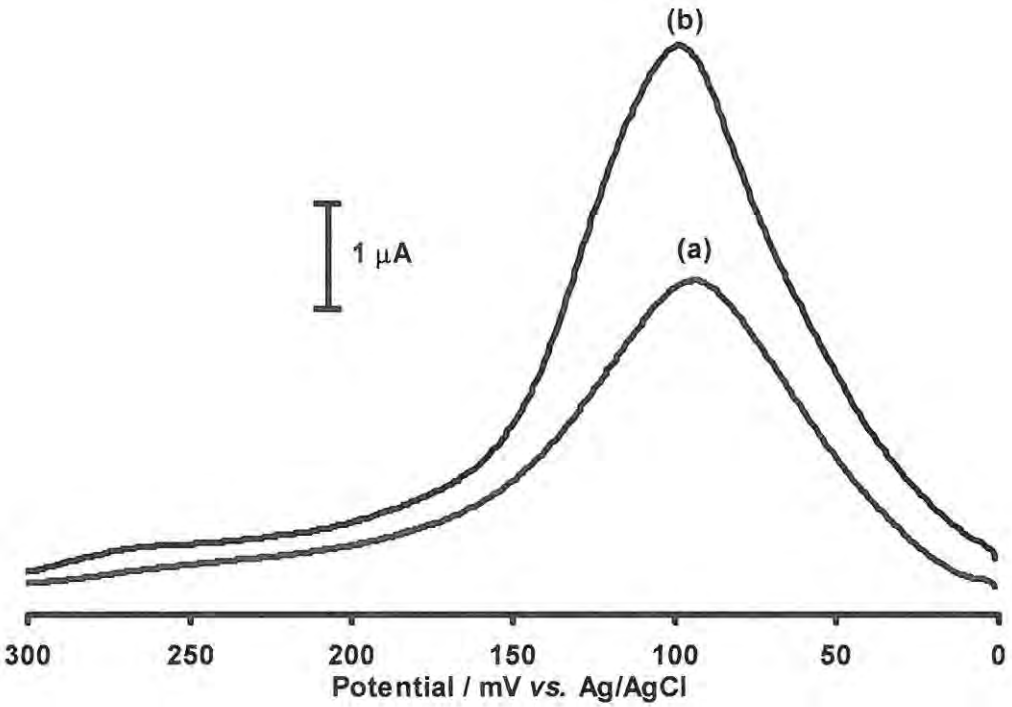

Figure 3.3 Adsorptive cathodic square wave stripping voltammograms obtained for mercury (1.0×10^{-8} mol dm^{-3}) in the absence (a) and presence (b) of acetylcholine (4.0×10^{-8} mol dm^{-3}) respectively.

Figure 3.4 (a) and (b) show the adsorptive cathodic square wave stripping voltammograms of Pb^{2+} chloride in the absence and presence of acetylcholine. The reduction peak for lead in the absence of acetylcholine on a gold working electrode, at neutral pH, is observed at 52 mV versus the reference electrode. To date this is the first observation of lead ions, under these conditions, on a gold surface electrode.

In previous studies, Limson *et al.* (1998) had observed lead alone on a mercury film glassy carbon electrode under acidic conditions at around –400 mV,[198] whilst Yao and Ramelow (1998) observed lead on a biomass modified carbon paste electrode at –530 mV *vs.* a

saturated calomel electrode,[227] whereas in this work Pb^{2+} is observed at +52 mV on a gold electrode. On addition of acetylcholine the lead peak is shifted in a positive direction (by 44 mV) and was also accompanied by an enhancement in peak current observed. The reduction of the metal-ligand complex is thought to occur at the metal site in a similar manner to that of mercury, since no OSWV for acetylcholine alone were recorded.

The enhancement in the reduction current on addition of acetylcholine to the solution containing Pb^{2+} or Hg^{2+} is an indication of the *in situ* formation and accumulation of the mercury- or lead-acetylcholine complex onto the gold electrode. The shift in the reduction peak to a more negative potential on addition of acetylcholine to the solution containing the mercury ion suggests that the mercury-acetylcholine complex formed is more difficult to reduce than the free metal. A positive shift, in the case of the lead-acetylcholine complex, suggests that the complex was more easily reduced than the metal ion itself. The extent of the shift in reduction peak potential of the metal on addition of acetylcholine is a good measure of the stability of the mercury- or lead- acetylcholine complex formed *in situ*.

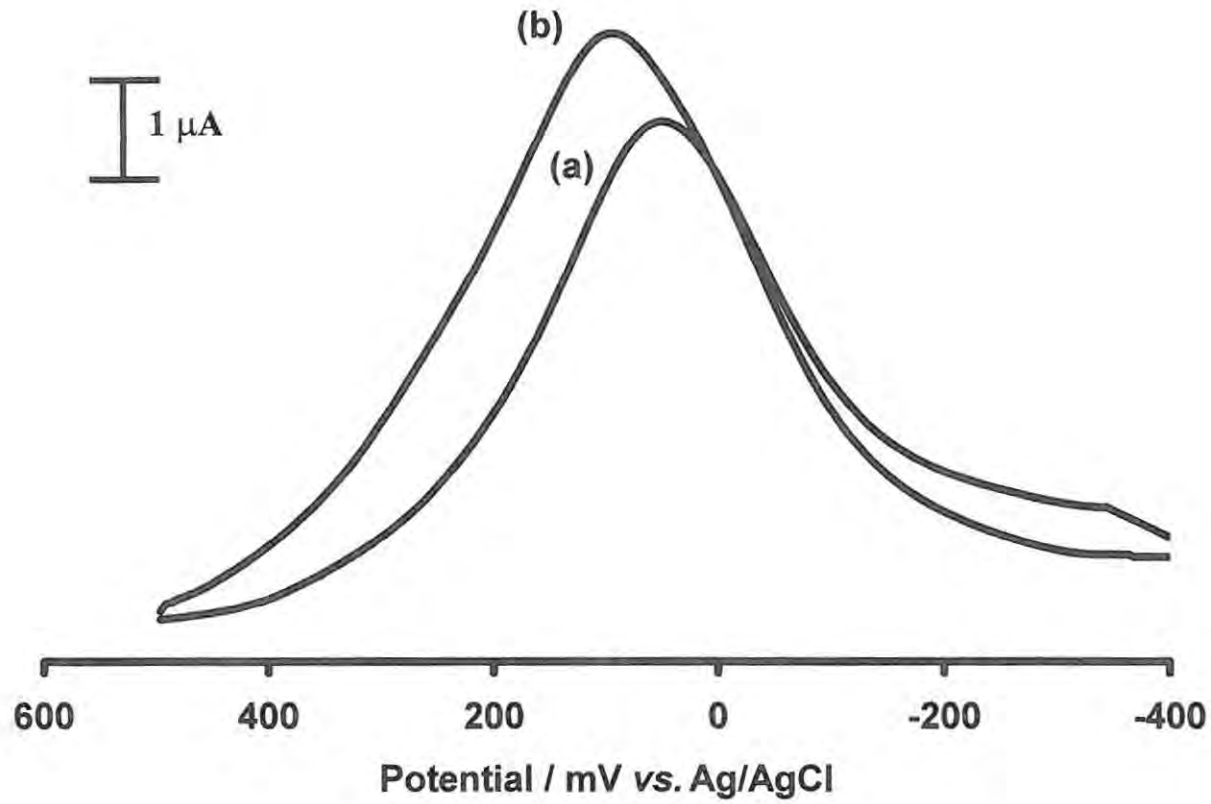

Figure 3.4 Adsorptive cathodic square wave stripping voltammograms obtained for lead (1.0×10^{-8} mol dm^{-3}) in the absence (a) and presence (b) of acetylcholine (4.0×10^{-8} mol dm^{-3}) respectively.

Figure 3.5 exhibits the linear concentration behaviour of acetylcholine with increasing concentrations of mercury (a) and lead (b) ions and a detection range of 2.5×10^{-10} to 2.0×10^{-9} mol dm^{-3}. The gold electrode demonstrated reproducibility with less than a 5% error margin for either metal investigated. The magnitude of the slope is an indication of the affinity of the ligand for the metal ion. Lead showed the largest slope and hence greatest affinity for acetylcholine in comparison to mercury.

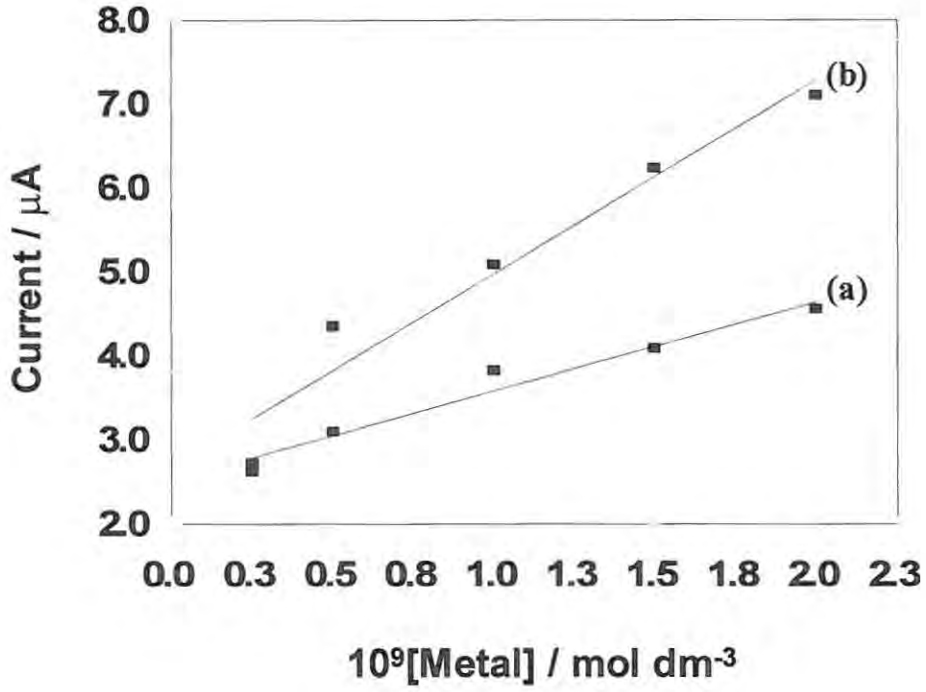

Figure 3.4 Effects of metal ion concentration on the adsorptive cathodic square wave stripping voltammogram currents of Hg^{2+} (a) and Pb^{2+} (b), in the presence of acetylcholine (1:4 ratio in ACh favour).

Cadmium, Copper and Zinc Study:

The CGME utilized in the cadmium, copper(II) and zinc study afforded reproducible results (less than a 4% error) in 50 seconds per sample run. Ghoneim *et al.* (2000) have described an electrochemical simultaneous determination method of detecting eleven trace metals in water samples utilizing variations on the differential pulse stripping voltammetry method at a HDME.[228] In the study [128], cadmium and copper(II) were observed, under pH = 1 at approximately –800 mV and –100 mV *vs.* a Ag | AgCl, respectively. Limson *et al.* (1998) made use of a mercury film electrode to observe cadmium in a similar region,

whilst copper(II) and zinc where reported at around –50 mV and –1200 mV, respectively.[198]

In the present study, cadmium, copper(II) and zinc, alone on the CGME, were observed at –593 mV, -220 mV and –1610 mV, *vs.* Ag|AgCl, respectively. On addition of acetylcholine to the solution, enhancements in peak currents were observed for all three metals concerned. Figures 3.6 (Cd^{2+}), 3.7 (Cu^{2+}) and 3.8 (Zn^{2+}) illustrate the AdCSV of the metal ion alone (a) and in the presence of acetylcholine (b). Table 3.1 highlights the shift in peak potential upon the addition of acetylcholine, ΔE_p. The direction of the shift is indicative of the ease of reduction of the complex on the electrode, whilst the magnitude of the shift is a measure of stability. A positive ΔE_p value for example may be interpreted as the complex being unstable.

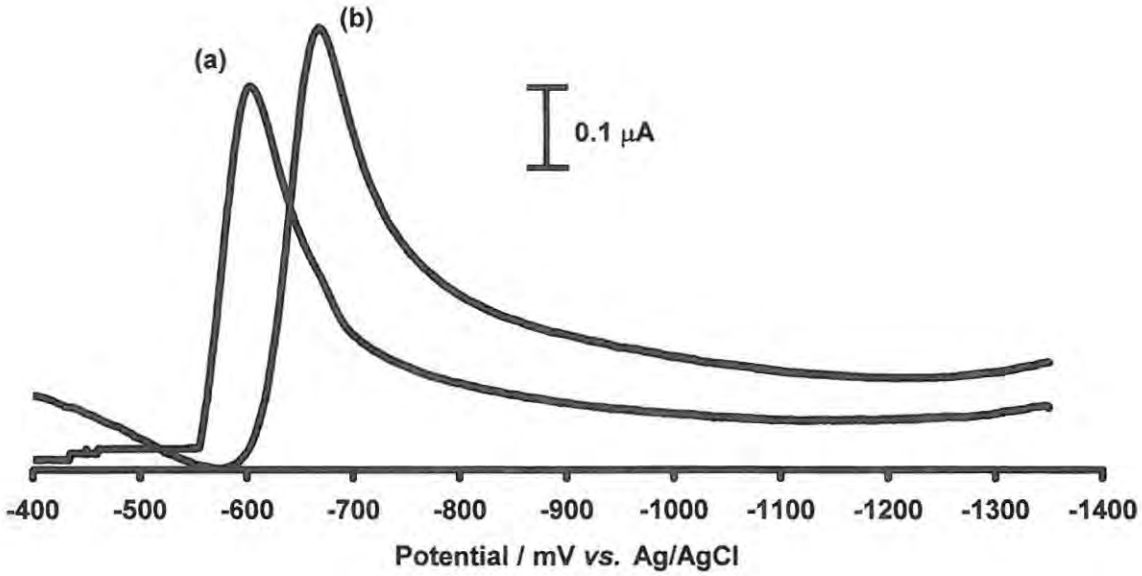

Figure 3.6 **Adsorptive cathodic stripping voltammograms obtained for cadmium (1.3×10^{-5} mol dm^{-3}) in the absence (a) and presence (b) of acetylcholine (4.0×10^{-4} mol dm^{-3}) respectively.**

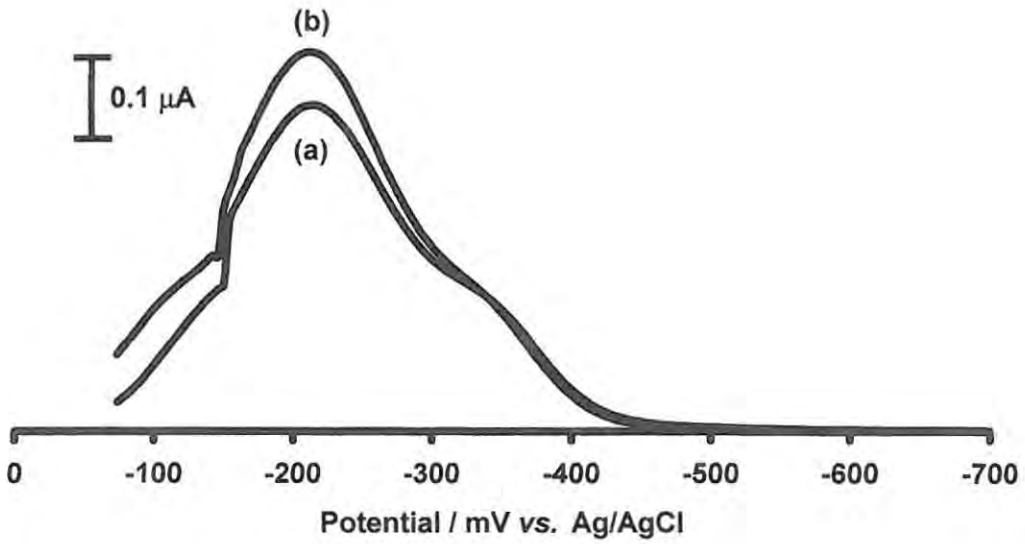

Figure 3.7 **Adsorptive cathodic stripping voltammograms obtained for copper(II) (1.3×10^{-5} mol dm^{-3}) in the absence (a) and presence (b) of acetylcholine (4.0×10^{-4} mol dm^{-3}) respectively.**

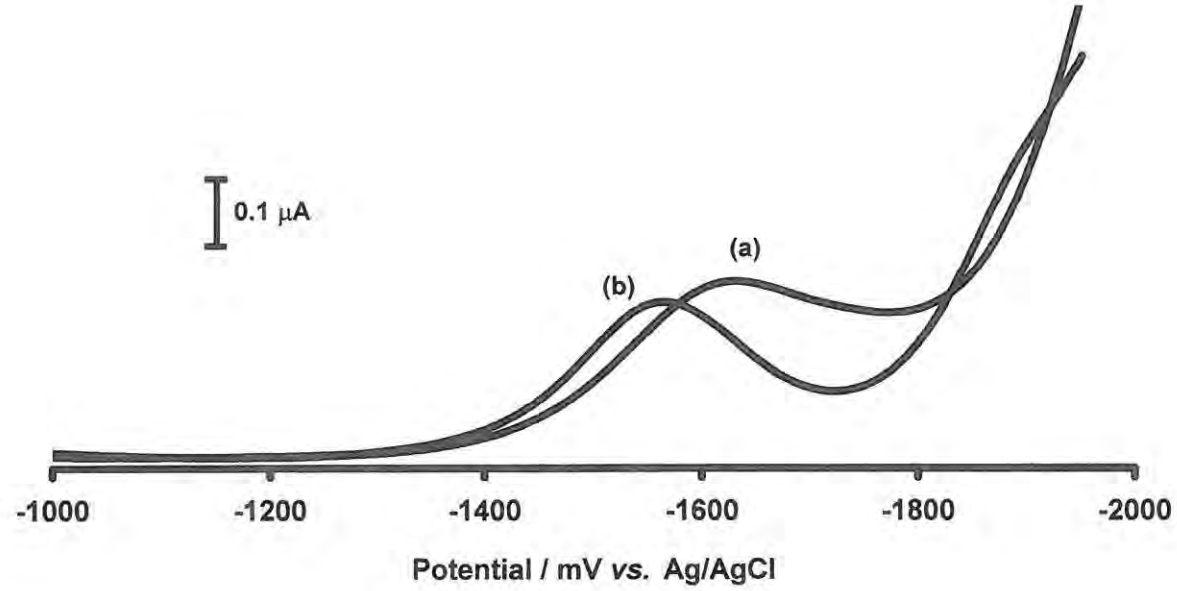

Figure 3.8 **Adsorptive cathodic stripping voltammograms obtained for zinc (1.3 x 10^{-5} mol dm^{-3}) in the absence (a) and presence (b) of acetylcholine (4.0 x 10^{-4} mol dm^{-3}) respectively.**

Table 3.1 AdCSV parameters for the metal-acetylcholine complexes:

[a]Metal	[b]ΔEp (mV)	[c]Slope (A/mol dm^{-3})
Cadmium	-49	2.21 (0.965)
Copper (II)	-10	0.88 (0.982)
Zinc	+56	2.14 (0.915)

[a]Metal concentration = 1.3 x 10^{-5} mol dm^{-3}, acetylcholine concentration = 4.0 x 10^{-4} mol dm^3. [b]ΔE_p is the difference between the peak potentials of the metal ions and those of the metal-ligand complexes. [c]Regression coefficients are shown in brackets.

Peak currents for the metal-acetylcholine complexes increased with an increase in the concentration of the metal as shown in Figure 3.9. The plots are linear, the slopes of which along with the regression coefficients are listed in Table 3.1. The highest currents were observed in the presence of cadmium, whilst lower currents and overlapping of lines were observed in the presence of copper (II) and zinc.

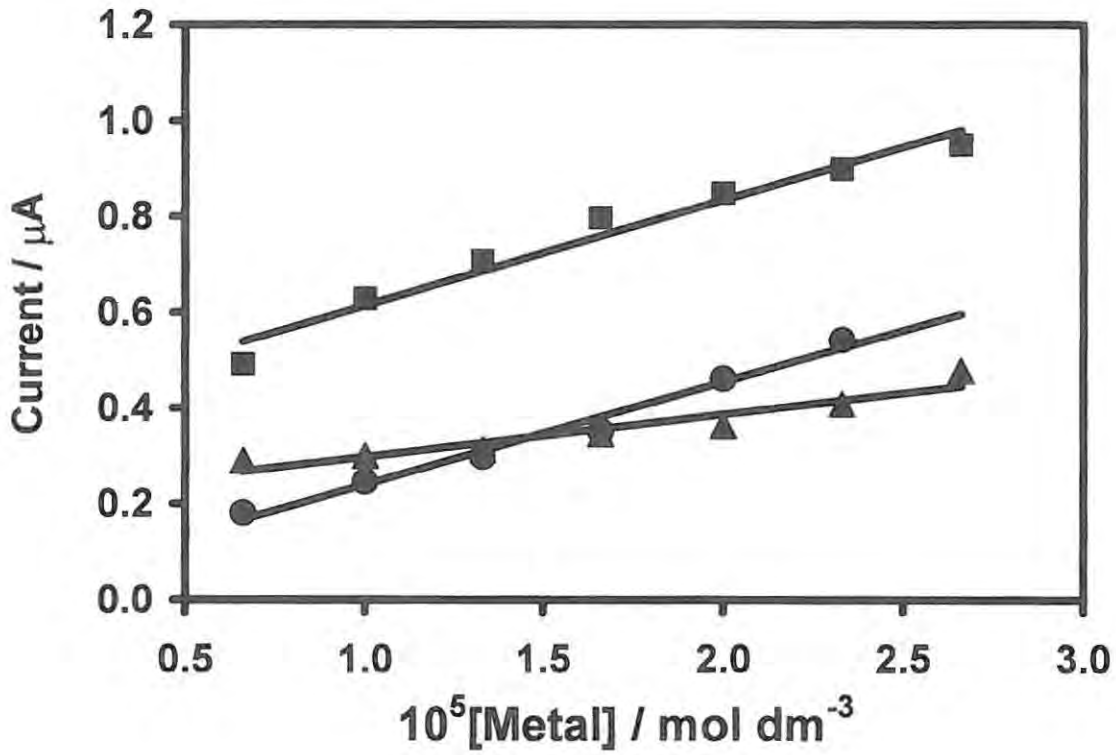

Figure 3.9 **Variation of currents with metal ion concentration for 4.0×10^{-4} mol dm^{-3} acetylcholine. Zn^{2+} (●), Cd^{2+} (■) and Cu^{2+} (▲)**

Solid sample analysis:

Apart from the visible structural differences between the freeze-dried acetylcholine sample and that containing the mercury ion, differences were also observed in the TGA decomposition plots, IR spectra and X-ray powder diffraction patterns. The mercury-acetylcholine freeze-dried complex was an off-white colour with a needle-like crystalline structure. The product was far less hydroscopic than the freeze-dried ligand form alone, which was a pure white colour.

The TGA mass loss observed in the freeze-dried ACh sample (Figure 3.10) is compared with that for the proposed Hg-Ach complex in Figure 3.11. For the ligand alone, a mass loss of 5% is observed in the temperature range of 96-159°C, which most likely corresponds to the loss of water from the sample. ACh is very hydroscopic in nature with a large quantity of the water being trapped in the crystal lattice of the sample. A single step decomposition stage is observed for the ligand with an onset temperature range of 159-263°C, corresponding to a mass loss of more than 90%.

A difference between the ligand and the proposed Hg-ACh complex is noted in Figure 3.11, where a two-step decomposition process is observed with higher onset temperatures than those seen for the ligand alone. In the temperature range of 124-204°C a mass loss of around 64% is noted. A further mass loss of 33% is observed in the region of 205-289°C. The increase of the onset temperature range suggests a more thermodynamically stable arrangement in the crystal structure indicative of a metal ion association with the ligand. The first mass loss may correspond to the loss of water trapped within the crystal structure as well as part melting of the ligand itself, whilst the second and final mass loss would

refer to the total decomposition of the solid. Interestingly there was no mass loss associated with water below 100°C as is often observed with uncoordinated water molecules in the Hg-ACh sample, which is in agreement with the visual observation that this sample is less hydroscopic than the ligand itself.

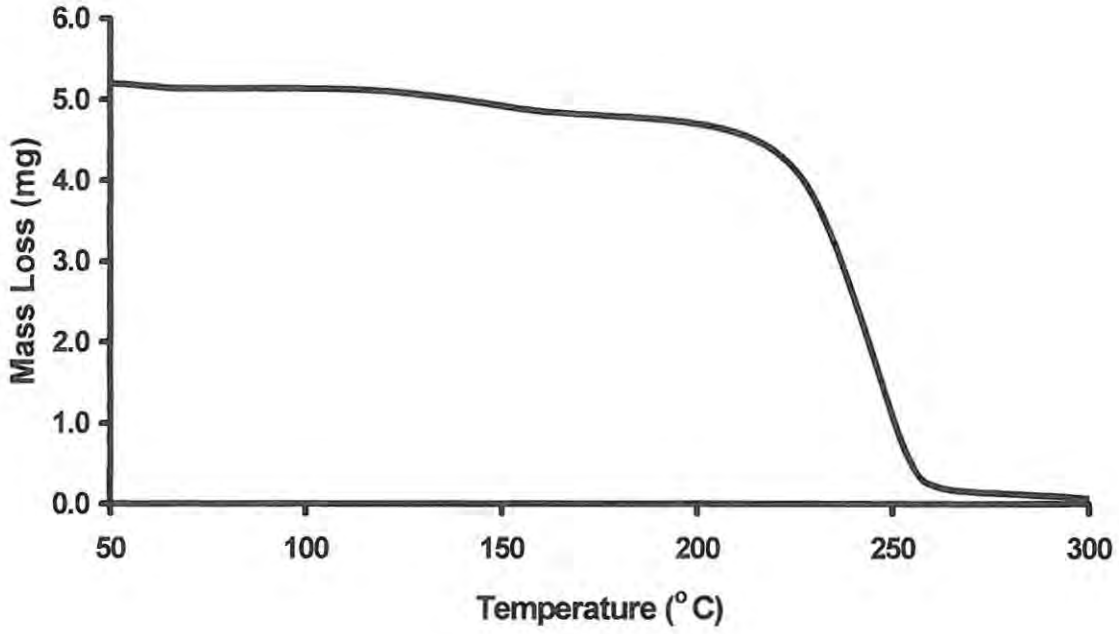

Figure 3.10 The TGA decomposition curve of the freeze-dried ACh sample.

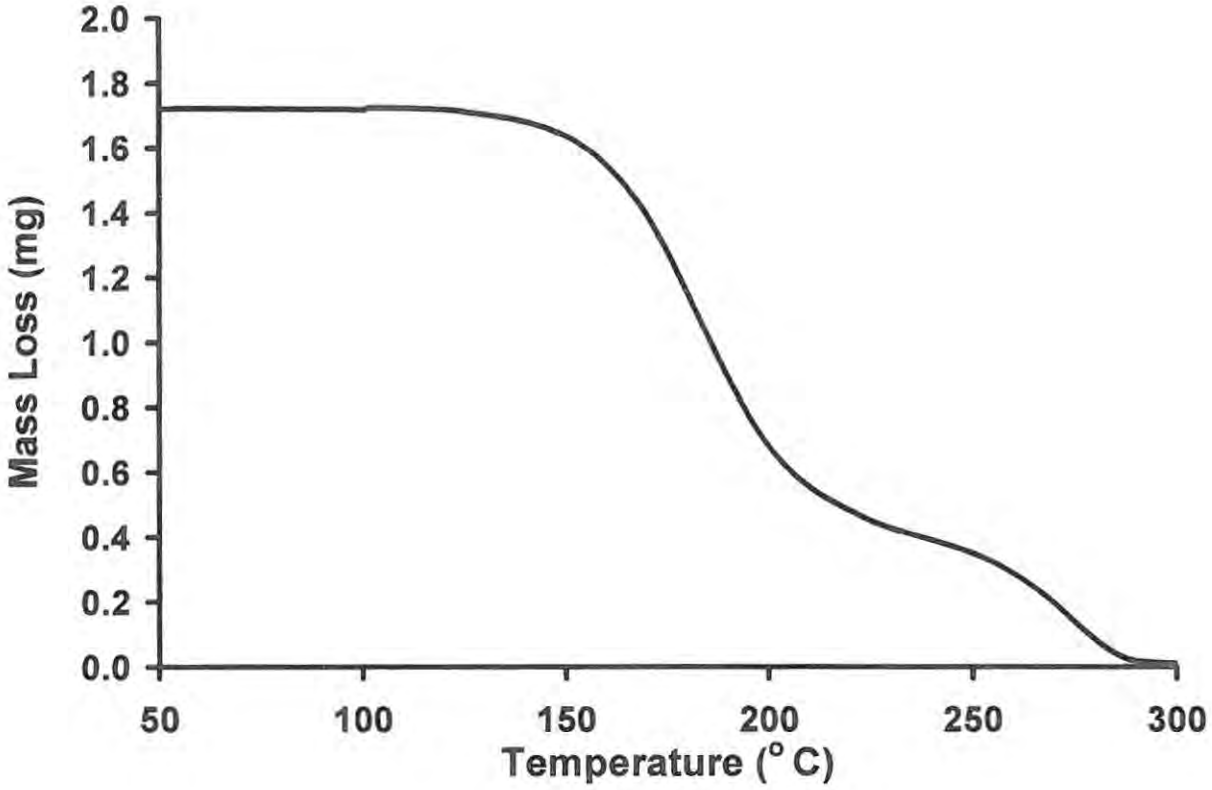

Figure 3.11 The TGA decomposition curve of freeze-dried Hg-ACh.

The IR spectra obtained for the freeze-dried ligand alone, Figure 3.12, and in combination with mercury, Figure 3.13, display significant changes indicative of complex formation between the metal ion and the ligand. The νC=O of the ligand alone was observed at the 1747 cm^{-1} band, whilst in the presence of the mercury ion the band is shifted to a lower wavenumber of 1727 cm^{-1}. The shift to a lower wavenumber is an indication of a more ordered structure, which is indicative of coordination between the metal and the ligand.[220]

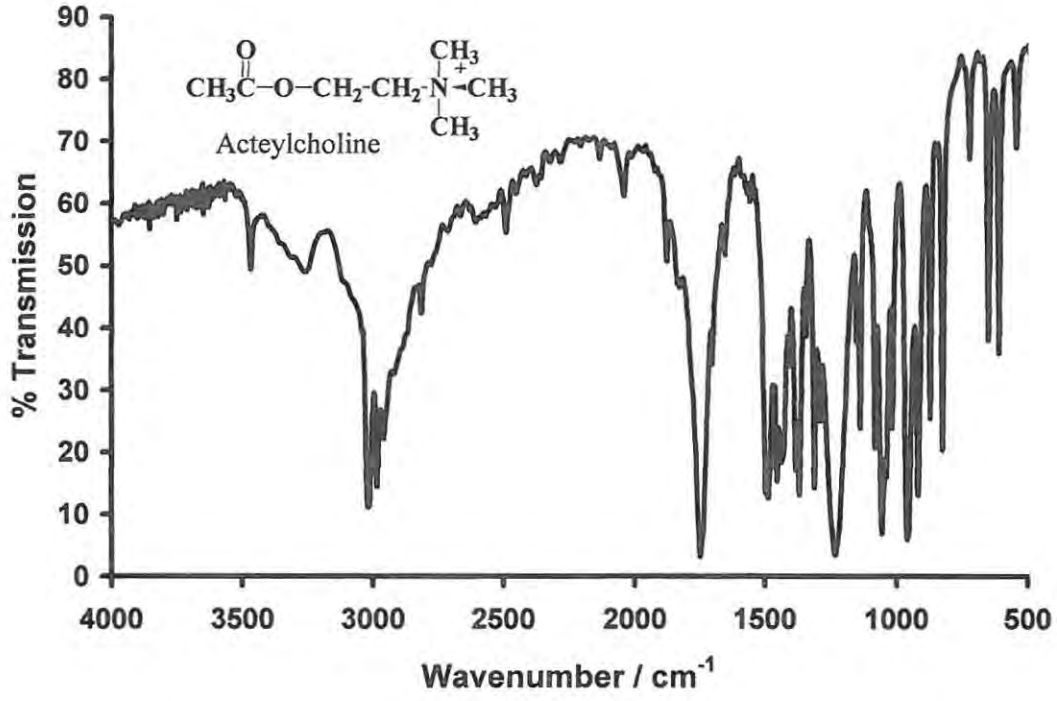

Figure 3.12 IR spectrum of the freeze-dried ACh sample alone.

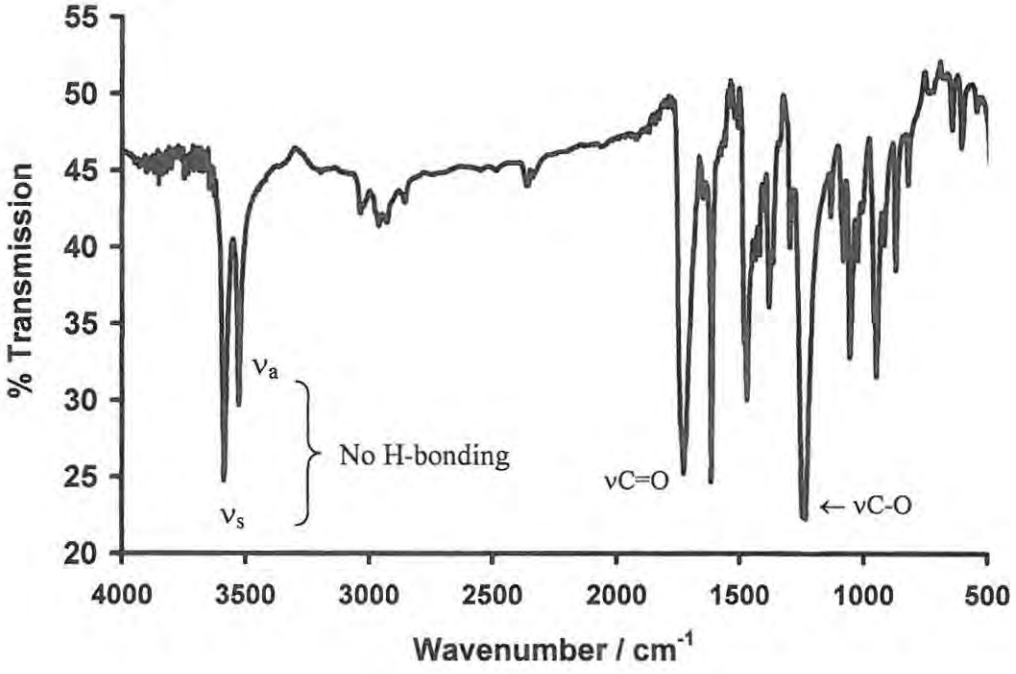

Figure 3.13 IR spectrum of the freeze-dried Hg-ACh sample.

Further evidence for coordination is observed in the presence of ν_a and ν_s stretches of the water molecules in the crystal structure of the proposed mercury-acetylcholine complex at 3587 and 3527 cm^{-1} respectively. The water molecules do not undergo hydrogen bonding and an δO-H bending stretch for the lattice water is noted at around 1614 cm^{1}. The water molecules are thought not to be coordinated to the structure, but instead trapped inside the crystal lattice as no rocking or wagging bands have been observed in the region between 800–500 cm^{-1}.

A change in the νC-O band is noted between the ligand and that of the proposed mercury complex. In the presence of the metal ion the band is split in two and there is a slight shift in wavenumber, indicating changes occurring in the O-C-O region of the acetylcholine molecule on addition of mercury.

Changes were also observed in the XRD samples. However, this technique is very dependent upon sample preparation. The crushing/grinding of the sample may cause significant differences in the spectra obtained, thus with the physical differences between the ligand and the Hg-ACh complex, the very hydroscopic nature of the ligand in particular should be noted and this technique should then only serve to corroborate existing evidence of complex formation.

The spectra depicted in Figure 3.14 and 3.15, for the ACh sample alone and in the presence of Hg^{2+} ions respectively, do however, show signs of metal-ligand interactions. Typically a shift in the peak positions seen between the two spectra indicates changes in the crystal structure, along with the disappearance of certain peaks and a more defined spectrum with

narrower peaks are all suggestive of the presence of a metal ion in the complex. Unfortunately the wet-like nature of the ligand may also account for many of the changes seen in the spectra and it was not possible to assign specific crystal lattice changes to the proposed metal-ligand complex.

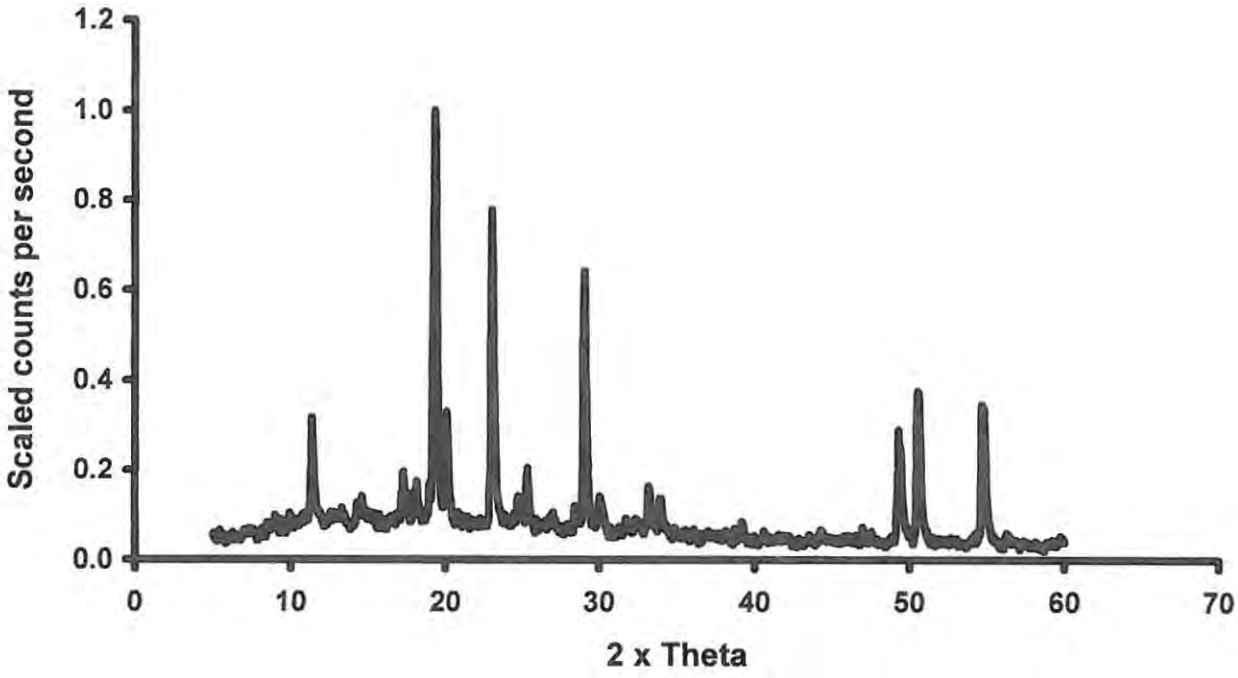

Figure 3.14 The XRD pattern observed for the freeze-dried ACh sample.

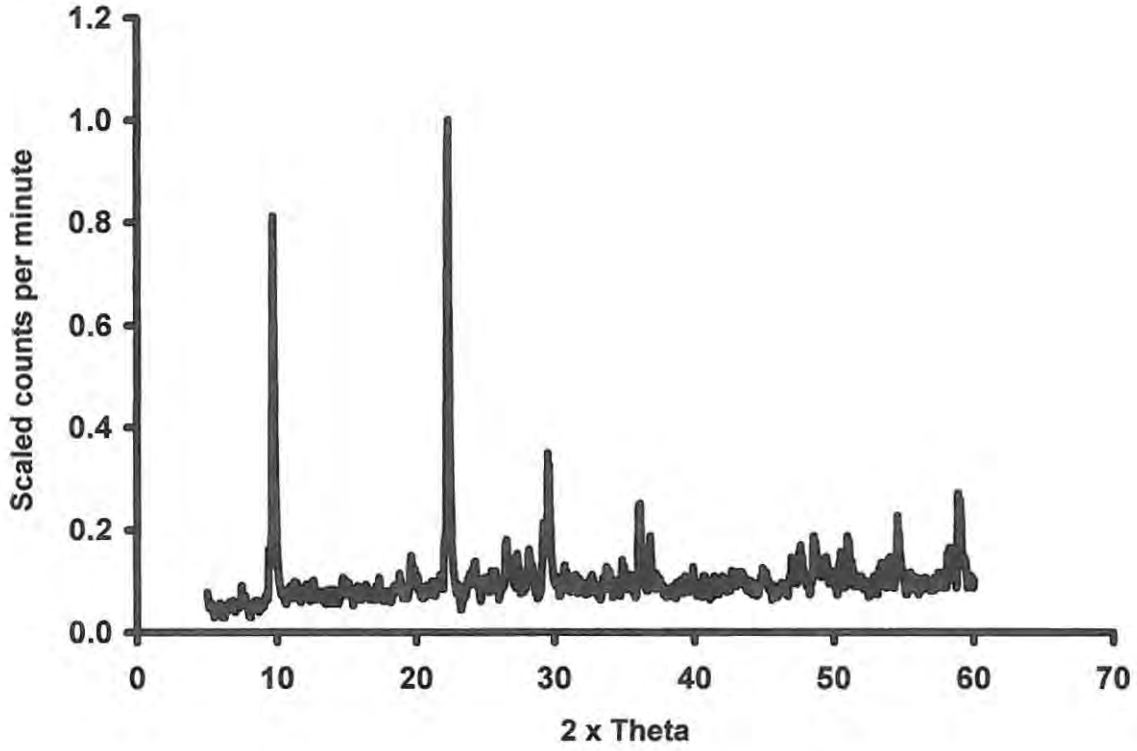

Figure 3.15 The XRD pattern observed for the freeze-dried Hg-ACh sample.

3.4 DISCUSSION:

From the results obtained it can be concluded that mercury, lead, cadmium, copper and zinc all form complexes with acetylcholine. However, in the lead and mercury comparative study, lead was shown to form a more stable complex with ACh than mercury. In addition, lead was also seen to possess a greater affinity for the ligand. Neurotransmitters such as acetylcholine are structurally specific for their receptors and any changes in their structure or polarity could have drastic consequences on the efficacy of the

neurotransmitter and its response to stimuli. The formation of an *in situ* complex with acetylcholine by both lead and mercury, imply that these metals could contribute to the acetylcholine deficiency observed in certain neurodegenerative disease cases such as AD. Both of these metals are common environmental toxins, with mercury dental fillings constituting the largest single source of mercury exposure in the general population, thus further research into the prolonged effects of mercury and lead intake and accumulation within the body is a future avenue of investigation.

In the study of ACh in the presence of cadmium, copper and zinc, the ligand showed the greatest affinity, based on the largest slope in Table 3.1, for the cadmium ion followed by zinc and then copper. The preference of ACh for environmentally toxic cadmium ion over those divalent cations that occur naturally in the body, such as the zinc and copper, should be noted as this may lead to further insight into metal accumulation or disturbances in ACh levels observed in some cases of degenerative disease states.

The formation and characterisation of a solid mercury-acetylcholine complex lends further strength to the *in situ* complex formation potential of ACh in the presence of various divalent cations and mercury itself in particular. Increased mercury levels and decreased ACh levels observed in postmortem brain tissue of AD suffers lead to the hypothesis that mercury may be involved in ACh complex formation, thus altering its efficacy in the neural network. An *in vivo* study is, however, needed to further validate the *in vitro* results observed thus far, but this study may go a long way to substantiate the removal of mercury from dental fillings.

CHAPTER 4

The pinealectomy study

4.1 INTRODUCTION:

A holistic view of brain function cannot ignore the growing awareness of the pineal gland in homeostatic control of the body and brain. In particular, as per the introduction in Chapter 2, two pineal indoleamine substrates of the pineal gland, namely melatonin and serotonin, have been shown to interact with a number of metal ions.[185,198] Such interactions have been shown to have possible biological significance, particularly with reference to melatonin's ability to protect against tissue damage.[185]

The life-long reduction of endogenous melatonin, due to a pinealectomy, has been positively linked to the increased accumulation of oxidatively damaged products as the animal ages.[229] Furthermore a pinealectomy, which eliminates the night-time rise in circulating and tissue melatonin levels, has been shown to worsen both reactive oxygen species-mediated tissue damage and brain damage after focal cerebral ischaemia and excitotoxic seizures. That melatonin protects against hippocampal neurodegeneration linked to excitatory synaptic transmission is fully consistent with the study undertaken by Skaper *et al.* (1999).[230] However, Willis and Armstrong (1999) have shown that melatonin may also have detrimental side effects, which may pose considerable problems

in neurological diseases characterised by dopamine degeneration.[231] The study highlighted the importance of aberrant amine production in neurological disease and demonstrate that treatments that reduce endogenous melatonin bioavailability can ameliorate experimental PD.[231]

Miguez *et al.* (1997) examined the influence of the pineal gland and its hormone melatonin on the metabolism of serotonin (5-HT) in discrete areas of the forebrain, such as the striatum and the nucleus accumbens, and the midbrain raphe.[232] The results point to the striatum as a target area for the interaction between pineal melatonin and the serotonergic function. However, a differential effect of the melatonin injected on areas containing serotonergic terminals and cell bodies is suggested, which may be relevant for the mode of action of melatonin and its behavioural effects.[232]

Beskonakli *et al.* (2000) investigated the effect of a pinealectomy on some immune parameters including zinc pool alterations.[233] The results showed that the plasma zinc level was significantly reduced in the third week after the pinealectomy. This was particularly noted in the pinealectomised neonatal rats and the wound healing process, affected only in pinealectomised neonatals, was restored to normal by melatonin administration.[233] Limson *et al.* (1998) further investigated the link between melatonin and metals by examining the possible interaction of melatonin and its precursors with aluminium, cadmium, copper, iron, lead and zinc.[198] Melatonin, serotonin and tryptophan exhibited variable affinity and sensitivity for the metals studied.[198] In addition, of the three ligands observed, only melatonin was found to bind all the metals, thus implicating melatonin in a metalloregulatory role and possible metal detoxification of the brain.[198] The metal binding role of melatonin is further favoured as a result of melatonin's

lipophilic, hydrophilic nature, permitting it to move freely across all cellular boundaries and thus facilitating the removal of toxic metal concentrations in the CNS.[234] Moreover the definite link between metals, essential and toxic, and the onset of neurodegenerative diseases cannot be ignored, as noted in Section 1.5.1.

In earlier works published by Earl (1961) [235] and Thompson (1961),[236] copper levels within the brain were shown to vary anatomically. Wong and Fritze completed a neutron activation detection of copper, manganese and zinc in the pineal body and other areas of brain tissue.[237] The study revealed an approximate fixed ratio of Cu:Mn:Zn in all brain regions investigated. However, the unexpected feature of the results was the high concentration of all three trace metals in the pineal body.[237]

In a more recent study Uitti *et al.* (1989) analyzed four brain regions (frontal cortex, caudate nucleus, substantia nigra, and cerebellum) in 36 human brains for concentrations of 24 metals (Ag, Al, As, B, Be, Ca, Cd, Co, Cr, Cu, Fe, K, Pb, Mg, Mn, Mo, Na, Ni, P, Se, Ti, V, W, Zn).[238] Regional metal concentrations, measured using atomic absorption and atomic emission spectroscopy, were compared between 9 Parkinson's disease (PD) brains, 15 brains from patients with other chronic neurological diseases, and 12 control brains. Parkinsonian brains showed lower concentrations of magnesium in the caudate nucleus and copper in the substantia nigra than control brains. These findings may represent an aetiologically important clue to parkinsonism.[238]

Finkelstein *et al.* (1998) discovered that within the brain, lead-induced damage occurs preferentially in the prefrontal cerebral cortex, hippocampus and cerebellum.[239] Interestingly, lead poisoning is one of the most significantly preventable diseases of

environmental origin and, in the USA, one of the top four diseases in young children.[240] The primary target for lead is the nervous system, however the target areas or mechanism by which this metal exerts its neurotoxic effects is still not clear today. The neuropharmacological toxicity effects include lead affecting the inhibition and facilitation of neurotransmitter release, modulation of ion conductance thereby affecting the electrophysiological output of the neuron.[172,240,241]

In a study conducted by Kumar *et al.* (1996), the effect of cadmium in brain has been shown to be region-specific and most pronounced in the olfactory bulb.[242] Gupta *et al.* (1990) have noted that cadmium significantly increases the levels of 5-HT and 5-HIAA in all brain regions of adult rats, while the levels of 5-HT and 5-HIAA were significantly decreased in most of the brain regions of growing rats.[243] The accumulation of cadmium in all the brain regions was significantly more marked in growing rats compared to adults after identical exposure.[243]

As discussed in Section 1.5.1, cadmium in its ionic form shows great chemical similarity with two biologically important metal ions, Zn^{2+} and Ca^{2+}. The metal ion may displace zinc from its cysteinated coordination due to its "softer" and more thiophilic nature, but cadmium may also be substituted for calcium in bone tissue. Cadmium is generally regarded to be more toxic than lead. However, under physiological conditions it cannot be bioalkylated to form potentially membrane-penetrating organometallic compounds such as R_2Cd or RCd^+.[84]

The pathological process in AD involves amyloid beta (Abeta) deposition and neuronal cell degeneration, but the link to copper mediated neurotoxicity was highlighted by White *et al.* (1999) in a recently reported study.[123] Here the neurotoxic Abeta peptide is derived from the amyloid precursor protein, which was shown to reduce copper(II) to copper(I) and this activity could promote copper-mediated neurotoxicity. However, copper has long since been known to play a role in neurodegeneration, but the mechanism behind the neuronal-specific toxicity of copper to date remains unclear.[123]

The present study aims to demonstrate the role of melatonin as a metal scavenger in the brain by comparing metal levels observed in pinealectomised male Wistar rats versus the control animal groups. Electrochemical detection was chosen as the tool for this study for its high sensitivity (typically in the order of 10^{-10}-10^{-13}M) and simultaneous determination of certain metal ions. The anodic stripping voltammetry (ASV) method was used in this study, as this technique has enjoyed much success in the analysis of a range of toxic heavy metals in flowing solutions, soil and biological samples. The simultaneous determination of zinc, cadmium, lead and copper in the urine of patients with Blackfoot Disease is an example of its application to biological samples.[244]

4.2 EXPERIMENTAL:

4.2.1 REAGENTS:

All reagents used were of analytical grade and unless otherwise stated, all solutions were prepared fresh daily with distilled deionised water. Melatonin was purchased from Sigma (M.O-USA), whilst the sodium chloride for the saline solution was a product of BDH chemicals (SA). Tetrabutylammonium bromide (TBABr), purchased from Sigma (M.O-USA) was the electrolyte of choice. Metal ion standards were prepared as per Section 3.2.1 from the corresponding metal chloride salts, all obtainable from SAARCHEM-HOLPRO Analytical (South Africa).

4.2.2 APPARATUS:

The animals were dosed subcutaneously (s.c) using 1 ml hypodermic syringes. Stripping voltammograms were obtained with the BioAnalytical Services (BAS, Lafayette, Indiana, USA) CV-50W voltammetric analyser. A silver | silver chloride (3 mol dm^{-3} KCl) electrode and a platinum wire were employed as the reference and auxiliary electrodes, respectively. A controlled growth mercury electrode (CGME), BioAnalytical Systems model MF-9058, was the working electrode of choice for this study.

4.2.3 METHOD:

Preliminary animal studies:

Initially the whole brain tissue of untreated animals (male rats of the Wistar strain weighing between 200-250g) was scanned using ASV to identify the metals observable in the homogenised brain tissue. The samples were prepared by homogenising the brain tissue with phosphate buffered saline (pH 7.2) in cold conditions. The homogenate was then boiled in a 2:1 ratio nitric to perchloric acid at 200°C till the solution had evaporated to dryness. The evaporate was then redissolved in 25ml distilled deionised water and kept in a sealed vessel in the fridge until the electrochemistry experiments could be performed on the samples. Once the metals in the ASV window were known, their parameters were optimised and work began on determining the metal content per gram of the three major sections of the brain namely: the cerebellum, cortex, and striatum.

Surgery:

The method used for all pinealectomies in this study was that of Hoffman and Reiter (1974).[245] A drill was fitted with a special drill bit, see Figure 4.1, made according to the specifications, consisting of a long shaft with serrated edges and an adjustable collar, fitted with Allen keys, was attached to the shaft.[245] The collar is used to vary the extent to which the bone of the skull could be penetrated, so as to prevent damage to the underlying brain tissue.

Figure 4.1 The drill bit adapted from Reiter and Hoffman [245] (the collar was removed to view the serration design of the bit).

The rats were anaesthetised with diethyl ether, and immediately, the head of the animal was rigidly mounted onto the stereotaxic apparatus so that it was temporarily immobilised, see Figure 4.2 (A). The fur around the skull region was then shaved and a neat antero-posterior incision was made along the midline of the skull, from the area posterior to orbit the suture. Alcohol swabs (70%) were used to wipe the area clean and the underlying tissue was carefully parted using a sharp scalpel.

The lambda axis, above the transverse and saggital sinuses was thus exposed. The drill was centered on this axis and a disc shaped hole was drilled into the skull to the desired depth, the region is indicated in Figure 4.2 (B). The bone was carefully removed so as to prevent excessive bleeding. A fine forcep was inserted into the junction of the two sinuses and the pineal gland was rapidly removed. The gland was easily discernible, being paler than the rest of the tissue and approximately the size of a pinhead. The invasive nature of

the procedure resulted in bleeding, which was eased by rapidly replacing the bone disc into its original position and applying gentle pressure on it using and alcohol saturated cottonwool swab. The skin flaps were then pulled together and held with a forceps, followed by deft suturing of the wound.

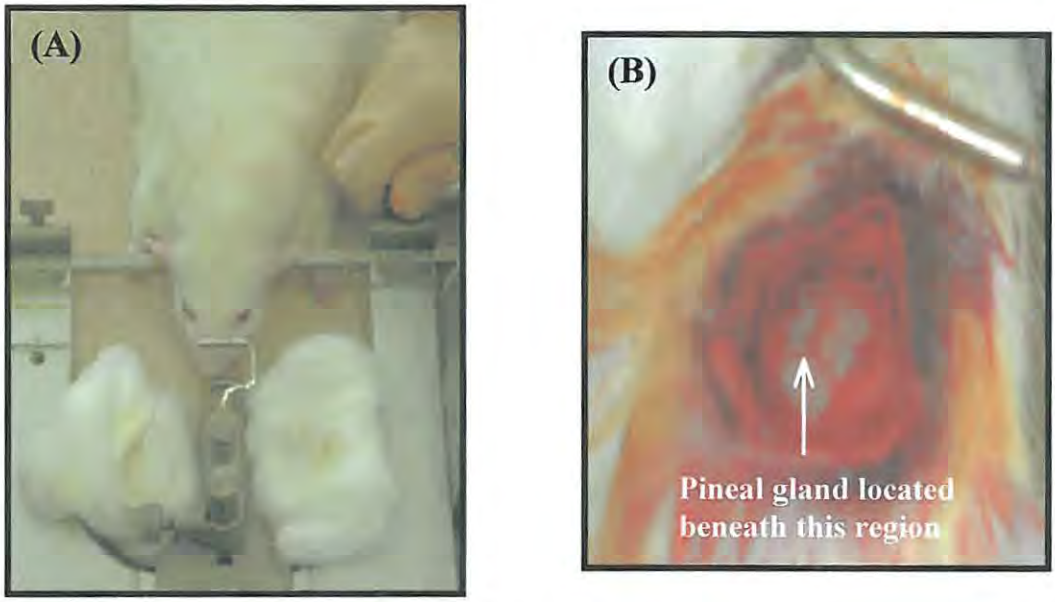

Figure 4.2 The sterotaxic mounting of the animal (A) and region of interest in the pinealectomy procedure (B).

The rat was then placed on a warm base near a thermostatically controlled oscillating heater. Recovery time from the anaesthetic ranged between 10 and 20 minutes. All the rats were housed in the animal room with an automatically regulated lighting cycle of Light:Dark 12:12 and allowed access to a standard diet and water *ad libitum*. The rats were housed individually for no less than six days after the operation, to prevent injury to

the operated area. Sham operations were carried out in a similar manner, except that the pineal was not removed. After removal of the bone disc of the skull the pineal gland was lightly touched without it being displaced. The bone disc was then replaced, the wound sutured and the animal was allowed to recover as described for the pinealectomies. Rats for the following study were then used after a minimum of a two week post-operation period.[245]

Treatment regimes:

The animals were divided into three groups of five animals each. Group 1 were the sham operated animals, group 2 included the pinealectomised rats dosed with saline, whilst group 3 consisted of the pinealectomised animals dosed with melatonin. All animals were treated continuously with saline or melatonin for a period of 1 month after the two week post-operation recovery time. The melatonin dosage was 0.5mg/kg bodyweight dissolved in a small amount of ethanol (not exceeding 0.5% of the total volume) whilst the bulk of the solution volume was saline. The pinealectomised animals were injected daily with 250µl of saline or melatonin in a saline vehicle. At the end of the treatment period, the animals were sacrificed by neck fracture and decapitation.

The brain was exposed by making an incision through the bone on either side of the parietal suture from the foramen magnum to near the orbit. The calvarium was removed exposing the intact whole brain, which was then extracted and dissected into the cortex, cerebellum and striatum regions. The various brain regions were weighed out before being acid digested (as per the preliminary method) for electrochemical metal analysis.

Electrochemistry:

The standard addition technique was utilised for the metals analysed.[246] A fixed volume of region specific digested brain tissue was analysed with increasing concentrations of the metal ion (copper(I), lead(II) and cadmium(II) – those metals observable in the preliminary study) and sufficient TBABr (0.05 M) electrolyte to maintain a constant cell volume. The optimised deposition potential and deposition time, following the method described in Sections 2.2.3 and 2.3, were –1200 mV and 300 second, respectively for the simultaneous detection of all three traceable metal ions. A minimum period of 5 minutes deaeration time was allowed, after which a flow of nitrogen gas was maintained over the solution throughout the measurements.

4.3 RESULTS:

The conventional method used to determine lead in blood and certain other biological tissues is atomic absorption. However, Jaenicke *et al.* (1998) have recently reported an automated electrochemical method, using flow injection analysis with a wall-jet detector.[247] The lead levels from the biological samples were quantified by stripping voltammetry on a mercury film electrode. The method allowed for a detection of 0.05 ppm Pb^{2+} with an accuracy of about 10%.[247] Daniele *et al.* (2000) have demonstrated the effectiveness of square-wave anodic stripping voltammetry for the determination of total copper and mercury content.[248] However, the technique may be used to determine the specific copper species present in solution as in the present application, hence surpassing atomic absorption as a detection tool for this type of brain metal analysis.

The ASV plot, Figure 4.3, displays the detectable peak positions of the 3 metal ions, namely copper(I), lead and cadmium. Identification of the peaks was done by spiking the sample with known standard solutions. The potential (-390 mV) for Pb^{2+} is different from that reported in Chapter 3, due to a different working electrode (Au *vs.* CGME) surface being employed. For Cd^{2+}, a potential of –597 mV *vs.* Ag | AgCl is observed in the brain sample, which corresponds well with the value obtained in Chapter 3. The presence of Cu^{+} as opposed to Cu^{2+}, was confirmed by spiking with a copper(I) standard, however, when repeating the process with a copper(II) standard, no peak enhancement was observed.

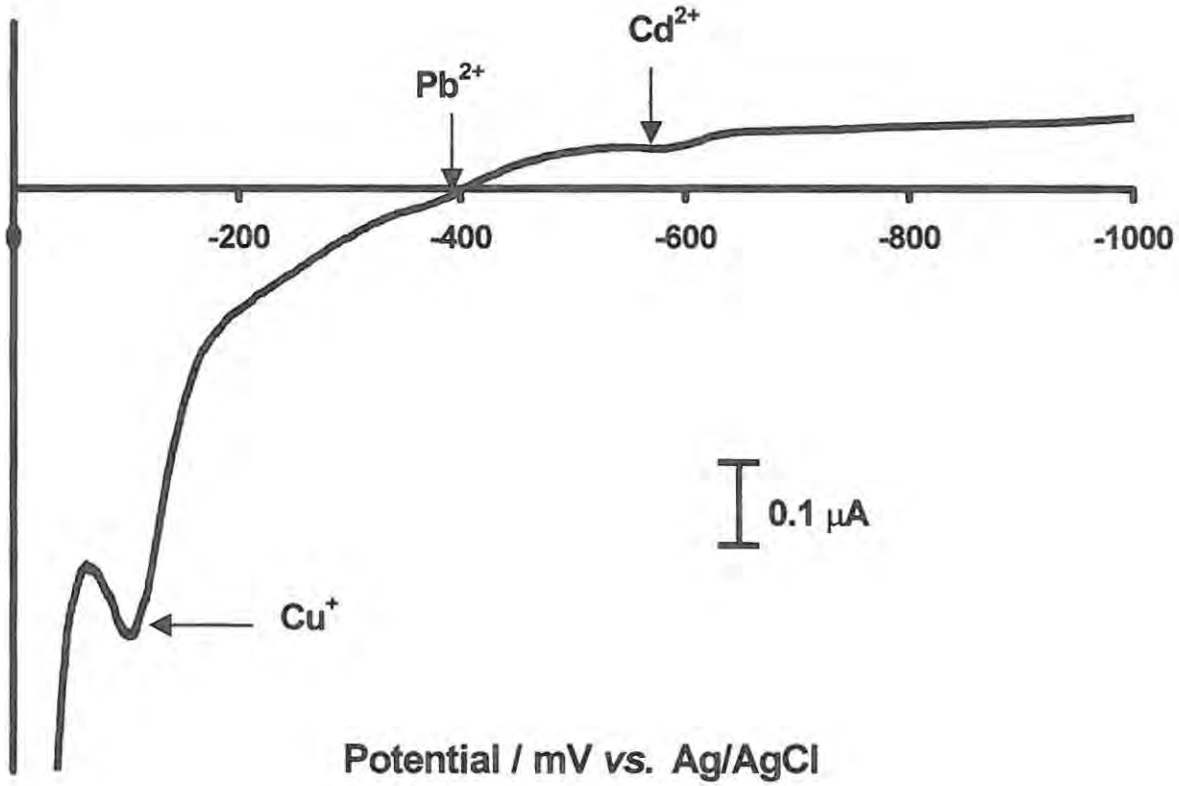

Figure 4.3 The ASV plot for whole brain tissue showing the three detectable metals in trace level quantities.

Standard addition curves (see for example Figure 4.4) derived from the ASV plots of each the three brain sections, were employed to determine the concentration of each detectable metal ion in the tissue. The data obtained for the sham operated and pinealectomised rats treated with either saline or melatonin is summarised in Figures 4.5, 4.6 and 4.7 for copper(I), cadmium and lead levels, respectively.

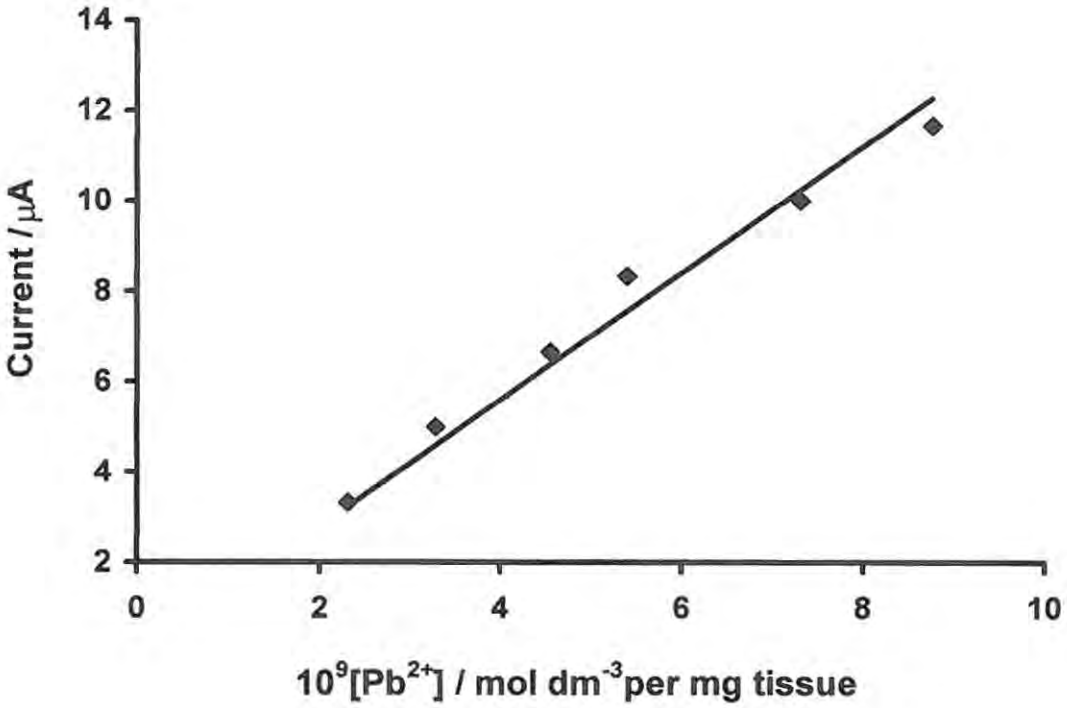

Figure 4.4 A typical standard addition curve for the determination of Pb^{2+} levels in the sham operated rat brain section.

The ANOVA one-way statistical analysis of variance method was used to analyse the significance of the data utilising the InStat® program software for Figures 4.5-7. The one-way analysis of variance compares the means of three or more groups. The null hypothesis

is that all column means are equal, and InStat® reports the P value testing this null hypothesis. If the F values were significant, the Student-Newman-Keuls test was used to compare the data of the treated (saline injected or melatonin dosed animals) and sham operated animals. The level of significance was accepted at $p < 0.05$.[249] The data for Figures 4.5, 4.6 and 4.7 have the standard deviation and standard error of the mean (SEM) as error bars above and below each data column, respectively. The metal levels in each of the plots have been quoted as a concentration per mg of tissue weighed.

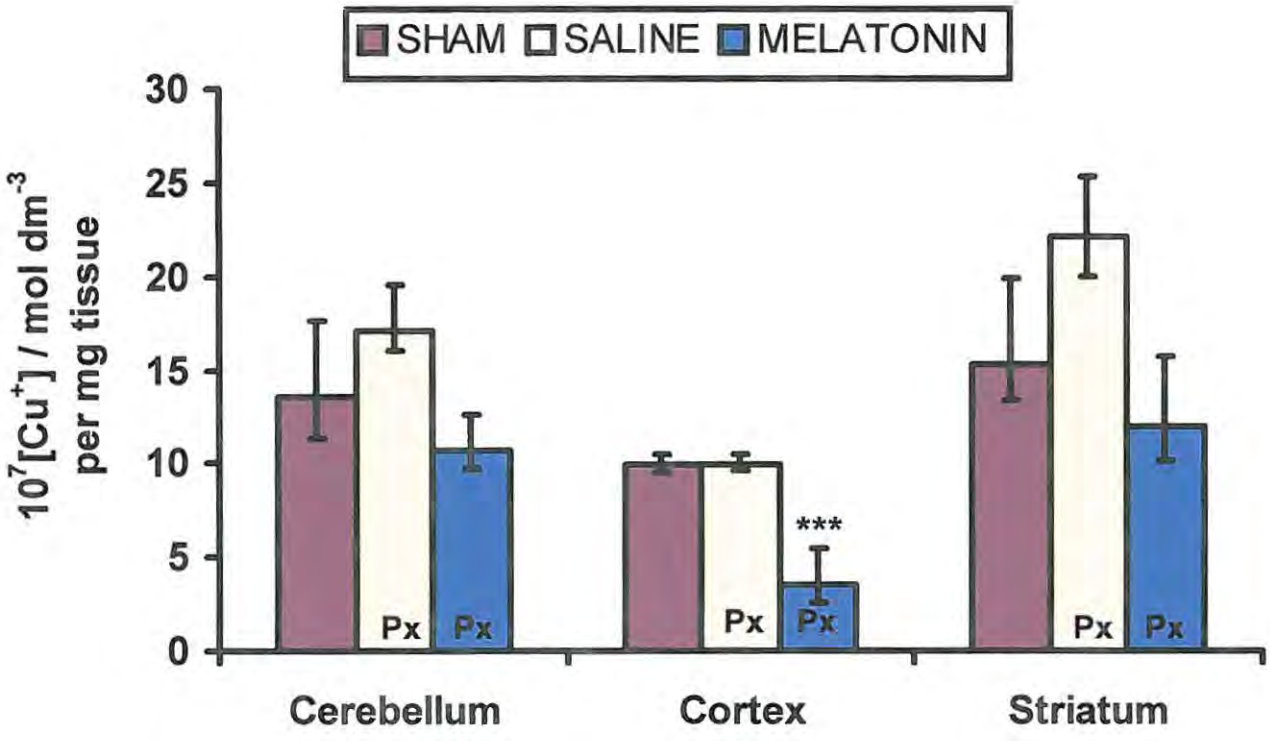

Figure 4.5 **Copper(I) levels assayed in the three brain regions of sham operated, saline injected or melatonin treated male Wistar rats. Values depicted represent the mean ± SEM (n=5), Px = pinealectomised (*** P < 0.001 in comparison with saline treated animals.)**

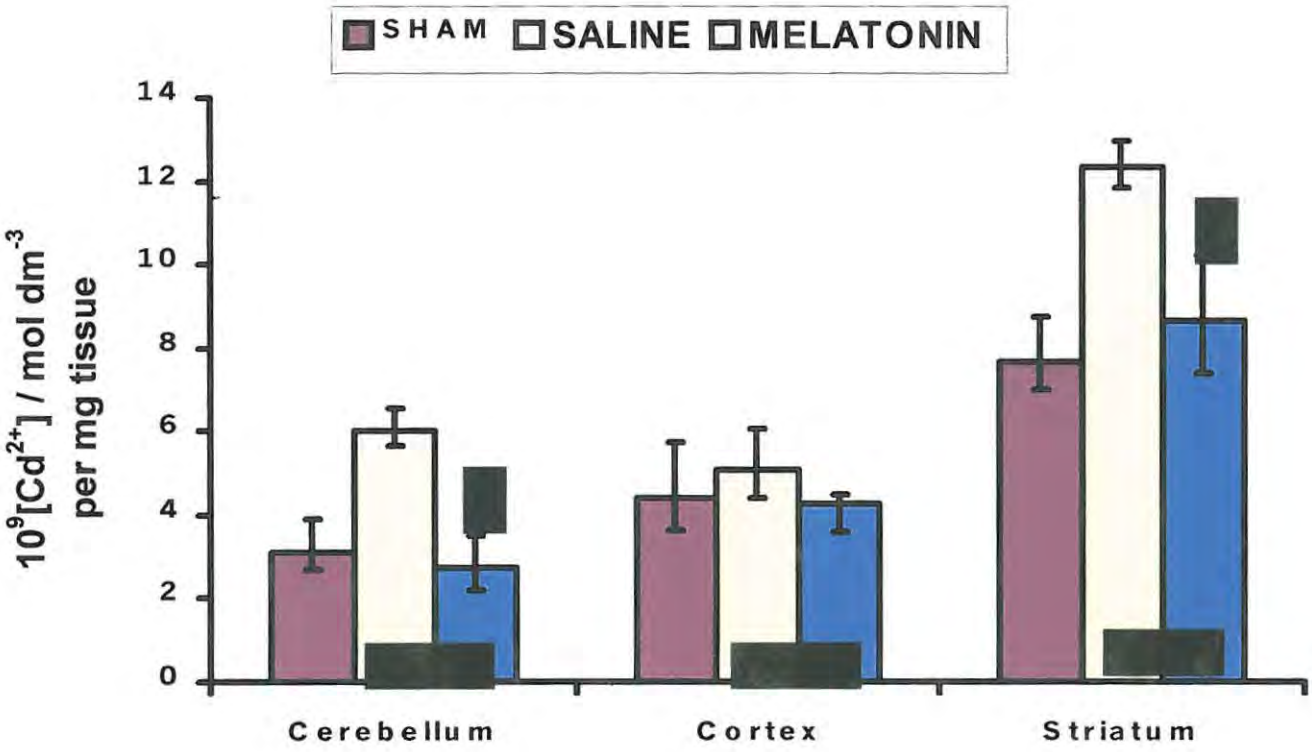

Figure 4.6 **Cadmium levels assayed in the three brain regions of sham operated, saline injected or melatonin treated male Wistar rats. Values depicted represent the mean ± SEM (n=5), (*P < 0.05 in comparison with saline treated animals.) Px = pinealectomised animals**

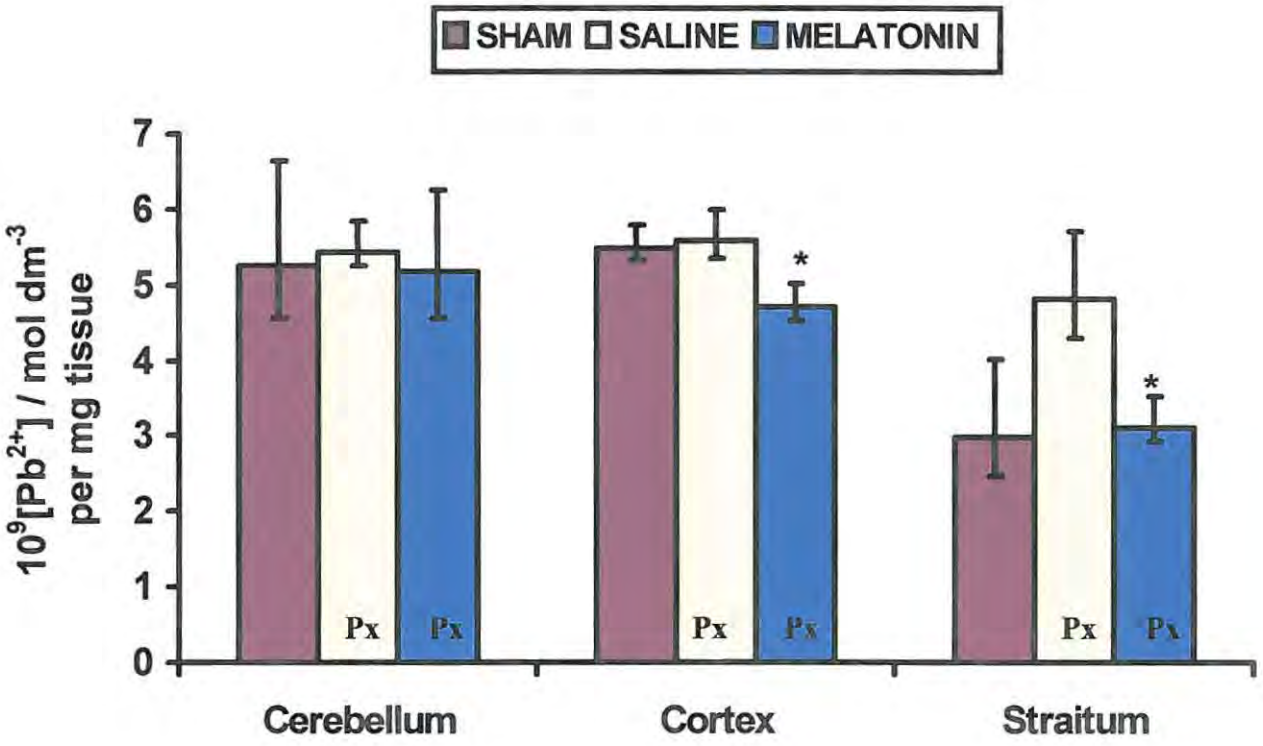

Figure 4.7 **Lead levels assayed in the three brain regions of sham operated, saline injected or melatonin treated male Wistar rats. Values depicted represent the mean ± SEM (n=5), (*P < 0.05 in comparison with saline treated animals.) Px = pinealectomised animals**

The copper(I) and cadmium metal levels assayed both indicated that the saline treated pinealectomised animals had the highest accumulated levels in the striatum region in particular, whilst in the case of lead the highest level was recorded in the cerebellar region. Interestingly in a study by Hasan *et al.* (1989) it was concluded that chronic low level lead exposure had no significant effect on the early structuring of the developing cerebellum.[250] Of the three metals studied, at least one brain region showed a significant decrease of accumulated metal upon treatment with melatonin. The most significant was

the copper(I) metal analysed in the cortex region. Interestingly the copper(I) levels were also much higher than those observed for lead or cadmium, but as copper occurs freely in the brain it is possible for the copper(I) species to be present in larger quantities, particularly as observed under oxidative stress conditions by White *et al.*(1999),[123] than either of the other two metals observed.

4.4 DISCUSSION:

Most metal species are cytotoxic at sufficiently high doses, resulting in neurochemical abnormalities and psychiatric disorders. Environmental exposure to toxic metals thus represents a biological hazard of growing concern,[215] particularly because the metals are in fact natural elements in the environment.[88] Furthermore, the increasing awareness of the negative effects of pollution to mankind over the last decade or two and the fact that the problems related to metal neurotoxicity have not yet been abated, is bound to make people concerned about copper and aluminium pots and possibly avoid leaded fossil fuels.[87]

However, in several animal studies it has been shown that metal ions do not always cross the blood-brain barrier if ingested, but the difference is the unknown factor of long term exposure to these metal ions and there is currently little evidence for or against this argument.[87] In addition the aging process is known to take its toll on the body and the blood-brain barrier is no exception, thus the importance of understanding metalloregulatory systems within the body may provide further clues to the mysteries of certain mental illnesses.

The proposed metalloregulatory or metal scavenging ability of melatonin was investigated in the present work. Limson *et al.* (1998) had previously demonstrated melatonin's ability to bind copper(II) in a concentration dependent manner,[198] whereas the present study has highlighted the presence of copper(I). Together with iron(II), copper(I) has been implicated in catalysing oxidative stress in the brain by converting hydrogen peroxide to the toxic hydroxyl radical in the Fenton reaction.[234]

Whether melatonin offers protection to brain tissue by binding to the metal ions concerned or through its antioxidative properties to scavenge both the hydroxyl and peroxyl radical species,[15] is beyond the scope of this study. However, it is clear that melatonin readily diffuses across membranes. Daily injections of melatonin was responsible for significantly decreasing copper(I), cadmium(II) and lead(II) levels in various regions of the rat brain of those animals that had undergone a pinealectomy in comparison to the saline injected group having undergone the same treatment.

Melatonin caused a noteworthy decrease in the copper(I) level in the cortex region compared to the controls, whilst it did not significantly change the levels of this metal in the cerebellar and corpus striatum regions. In the case of cadmium and lead, melatonin dosing in the pinealectomised animals significantly decreases both metal levels in the corpus striatum. Furthermore, cadmium levels are significant decreased in the cerebellar region, whereas lead showed a significant change in the cortex region upon melatonin treatment.

The *in vitro* study by Limson *et al.* (1998), demonstrated that melatonin and its precursors have the greatest affinity for cadmium followed closely by copper(II) and lead, but that the lead complex formed showed the least stability. Both lead and cadmium are highly toxic to living systems, since they may easily displace softer biologically important metals such as zinc at the active sites of proteins or enzymes and thereby render them inactive.[84] The study by Limson *et al.* (1998) then attempts to confer a metal detoxification role on melatonin and its precursors.[198] The idea was rewarded in the present study where it is clear that melatonin has a region specific detoxification potential dependent on the metal type present.

The most significant decrease in metal levels observed was that of copper(I) in the cortex region upon melatonin supplementation. Although in mammalian cells the chief copper sequestration or chelation into relatively innocuous complexes is carried out through the binding of Cu^{+} to a series of metallothioneins.[251] Metallothionein has also been identified in the rat pineal gland,[252] but only in the peripheral organs has this metal binding protein been shown to bind a broad range of essential and toxic metals. Melatonin may well support this process. In the brain, however, evidence to support metallothionein involvement in zinc and calcium homeostasis has been reported.[130]

The role of melatonin as a metalloregulator may thus compliment the metallothioneins in the brain as its potential to bind a series of metal ions has been demonstrated *in vitro*.[198] Furthermore, the depletion of melatonin with age has been associated with neurodegenerative diseases such as AD.[16] Coupled to that a growing number of researchers now suspect that mishandling metals in the brain is in part responsible for neurological disorders.[87] Overlaid upon that belief is the fact that levels of exposure to

neurotoxic metals are not much above the levels known to cause disease.[88] The implications of melatonin's metalloregulating ability are thus noteworthy in light of slowing down the natural aging process and perhaps stalling the onset of certain neurodegenrative disease states related to metal toxicity.

CHAPTER 5

In Vivo Aluminium Toxicity

5.1 INTRODUCTION:

Aluminium exposure leads to neurotoxicity and is considered a possible aetiological factor for many neurodegenerative disorders. Al^{3+} has been known to impair the glutamate-nitric oxide pathway in neurons and the suggested specific targets are the cortical nitroxidergic neurons and granule cells.[253] Colomina *et al.* (1999) investigated the influence of restraint stress on potential Al-induced behavioural changes assessed in mice.[254] The study showed lower motor resistance and coordination in the rotarod tests, following exposure of 600 mg Al^{3+}/kg/day. Furthermore, the levels of Al^{3+} in whole brain and cerebellum regions were significantly enhanced in mice exposed to Al^{3+} plus restraint.[254]

Al^{3+} is found in the developing conceptus, but little information is available concerning its tissue distribution and its changes in concentration with age.[255] In addition Al^{3+} has an affinity for many of the same biological ligands as the essential mineral cations Ca^{2+}, Mg^{2+}, Zn^{2+}, Fe^{n+}, and Mn^{n+} and it has been hypothesized that Al^{3+} might show a pattern of developmental concentrations that are similar to one or more of these elements in the brain. However, the study by Golub *et al.* (1996) on concentrations of Al^{3+}, Ca^{2+}, Mg^{2+}, Zn^{2+}, Fe^{n+}, and Mn^{n+} measured in spinal cord, brainstem, cerebellum, and forebrain of guinea pig

fetuses, after the dams were fed commercial guinea pig chow, indicated that Al^{3+} was the only element to show higher concentrations in the spinal cord at birth.[255] The tissue distribution of Al^{3+} was also shown to not to follow that of the essential cations examined in the study.

A recent histochemical and immunocytochemical study by Platt *et al.* (2001) was undertaken to investigate changes induced by intracerebroventricular Al^{3+} injections (5.4 micrograms in 5.5 microlitres, daily over a period of 5 successive days) in the adult rat brain after survival periods of either 1 or 6 weeks.[256] For both the Al- and saline-infused controls, no major signs of gross histological changes were evident in cresyl violet-stained sections. However, Al^{3+} was seen to be concentrated in the white matter of the medial striatum, corpus callosum, and cingulate bundle. An immunoreactivity test revealed a greater inflammatory response in the Al-injected animals compared to controls. In addition, damage to the cingulate bundle in Al-treated animals led to a severe anterograde degeneration of cholinergic terminals observed in the cortex and hippocampus regions.[256]

Aluminium exposure has also been known to produce a significant increase in lipid peroxidation, a condition which has been positively linked to increasing oxidative damage observed in the elderly.[257] Nonetheless the controversy over Al^{3+} and the link to neurodegenerative disease is an ongoing saga, in particular Al^{3+}'s role in the aetiology of AD is still disputed. The purported association of Al^{3+} with the disease has been based on: (1) the experimental induction of fibrillary changes in neurons of animals by the injection of Al salts into brain tissue, (2) reported detection of the metal in neuritic plaques and tangle-bearing neurons, (3) epidemiological studies linking Al^{3+} levels in the environment, notably water supplies, with an increase in the prevalence of dementia and (4) a reported

decrease in the rate of disease progression following administration of an Al^{3+} chelator, desferroxamine, to clinically diagnosed sufferers.[258] The latter point has lead to the mushrooming effect of numerous agents with claims to be neuroprotective or acting as possible "cures" to AD or other related disease states.

Limson *et al.* (1998) published an earlier study on the possible *in vitro* neuroprotective effects of melatonin and its precursors.[198] However, to date no *in vivo* studies have been embarked upon to investigate the protective effects of melatonin on Al^{3+} neurotoxicity. The present study is thus two fold in aiming to generate firstly a picture of Al^{3+} related toxic effects on the hippocampal cells and secondly to quantify the protective nature of melatonin. Histological and electrochemical, in particular ASV- see Section 1.8.1, procedures were undertaken for the study.

The hippocampus was the chosen region for this study as it is the area of the brain whose primary function is associated with that of declarative memory consolidation.[43] Furthermore, earlier literature implied that the neurofibrillary tangles and senile plaques occur more or less randomly throughout the cortex. However, more recent studies have noted the hippocampal predisposition toward the formation of both of these neurodegenerative species.[52] The region consists of two thin sheets of neurons folded onto each other, one sheet is the dentate gyrus and the other is known as the Ammon's Horn. The latter is comprised of four divisions of which the most important are the CA1 and CA3 regions.[43] In the rat, the hippocampus is located approximately 1 mm anterior to where the cerebrum starts (from where the cerebellum ends, if one looks at the dorsal view of the brain) and extends about 4mm posterior and approximately 2.5mm lateral of the

midline separating the two hemispheres.[43] Histological evidence of the rat CA1 and CA3 regions are shown in a Nissl-stained coronal section, see Figure 5.1.

Figure 5.1 A magnified view of the rat hippocampus. A Nissl-stained slide showing CA1 and CA3 regions as adapted from Bear *et al.* (2001).[43]

Histology is derived from the Greek word for web or tissue, and involves the examination of preserved, sectioned and stained tissues. Most of our knowledge of internal tissue structure has come from this branch of science.[259] The Nissl stain, introduced by the German neurobiologist Franz Nissl in the late nineteenth century, is commonly used to study neurons under the light microscope. The Nissl granules themselves are thought to consist of ribonucleiprotein and are associated with protein synthesis.[260] This stain is particularly useful as it suitably distinguishes between neurons and glia, allowing histologists to study the arrangement of neurons in different parts of the brain.[43]

Matlaba *et al.* (2000) [224] and Limson *et al.* (1998) [198] have both published papers on the electrochemical detection of aluminium as an AdCSV study for the interaction with acetylcholine or melatonin respectively. However, Limson *et al.* (1998) were unable to

detect an Al^{3+} peak in the absence of a ligand as it was thought that the chosen solvent masked the metal's reduction peak. However, Al^{3+} is known to exhibit complex solution chemistry existing in a large variety of species whose nature and amounts are pH dependent.[89]

The electrochemical study conducted by Matlaba *et al.* (2000) observed the reduction peak of Al^{3+} in the region of around –1700 mV.[224] Wang (1996) has also reported on Al^{3+} detection by AdCSV with a 1,2-dihydroxyanthraquinone-3-sulfuric acid complexing agent and a detection limit of 1.0 nano mol dm^{-3} was afforded.[171] Brett and Brett (1993) have observed a standard electrode reduction potential of Al^{3+} at –1670 mV *vs.* the normal hydrogen electrode for the stripping analysis of the metal ion.[162]

In this study, it is likely that the CSV is in fact AdCSV in the presence of unknown biological ligand(s), since the tissue sample was not acid digested. Equations 2.1 –2.3 thus apply, where L is an unidentified biological substrate.

5.2 EXPERIMENTAL:

5.2.1 REAGENTS:

Melatonin was purchased from the Aldrich Chemical Company (USA) and the paraffin wax was obtained from Lasec (South Africa). Cresyl violet stain was purchased from BDH Chemicals Ltd (England) along with the aluminium chloride salt, whilst DPX® was purchased from Philip Harris Ltd (England). Haupt's adhesive consisted of the following: 1 g gelatine, 100 ml water, 2 g phenol and 15 ml glycerol. For the electrochemical section

of the study, TBABr purchased from Sigma (M.O-USA) was the electrolyte of choice. $AlCl_3$ is a product of SAARCHEM-HOLPRO Analytical (South Africa).

5.2.2 APPARATUS:

Thin sections of the embedded brain tissue were obtained with the aid of a rotary microtome. The slides were photographed using a combination Olympus camera and light microscope. AdCSV (OSW mode) data was obtained on the electrochemical apparatus described in Section 4.2.2.

5.2.3 METHOD:

Treatment Regimes

Male rats of the Wistar strain were divided into three groups, as shown in Table 5.1, and treated as follows:

Table 5.1 The treatment regime of each animal group:

Treatment Group	Daily Dosing quantities (s.c injections)
Control	250 µl saline
MEL & Al^{3+}	0.5 mg/kg saline based MEL solution before 5mg/kg Al^{3+}, administered 30 min. later
Al^{3+}	5 mg/kg Al^{3+} solution

The animals were dosed for a total period of 3 months. Initially 4 weeks of daily injections were given between 8:30 am and 12:30 pm followed by 1month of recovery and then finally a repeat of the prior 4 week treatment program.

Histological Techniques:

The technique was carried out according to the method described by Southgate (1998).[192]

Fixing the brain: The male Wistar rats, weighing between 200 and 250g, were sacrificed and the whole brains were removed as described in the treatments regime of Section 4.2.3. Immediately after death, animal tissue begins to break down as a result of autolysis and bacterial attack, thus it is imperative to fix this tissue. The fixation procedure functions to chemically stabilize the protein content enabling the preservation of the structure. Whole brains were rapidly fixed in a mixture of formol (30%), glacial acetic acid and ethanol (2:1:7v/v) for a minimum period of 2 hours. After fixation the brain tissue was stored in 70% ethanol.

Specimen preparation and embedding: In order to be cut, the slices need to be supported as brain tissue alone is too soft. Embedding involves the infiltration and orientation of tissue in the paraffin wax support medium. The tissue was dehydrated (using increasing concentrations of ethanol), followed by the removal of the ethanol using xylene. Finally the tissue was immersed in molten paraffin wax, which removed the xylene, while infiltrating the tissue without encountering water. The method used is summarised in Table 5.2 (I = 1st aliquot and II = 2nd aliquot after I has been poured out of the container for Table 5.2 and subsequent Tables).

Table 5.2 Procedure for embedding brains in paraffin wax:

Step	Processing Agent	Time (Hours)
1	70% Ethanol	1
2	90% Ethanol	1
3	Absolute Ethanol I	1
4	Absolute Ethanol II	1
5	Xylene I	1
6	Xylene II	1
7	Melted Paraffin Wax I	1
8	Melted Paraffin Wax II	1

Blocking the sample: The brain material was fixed into a block so that it could be cut with a microtome. A plastic ice tray, coated with ethanol-glycine to prevent sticking, was chosen as a suitable mould in which to set the wax blocks containing the tissue. The brain was removed from the final molten wax stage (previous section) and placed into the mould with warmed forceps. Molten wax was then poured over the brain and air was gently blown over the surface of the wax until the top layer hardened. The blocks were left over night to ensure that the wax had completely solidified.

Sectioning and slide preparation: The wax block was trimmed with a razor blade so that two of the sides were parallel, while the other two converged slightly. The sides were cut so as to leave about 2 mm of wax around the tissue. The wax block was attached to a similar sized wooden block using a small amount of molten wax. Sectioning was done using a rotarty microtome set to cut sections with a thickness of 10 μm.

As sections were cut, they would stick to one another, so as to form long ribbons. When the part of the brain containing the hippocampus was reached, every second section was removed and placed in a water bath (40°C) using forceps. Three sections at a time were removed from the water bath and placed onto microscope slide containing a thin layer of Haupt's adhesive. The slides were left over night in an oven at 40°C.

Staining: The sections were Nissl-stained using a cresyl violet solution. The stain is known to stain the nuclei a purple colour, Nissl substances are seen as intense purple shade, but the background remains clear.[261] Before the section could be stained, it first had to be dewaxed and dehydrated as the stain is water soluble. The procedure is outlined in Table 5.3. Sections were stained by being placed upright in a staining tank containing 0.1% cresyl violet solution for 2 hours. The cresyl violet solution consisted of 0.25 g cresyl violet, 250 ml MilliQ water, 0.75 ml glacial acetic acid and 0.0512 g sodium acetate. The pH was adjusted to 3.5 before use. The slides were differentiated in 95% ethanol by rinsing in a flat dish until the background became clear. Sections were then dehydrated again after staining, as shown in Table 5.4.

Table 5.3 Procedure for dewaxing and dehydrating brain sections:

Step	Processing Agent	Time (Minutes)
1	Xylene I (dewaxing)	5
2	Xylene II	5
3	Xylene/Absolute Ethanol (1:1)	3
4	Absolute Ethanol I	5
5	Absolute Ethanol II	Overnight at 30°C

Table 5.4 Procedure for dehydrating brain sections after staining:

Step	Processing Agent	Time (Minutes)
1	Absolute Ethanol I	5
2	Absolute Ethanol II	5
3	Xylene I	5
4	Xylene II	5

Mounting of the slides: Whilst the slides were kept under a thin film of xylene, enough DPX® was added to just cover the tissue. A cover slip was placed over the tissue and the slides were allowed to air dry on a flat surface for at least 48 hours.

Electrochemistry:

The standard addition technique, as in Section 4.2.3, with an OSW stripping voltammetry was utilised for the Al^{3+} analysis.[246] A known weight of dissected out hippocampal brain tissue was ground finely with mortar and pestle and mixed with a little TBABr. The tissue was then analysed with increasing concentrations of the metal ion and sufficient TBABr (0.05M) electrolyte to maintain a constant cell volume. As with all other electrochemical experiments performed, a minimum period of 5 minutes deaeration time was allowed, after which a flow of nitrogen gas was maintained over the solution throughout the measurements.

The optimised deposition potential and deposition time chosen were –450 mV and 100 seconds, respectively as described in Chapter 2. The square wave key parameters included: a step potential of 4 mV, amplitude of 25 mV and a frequency set at 15 Hz.

5.3 RESULTS:

Histological study:

The photomicrographs in Figure 5.2 and 5.3 demonstrate that melatonin offers some protection to the hippocampal neurons against Al-induced neuronal damage. The hippocampal neurons in the control group from both the CA1 and CA3 regions (see Figure 5.1) appear undamaged, see Figure 5.2 (a) and 5.3 (a) respectively. In the Al^{3+} treated animals, neurons in the CA1 and CA3 sections showed signs of neuronal damage as is evident in the swelling of the cells and overall degeneration. The CA3 region appears to be the most affected. Figure 5.2 (c) and 5.3 (c) illustrate the cell damage observed as a result of Al^{3+} treatments. The animals which received a daily dose of melatonin before their aluminium injections, did show signs of cell swelling and degeneration, but to a lesser degree than those without the melatonin supplement, Figure 5.2 (b) and 5.3 (b).

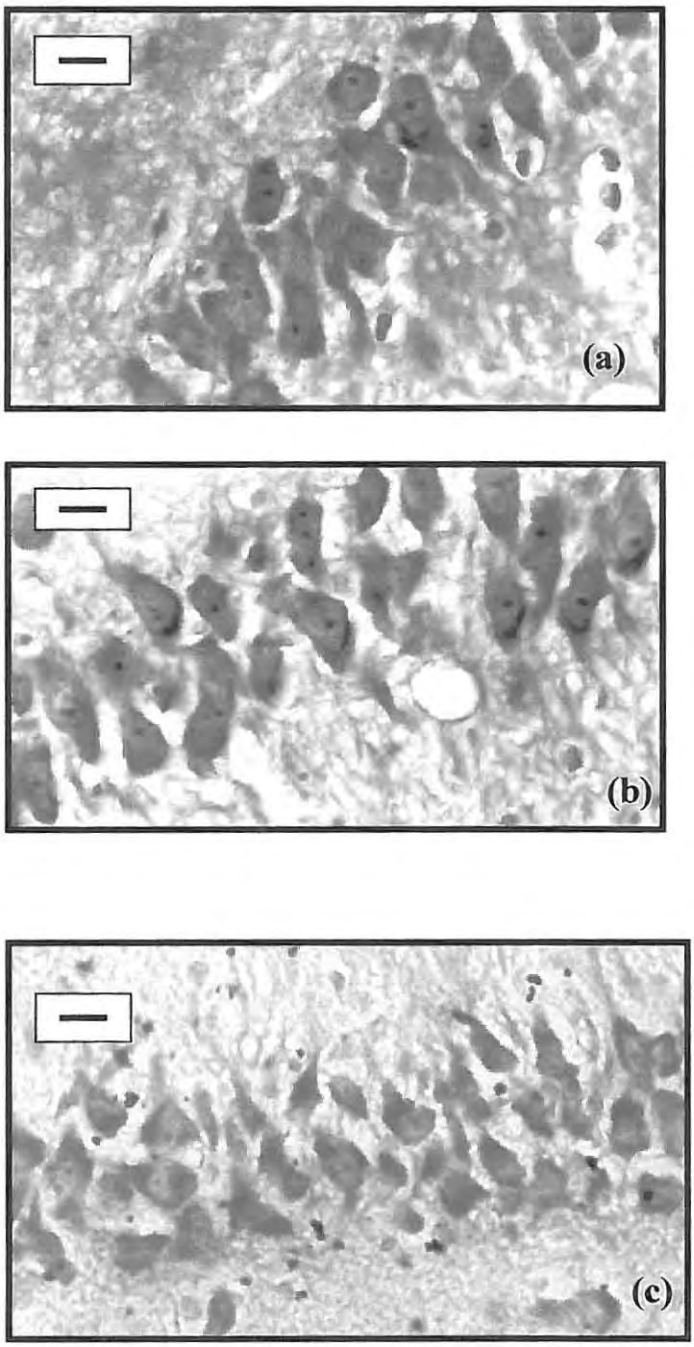

Figure 5.2 **Al^{3+} toxicity and the protective effects of melatonin on hippocampal neurons of the CA1 region of the control (a), Al^{3+} & MEL treated (b) and Al^{3+} dosed (c) male Wistar rats. (Bar = 10μm)**

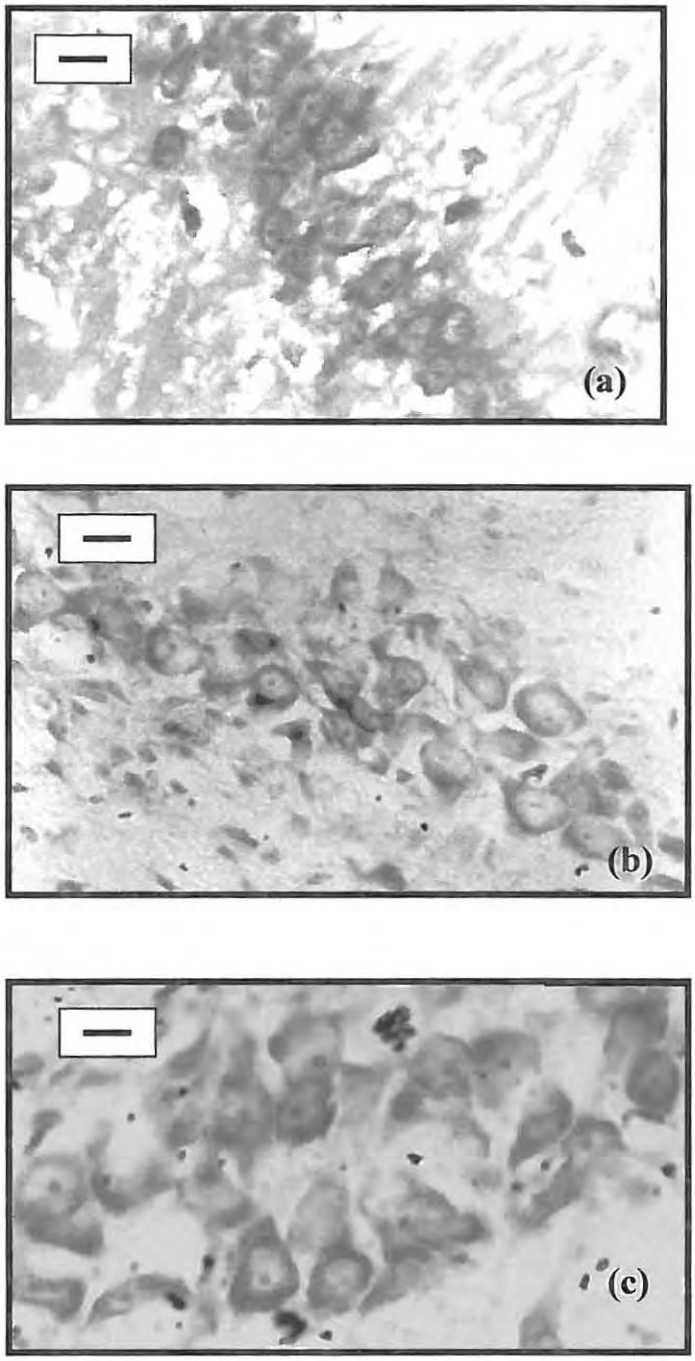

Figure 5.3 **Al^{3+} toxicity and the protective effects of melatonin on hippocampal neurons of the CA3 region of the control (a), Al^{3+} & MEL treated (b) and Al^{3+} dosed (c) male Wistar rats. (Bar = 10μm)**

Electrochemical study:

Figure 5.4 illustrates the AdCSV peak obtained for Al^{3+} at –1624 mV. A standard curve was set up in the concentration ranges of 6.67×10^{-9} mol dm $^{-3}$ to 2.33×10^{-8} mol dm $^{-3}$, as shown in Figure 5.5. A linear relationship exists between the current increase and the concentration of the Al^{3+} ions with a regression value of 0.978. The Al^{3+} concentrations obtained from the standard curve for the control, Al^{3+} treated and Al^{3+} and MEL dosed animals were plotted against each other and compared in a statistically significant manner, Figure 5.6.

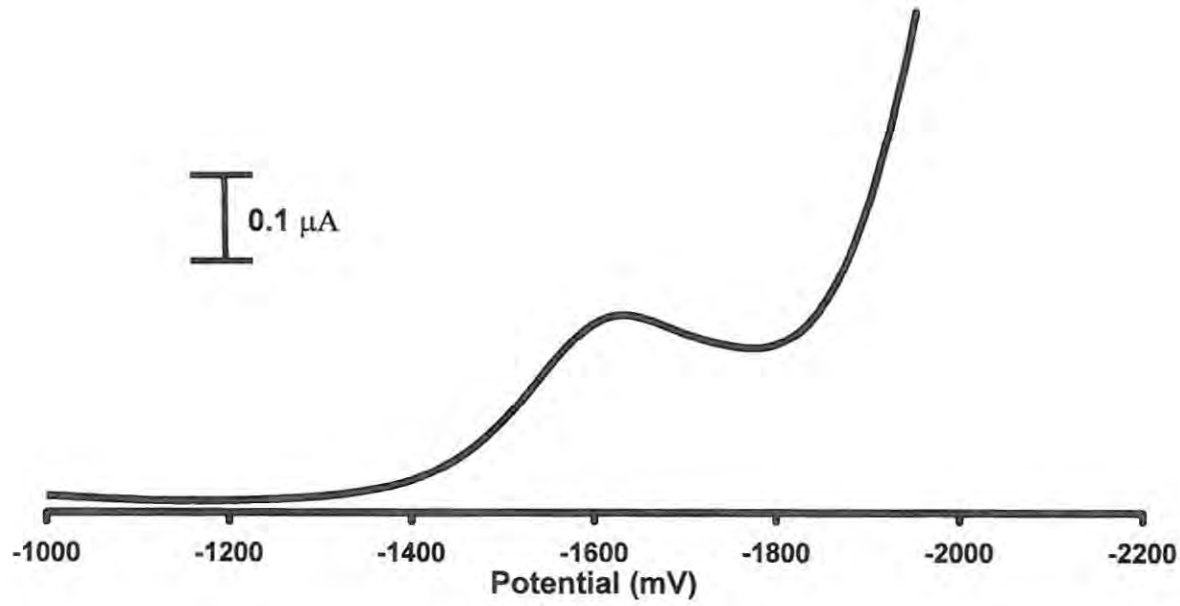

Figure 5.4 The AdCSV plot, OSW mode, in the presence of an unknown biological ligand and of Al^{3+}(1.33×10^{-8} mol dm^3). [TBABr] = 0.05 mol dm^{-3}. Deposition potential was –450 mV for 100 s.

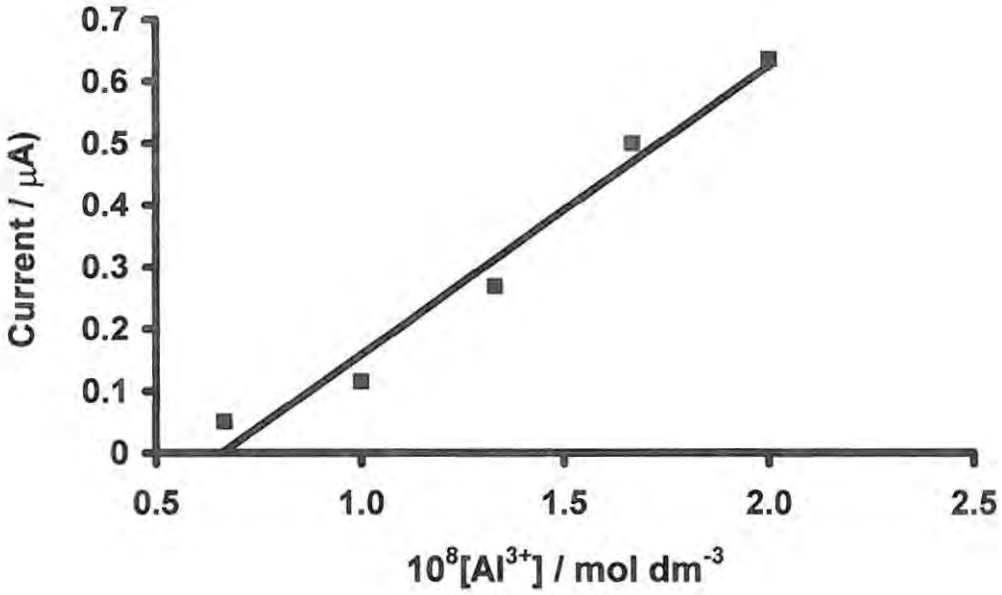

Figure 5.5 Variation of peak current with increasing metal concentration.

In Figure 5.6, the aluminium levels were compared with either the control group or the Al^{3+} and MEL treated animals in a statistical manner as described in Section 4.3. The results show that Al^{3+} levels were appreciably higher in the neurons of Al^{3+} injected animals. This rise was significantly reduced, but not abolished by melatonin administration. From the data obtained, melatonin is shown to significantly reduce the level of Al^{3+}in the hippocampal neurons in comparison with those animals that received only Al^{3+}.

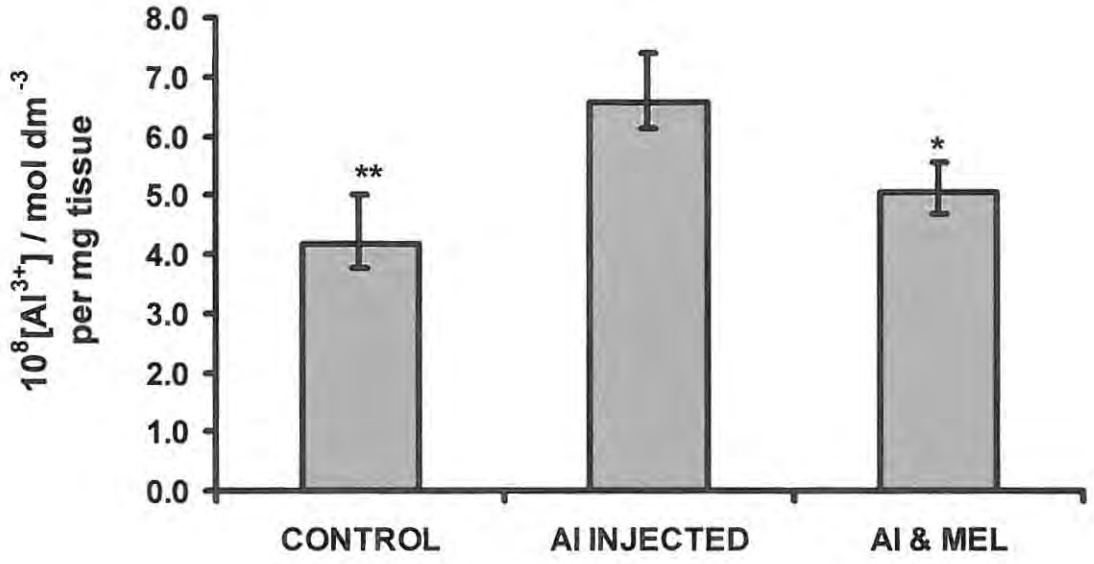

Figure 5.6 **Al^{3+} levels assayed in the three treatment groups. Values depicted represent the mean ± SEM (n=5), (*P < 0.05, ** P < 0.01 in comparison with Al^{3+}).**

5.4 DISCUSSION:

The cell damage induced by daily Al^{3+} injections is in part to be alleviated by dosing with melatonin. However, since the pathophysiology of aluminium toxicity is largely unknown, it is not possible to establish from this study whether a higher dosage of melatonin would have been more beneficial or what the mechanism was by which Al^{3+} induced hippocampal neuronal damage.

In agreement with the recent histochemical publication by Platt *et al.* (2001) on Al^{3+} toxicity in the rat brain,[256] no major signs of gross histological changes were evident in cresyl violet-stained sections of the hippocampus. However, more prominent signs of neuronal swelling and cell damage were noted in both the CA1 and CA3 regions of the Al^{3+} treated animals in comparison to the control group and / or the group additionally receiving melatonin. The observations further imply that aluminium neurotoxicity may be mediated by a mechanism other than the more commonly accepted physiological consequences of excitotoxicity, that is through the extracellular calcium entry into the cell leading to neuronal swelling and finally cell death. A study by Brenner and Yoon (1994) on the Al^{3+} toxicity in cultured rat hippocampal neurons corroborates the concept of an alternative mechanism of Al^{3+} toxicity other than the expected excitotoxicty response.[262] Instead, the study suggests Al^{3+} toxicity may be directly linked to the ion flux across the cell membrane.

Although the electrochemical study did not address the issue of metal influxes across the cell membrane directly, the levels of Al^{3+} were compared between the control group and those receiving melatonin supplements. From the data, it is clear that there is a significant decrease of Al^{3+} levels in the hippocampus of the animals that received a daily dose of melatonin along with Al^{3+} injections. However, that the control group showed the greatest significant lowering of Al^{3+} levels, implies that the melatonin may not completely prevent Al^{3+} accumulation in the hippocampus, which has been associated with neurodegeneration.

Furthermore, the dosage of melatonin may need to be increased in order to observe a more pronounced effect, but this is an avenue of future study. However, from the current study it should be noted that Al^{3+} levels were enhanced in the hippocampal region of the brain

upon daily s.c injections of Al^{3+}. This is not unexpected, as Brenner and Yoon (1994) [262] have reported high levels of Al^{3+} (between 1.3 and 2.7 μM) in renal dialysis patients with dementia, patients suffering from kidney failure are more prone to Al^{3+} toxicity as a direct result of their dialysis treatments. The implications of high Al^{3+} levels in the brain regions, particularly the hippocampus, has been synonymously linked to various neurodegenerative diseases including AD.[198,258] The debilitating nature of this disease alone would warrant further study into any substance that would show the slightest possibility of a reprieve from the symptoms. Melatonin has shown signs of promise in indirect symptom alleviation by decreasing neuronal swelling and cell degeneration linked to Al^{3+} toxicity, but a more indepth study into its mode of protection is still required.

CHAPTER 6

Calcium Ion Sensing: A preliminary study

6.1 INTRODUCTION:

A casual observer would state there is an obvious difference between a living organism and something which is dead. Scientists on the other hand have over the past centuries not found it easy to define life and death precisely at the cellular level, particularly in chemical terms. Pathological conditions cause disruption and impairment of cell structure, metabolism and function, but in many cases these changes are reversible and the cell may recover when the cause of injury has been removed. However, a point of no return may well be reached where injury to the cell is so severe that within a relatively short space of time, the cell is morphologically dead. At this point the cell is recognizable under the microscope as being necrotic and calcium seems to play an important part in the chemical changes associated with this necrosis.[263]

Interestingly, the concentration of free cytoplasmic Ca^{2+} in resting cells is in the order of 0.1 μM. A resulting concentration gradient across the cell membrane is then created (between 10000 and 100000-fold), which in turn suggests why calcium has been utilized by the cell in several regulatory phenomena.[263] In neuronal cells though damage is initiated via overactivation of the excitatory neurotransmitters, excitotoxicity. The damage

results from fluctuations in intracellular calcium, which in turn leads to intracellular enzymatic degradation of lipids, proteins and nucleic acids. In addition, the neurons suffer swelling as a result of water uptake.[43] The ability to thus monitor intracellular calcium levels is applicable to the study of neurodegenerative disease states.

However, to date only three suitable methods exist for intracellular calcium studies. These methods include: (1) Ca^{2+}-activated luminescent proteins, photoproteins, (2) metallochromic and fluorescent dyes and (3) Ca^{2+} microelectrodes. Of the three methods available, in terms of quantification and response time the microelectrodes are superior since they measure the Ca^{2+}-activity directly, whilst the dyes often lack selectivity over other divalent cations.

The design of such an indicator electrode varies greatly depending on the particular application.[165] A liquid-membrane electrode develops a potential across the interface between the solution containing the analyte and a liquid-ion exchanger that selectively bonds with the analyte ion. These electrodes have been developed for the direct potentiometric measurement of numerous polyvalent cations as well as certain anions and are referred to as ion selective electrodes (ISE).[246] Potentiometric measurements involve the determination of the electrical potential between two electrodes at zero current flow. The variation in potential occurs at the outer membrane boundary of the indicator electrode in contact with the sample solution. The other electrode is a reference electrode.

The first two types of calcium selective liquid membrane microelectrodes were developed in 1976: using a membrane based on the charged lipophilic esters of phosphoric acid in one case [264,265] and a membrane solution form containing a synthetic neutral carrier in

another.[266] Both types of microelectrodes exhibited a high preference of Ca^{2+} over Na^{+} and K^{+}, however the neutral carrier-based microelectrodes demonstrated better Ca^{2+}/Mg^{2+} and Ca^{2+}/H^{+} selectivities. Recently the calcium ISE liquid membrane electrodes have been superseded by the polyvinyl chloride (PVC) membranes based on ionophores such as the ETH® series (Fluka Chemie, AG, Switzerland) and lipophilic hexapeptides that act as perm-selective agents for Ca^{2+}.[165]

The addition of PVC to the microelectrodes resulted in improvements in electrode function for small tip diameter electrodes (<1μm) and lower detection limits. The improvement was thought to be due to the elimination of electrical shunts through the glass wall at the tip of the microelectrode.[267] The PVC matrix membrane ion-selective electrodes have been shown to have longer lifetimes and considerable economy of the sensor material in comparison to their liquid-membrane counterparts. The calcium selective microelectrodes are the most widely used of the neutral carrier-based types available.[267,268] In this preliminary study, work was completed on the construction and standardization of a neutral carrier-based Ca^{2+} microelectrode for the measurement of intracellular calcium levels.

6.2 EXPERIMENTAL:

6.2.1 REAGENTS:

Triply distilled deionised water was used for all experiments to avoid contamination of the calcium standards. Solutions of Ca^{2+} containing 125 mM K^{+}, as it is the most strongly interfering ion as well as the ion that determines the ionic strength of the solution, were prepared from the corresponding metal chloride salts (SAARCHEM-HOLPRO Analytical, South Africa). The calcium ionophore II, sodium tetraphenylborate, *o*-nitrophenyl-n-octyl ether and PVC were all products of Fluka (Switzerland). Tetrahydrofuran (THF, membrane solvent) was a product of Aldrich Ltd.

6.2.2 APPARATUS:

The microelectrode casing was pulled from a Kwik Fil® borosilicate glass capillary on a Narishige PB-7 glasspuller and after filling, sealed with gold-plated connector points obtainable from World Precision Instruments (Florida). Visualization of the cells was done on an Olympus BH2-RFCA microscope, whilst the electrometer readings were recorded with a Duo 773 Electrometer (World Precision Instruments - Sarasota, Florida). A Piezo PM10 manipulator was utilized to control the impalement procedure of the microelectrode tip into the cell. The pseudo reference electrode employed, a silver wire, was placed in the bathing medium. Hippocampal brain slices were cut with a standard surgical blade.

6.2.3 METHOD:

A double-pull system was used to create a suitably shaped microelectrode tip, which was then allowed to stand tip-face upwards to draw up the carrier molecule membrane solution through the wicked capillary. The microelectrode needles were then viewed under a light microscope to ensure sufficient membrane material was present and no air bubbles or faults in the shape were noticeable. The carrier membrane composition, summarized in Table 6.1, was according to the method of Lanter *et al.* (1982).[269]

Table 6.1 The calcium ion selective electrode membrane composition:

Membrane Composition	Quantity (wt.)
Ca^{2+} carrier molecule: Calcium Ionophore II	10.0%
Sodium tetraphenylborate	1.0%
o-nitrophenyl-n-octyl ether	89.0%

For tip diameters of < 1 μm, 86% of the membrane composition is added to 14% PVC and the mixture is then dissolved in 3 times its weight of THF. The neutral carrier-based microelectrode was then allowed to air dry for a day before being filled with a 3 M solution of lithium chloride and tested in the calcium standard before cell impalement experiments were run. Figure 6.1 shows the structure of a completed neutral carrier-based Ca^{2+} selective microelectrode.

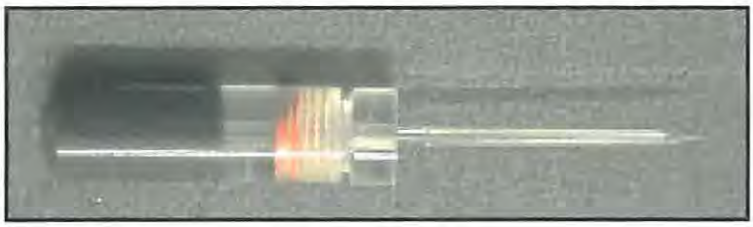

Figure 6.1 The Ca^{2+} selective microelectrode.

6.3 RESULTS:

The standard curve shown in Figure 6.2 can be used for the intracellular determination of calcium ions. Concentration detection limits in the order of 10^{-7} mol dm^{-3} were obtained.

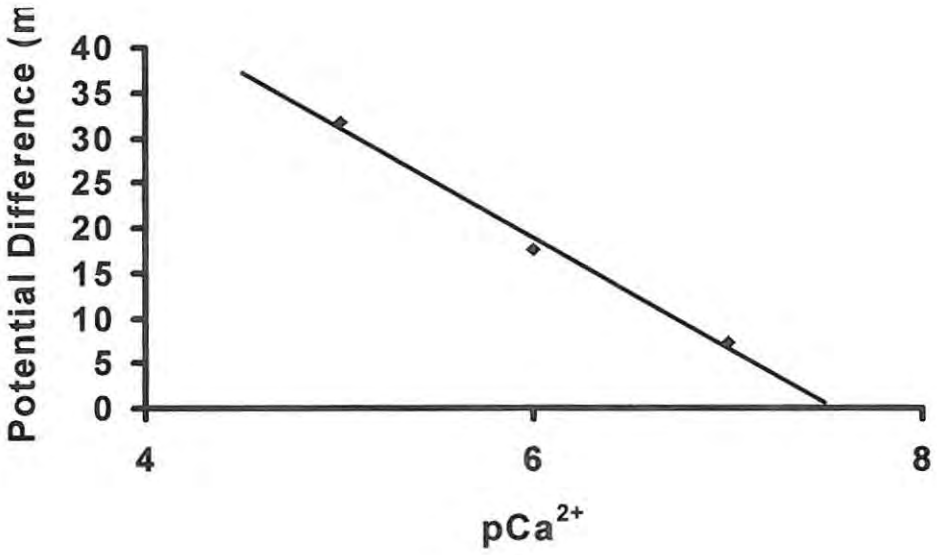

Figure 6.2 Ca^{2+} microelectrode standard curve in the presence of 125 mM K^+ where $pCa^{2+} = \log a_{calcium}$. A regression value of 0.9915 was obtained.

The microelectrode was then applied to the measurement of intracellular calcium levels of a male Wistar rat hippocampal slice. Readings were taken and values were extrapolated from the standard curve resulting in a measured value of 0.18 ± 0.02 μM free calcium (where number of measurements = 3). However, the continual impalement of the microelectrode into the cell resulted in damage after the third reading. Lacking a proper tissue slicing facility and the difficulty in working with soft brain tissue, had made thin hippocampal slicing impossible. The slices had been too thick to view individual cells under the microscope, making the manipulation and angle of cell entry by the microelectrode difficult to obtain. Hence, only a preliminary study is reported here and more work needs to be done in the future to optimise Ca^{2+} analysis, and the implications thereof, in brain tissue.

6.4 DISCUSSION:

The preliminary study on calcium microelectrode sensing resulted in a standard curve with electrode reproducibility and an error level of less than 5%. The standard curve was obtained in the presence of 125 mM K^+ ions as it is the most strongly interfering ion as well as the ion that determines the ionic strength of the solution, thereby approximating *in vivo* intracellular conditions. However before comparing the value of intracellular calcium obtained for the hippocampal slice, there are several sources of error to be considered with respect to the indicator microelectrode. Firstly the ions of interest must be in the form the electrode will be sensitive to. The ions that are in complex form as a result of ionic complexes, cellular constituents or structures and/or complexation by polyelectrolytes will render the indicator electrode insensitive. Furthermore, if heterogenous ion distribution

occurs because of compartmentalization within the cell, the comparison of microelectrode measurements with analytical methods that measure total concentration will be invalid.[246,270] The response of an ISE may be affected by the presence of proteins and other organic constituents, which can coat the surface of the electrode membrane. This often leads to a sluggish response, but may also shift the observed potential due to the presence of active sites in the coating molecules and changes in membrane selectivity. In intracellular measurements, errors due to the presence of "bound" water may in addition result in anomalous ionic activities when compared to solutions of similar ionic strength *in vitro*.[270]

Despite the commonly occurring errors in ISE work, the value of 0.18 μM obtained for intracellular calcium was within the order observed by Tsien (1981) for the arsenazoIII dye method.[271] Campbell (1985) [263] has reported free cytoplasmic Ca^{2+} concentrations of between 0.1 and 0.2 μM in liver cells, whilst the resting lymphocyte concentration was measured at 0.12 μM utilizing the microelectrode method. Further work is still required on this study, but thinner tissue slices are needed to identify cell types and impale the microelectrode efficiently.

CHAPTER 7

Overall Conclusions and Future Work

Metal interactions with neural substrates and their role in neurodegeneration has broad stroked the importance of understanding metal-ligand chemistry and the application of techniques available in order to obtain a greater understanding of the link between metal ions and neurochemical dysfunction. The multidisciplinary approach to this study has encompassed *in vitro* and *in vivo* aspects of metal-ligand interaction chemistry utilising electrochemical methods in particular to analyse the complex metal-ligand interactions, an integral part of any biochemical pathway. The basic principles of electroanalytical chemistry, highlighting the benefits of this technique towards research aims of this work, have been discussed in detail in Chapter 1. Relevant aspects of metal-ligand chemistry, the neural substrates studied (melatonin, serotonin and acetylcholine) and topical neurodegenerative diseases tied in with these factors are also reviewed.

Chapter 2 attempts to emphasize the binding ability and complex formation of melatonin and serotonin toward three biologically active metals, namely calcium, potassium and sodium, as well as two other metals linked to neurochemical alterations in the brain - that of lithium and aluminium. An attempt is also made to explain the observed interactions in terms of different structural and chemical aspects of the bond formation between the

metals and these ligands of interest. Adsorptive cathodic stripping voltammetry provided suitably feasible information by utilising the current responses and potential shifts of the metals alone and upon addition of the ligands as the criteria for plausible metal-ligand interactions. The IR, NMR and computer modeling data corroborated the interactions and highlighted certain binding features. All the metals investigated were shown to form complexes with both serotonin and melatonin. However, the stability and affinity for the ligands to the various metals varied greatly. Both Li^+ and K^+ formed more stable complexes with serotonin and melatonin when compared to the other metal complexes under consideration, whilst coordination to Ca^{2+} was not favoured by either ligand.

Mercury, lead, cadmium, copper and zinc complexation studies with acetylcholine was the objective of Chapter 3. Adsorptive cathodic stripping voltammetry was employed using more than one type of working electrode for the study. Comparatives were drawn between the interactions of lead and mercury with acetylcholine on a solid gold working electrode as well as the binding ability of acetylcholine toward cadmium, copper and zinc utilising the hanging drop mercury electrode. The formation and characterisation of a solid mercury-acetylcholine complex lends further strength to the *in situ* complex formation potential of ACh in the presence of various divalent cations and mercury itself.

Neurotransmitters such as acetylcholine are structurally specific for their receptors and any changes in their structure or polarity could have drastic consequences on the efficacy of the neurotransmitter and its response to stimuli. The formation of an *in situ* complex between acetylcholine and the metals studied, imply that these metals could contribute to the acetylcholine deficiency observed in certain neurodegenerative disease cases such as AD. Of these metals, three are common environmental toxins, with mercury dental fillings

constituting the largest single source of mercury exposure in the general population. The preference of ACh for environmentally toxic heavy metals over those divalent cations that occur naturally in the body, such as the zinc and copper forms studied, should be noted as this may lead to further insight into metal accumulation or disturbances in ACh levels observed in some cases of degenerative disease.

The view that most metal species are cytotoxic at sufficiently high doses, the belief that levels of exposure to neurotoxic metals are not much above the levels known to cause disease and the fact that a growing number of researchers now suspect that mishandling of metals in the brain is in part responsible for neurological disorders has prompted a closer look into metal levels within the various brain regions of our animal model. In particular, Chapter 4 focussed on the possible metalloregulatory role melatonin played in the three brain regions: cerebellum, cortex and corpus striatum, as such an *in vivo* extension of the earlier *in vitro* studies. The implications of this are vast, especially since the depletion of melatonin with age has been associated with neurodegenerative diseases such as AD.

In Chapter 5, histological and electrochemical stripping techniques were applied to investigate the implications of high Al^{3+} levels in the brain regions, particularly the hippocampus. The region has been synonymously linked to various neurodegenerative diseases including AD. The debilitating nature of this disease alone would warrant further study into any substance that would show the slightest possibility of a reprieve from the symptoms. Melatonin has from this study shown signs of promise in indirect symptom alleviation, by decreasing neuronal swelling and cell degeneration linked to Al^{3+} toxicity, and by significantly decreasing Al^{3+} levels in rats that had been dosed with melatonin prior to Al^{3+} treatments in comparison with the control groups.

The preliminary study in Chapter 6, outlines a method for the production of a calcium selective microelectrode which was applied to measuring intracellular calcium levels in brain slices. Further work is still needed to optimise the microelectrode production as well as the applications of this electrode in sensing real-time intracellular Ca^{2+}-induced exitotoxicity and neuronal damage by various neurodegenerative substrates.

"Life" may be characterized as a controlled stationary flow equilibrium, maintained by energy consuming chemical reactions. In this work, the delicate link between metal homeostasis and neural substrates has been brought to the fore through the application of various inorganic analytical techniques and metal-ligand chemistry. In a publication by Brennan (1999) [272] the endless frontier of neuroscience is analogous to a giant jigsaw puzzle requiring a multidisciplinary approach and the tools afforded to chemists set them at the centre stage in terms of structural and mechanistic elucidation. The overall conclusions of this study may indeed only be in effect one piece of a very large puzzle, but that piece will no doubt serve as a building block for further ideas and work in this field.

REFERENCES:

1. Erlich S.S and Apuzzo M.L.J (1985) J. Neurosurg. 63:321.
2. Reiter R.J. (1981) in *The Pineal Gland: Anatomy and Physiology*. Vol. 1, edited by Reiter R.J. CRC Press, Florida.
3. Ariens-Kappers J. (1981) in *The Pineal Gland: Anatomy and Physiology*. Vol. 1, edited by Reiter R.J. CRC Press, Florida.
4. Boyd C.S. (1999) PhD Thesis, Rhodes University, Grahamstown.
5. Kappers J.A. (1965) Progress Brain Research 10:87.
6. Wurtman R.J. and Axelrod J (1965) Sci. Am. 213:50.
7. Cardinali D.P and Vacas M.I. (1978) J. Neural. Transm. 42:193.
8. Reiter R.J. (1989) in *De Groot's Endocrinology* Vol. 1 edited by De Groot L.J. Saunders Publishers, Philadelphia. Pg. 240.
9. Zhang E.T., Mikkelsen J.D. and Møller M. (1991) Cell Tissue Research 265:63.
10. Arendt J. (1989) Br. J. Psych. 155:585.
11. Daya S. (1994) Specialist Medicine Sep.:58.
12. Arendt J., Middleton B., Stone B. and Skene D. (1999) Sleep 22:625.
13. Skene D.J. (1996) Chemistry and Industry Sept. 637.
14. Reiter R.J. and Robinson J. (1995) in *Melatonin: Your body's natural wonder drug.* Bantam Books, New York.
15. Reiter R.J. (1995) Front. Neuroendocrinol. 16:383.
16. Reiter R.J. (1996) Annals New York Academy of Sciences 786:362.
17. Reiter R.J. (1991) Endocrine Reviews 12:151.
18. Saarela S. and Reiter R.J. (1993) Life Sciences 54:295.
19. Bender D.A. (1982) Molecular Aspects of Medicine 6:101.
20. Reiter R.J. (1987) Life Sciences 40:2119.
21. Freur G. (1990) Drug Metabolism and Drug Interactions 8:203.
22. Klein D.C. and Notides A. (1969) Analytical Biochemistry 31:480.
23. Van Wyk E.J. (1993) MSc Thesis, Rhodes University, Grahamstown. South Africa.

24. Cardinali D.P., Lynch H.J. and Wurtman R.J. (1972) Endocrinology 91:1213.

25. Pang S.F. and Allen A.E. (1986) Pineal Research Review. 4:55.

26. Bubenick G.A., Brown G.M. and Grota L.J. (1976) J. Histochem. Cytochem. 24:1173.

27. Reiter R.J. (1988) ISI Atlas of Science: Animal and Plant Sciences. 1:111.

28. Gibbs F.P. and Vriend J. (1981) Endocrinology 109:1796.

29. Kennaway D.J., Matthews C.D. and Seamark R.F. (1981) in *Pineal Function.* editors: Matthews C.D. and Seamark R.F. Elsevier, Amsterdam. Pg.123.

30. Kopin I.J., Pare C.M.B., Axelrod J. and Weissbach, H. (1961) The Journal of Biological Chemistry 236:3072.

31. Valtonen M., Laitinen J.T. and Eriksson L. (1993) J. of Endocrinology 138: 445.

32. Wurtman R.J., Axelrod J. and Potter L.T. (1964) Journal of Pharmacology and Experimental Therapeutics 143:314.

33. Klein D.C., Auerbach D.A. and Namboodiri M.A.A. (1981) in *The Pineal Gland* edited by: Reiter R.J. CRC Press, Boca Raton. Pg. 199.

34. Cagnacci A. (1996) J. Pineal Research. 21:200.

35. Green J.P. (1989) in *Basic Neurochemistry*, edited by Siegel G, Agranoff B, Albers R.W. and Molinoff P. 4th edition Raven Press New York. Pg. 253.

36. Nutt D. (1993) in *Seminars in Basic Neurosciences* edited by Morgan G and Butler S, Gaskell Publishers, London, Pg. 71.

37. Bradford H.F. (1986) in *Chemical Neurobiology: An introduction to neurochemistry.* W.H. Freeman and Company. New York.

38. Louw D.A. and Edwards D.J.A. (1993) in *Psychology An Introduction for Students in South Africa*, Lexicon Publishers, Johannesburg.

39. Taylor P. and Brown J.H. (1989) in *Basic Neurochemistry*, edited by Siegel G , Agranoff B., Albers R.W. and Molinoff P. 4th edition, Raven Press New York Pg. 203.

40. Canepa F.G., Pauling P. and Sorum H. (1966) Nature 210:907.

41. Lopez M.G.D., Gauthier S., Ruiz J.S., Van Den B., Antonine M.S. and Gasca A.T. (1993) in *Essential Brain - Current Topics in Science and Medicine.* Merk. Spain.

42. Kaita A.A. and Goldberg A.M (1969) J. Neurochem. 16:1185.

43. Bear M.F., Connors B.W. and Paradiso M.A. (2001) in *Neuroscience: Exploring the Brain.* 2nd edition. Lippincott Williams and Wilkins Publishers. Philadelphia.

44. Mahabeer R. (1996) Masters Degree, Rhodes University, Grahamstown.

45. Calne D.B., Hochberg F.H., Snow B.J. and Nygaard T. (1992) Annals New York Academy Science 648:1.

46. Cooper J.R., Bloom F.E. and Roth R.H. edited. (1996) in *The Biochemical Basis of Neuropharmacology*. 7th edition Oxford Press, New York.

47. Sourander P. and Sjögren H. (1970) in *Alzheimer's Disease and Related Conditions* edited by Wolstenholme G and O` Connor M, Longman Group Ltd, London.

48. Goodman Y., Bruce A.J., Cheng B. and Mattson M.P. (1996) Journal of Neurochemistry 66:1836.

49. Behl C., Davis J.B., Lesley R. and Schubert D. (1994) Cell 77:817.

50. Goodman Y. and Mattson M.P. (1996) Journal of Neurochemistry 66:869.

51. Mattson M.P., Cheng B., Davis D., Bryant K., Lieberberg I. and Rydel R.E. (1992) Journal of Neuroscience 12:376.

52. Zec R.F. (1993) in *Neuropsychology of Alzheimer's Disease and Other Dementias* edited by Parks R.W., Zec R. and Wilson R.S. Oxford University Press, New York.

53. Issa A.M. and Keyserlingk E.D. (2000) Prog. Neuro-Psychopharmacol. and Biol. Psychiat. 24:1229.

54. Quirion R., Auld D., Befert U. Poirier J and Kar S. (1998) in *Handbook of The Aging Brain* edited by Wang E and Snyder D.S. Academic Press, San Diego.

55. Nash M. (2000) Time Magazine 156:53.

56. Pappolla M.A., Sos M., Bick R.J., Omar R.A., Hickson-Bick D.L.M., Reiter R.J., Efthimiopoulos S., Sambamurti K. and Robakis N.K. (1997) in *Alzheimer's Disease: Biology, Diagnosis and Therapeutics* edited by Iqbal K., Winblad B., Nishimura T., Takeda M. and Wisniewski H.M. John Wiley and Sons, New York. Pg. 741.

57. Pappolla M.A., Sos M., Omar, R.A., Bick R.J., Hickson-Bick, D.L.M., Reiter R.J., Efthimiopoulos S. and Robakis N.K. (1997) The Journal of Neuroscience 17:1683.

58. van Someren E.J.W., Mirmiran M. and Swaab D.F. (1993) Behavioral Brain Research 57:235.

59. Bevier W.C., Bliwise D.L., Bliwise N.G., Bunnell D.E. and Horvath S.M. (1992) Journal of Clinical and Experimental Gerontology 14:1.

60. Daniels W., van Rensburg S., van Zyl J. and Taljaard J. (1998) J. Pineal Research 24:78.

61. Poeggeler B., Reiter R.J., Tan D-X., Chen L-D. and Manchester L.C. (1993) J. Pineal Research 14:151.

62. Meldrum B. and Garthwaite J. (1990) Trends in Pharmacological Sciences. 11:379.

63. Benveniste H., Drejer J., Schousboe A. and Diemer N.H. (1984) Journal of Neurochemistry 43:1369.

64. Luthert P. (1993) in *Seminars in Basic Neurosciences* edited by Morgan G and Butler S, Gaskell Publishers, London, Pg. 186.

65. Sapolsky R.M. and Pulsinelli W.A. (1985) Science 229:1397.

66. Walz W., Klimaszewski A. and Paterson I.A. (1993) Developmental Neuroscience 15:216.

67. Crain B.J., Westerkam W.D., Harrison A.H. and Nadler J.V. (1988) Neuroscience 27:387.

68. Cho S., Joh T.H., Baik H.H., Dibinis C. and Volpe B.T. (1997) Brain Research 755:335.

69. Manev H., Uz T., Kharlamov A. and Joo J.-Y. (1996) FASEB Journal 10:1546.

70. DiFiglia M. (1990) Trends in Neurosciences 13:286.

71. Ludolph A.C. (1995) in *Neurotoxicology: Approaches and Methods* edited by Chang L.W. and Slikker W. (Jr.), Academic Press, Inc, London. Pg. 671.

72. Bird E.D. (1980) Annual Review of Pharmacology and Toxicology 20:533.

73. Figueredo-Cardenas G., Anderson K.D., Chen Q., Veenman C.L. and Reiner A. (1994) Experimental Neurology 129:37.

74. Isacson O., Dunnett S.B. and Bjorklund A. (1986) Proceedings of the National Academy of Sciences, USA 83:2728.

75. Stahl W.L. and Swanson P.D. (1974) Neurol. 24:813.

76. Jackson M., Gentleman S., Lennox G., Ward L., Gray T., Randall K., Morrell K and Lowe J. (1995) Neuropathol. Appl. Neurobiol. 21:18.

77. Lange K.W., Kornhuber J. and Riederer P. (1997) Neuroscience and Biobehavioural Reviews 21:393.

78. Cohen G. and Spina M.B. (1989) Annals of Neurology 26:689.

79. Sandyk R. (1990) Int. J. Neurosci. 50:37.

80. Leong A.S.Y., and Mathews C.D. (1979) Med. Hypotheses. 5:265.

81. Reiter R.J., Melchiorri D., Sewerynek E., Poeggler B., Barlow-Walden L., Chuang J., Oritz G.G. and Acuña-Castroviejo D. (1995) J.Pineal Research 18:1.

82. Partonen T. (1994) Annals of Medicine 26:239.

83. Waldhauser F., Erhart B. and Förster E. (1993) Experentia 49:671.

84. Kaim W. and Schwederski B. (1994) in *Bioionorganic Chemistry: InorganicElements in the Chemistry of Life An Introduction and Guide*. Wiley Publishers, New York, Pg. 7 and 330-348.

85. Mathews C.K. and van Holde K.E. (1990) in *Biochemistry*. Benjamin/Cummings Publishing Company, California.

86. Harrison P.M. and Hoare R.J. (1980) in *Metals in Biochemistry*. Chapman and Hall, New York.

87. Bush A. (2000) Current Opinion in Chemical Biology 4:184.

88. O Carpenter D. (1994) Cellular and Molecular Neurobiology 14:591.

89. Kendirck M.J., May M.T, Plishka M.J and Robinson K.D. (1992) in *Metals in Biological Systems*, Ellis Horwood Ltd, West Sussex Pg. 18.

90. Cowan J. (1997) in *Inorganic Biochemistry: An Introduction* Wiley-VCH Inc. New York Pg. 5-7 and 338-342.

91. Stollery B. T., Banks H.A. Broadbent D. E. and Lee W.R. (1989) Br. J. Indust. Med. 46:698.

92. Fergusson J. E. (1990) in *The Heavy Elements: Chemistry, Environmental Impact and Health Effects* Pergamon Press, New York.

93. Luthert P. (1993) in *Seminars in Basic Neuroscience*, edited by Morgan G. and Butler S., Gaskell Publishing London Pg. 208.

94. Goldstein G.W. and Betz A.L. (1986) Sci Am. 255:70.

95. Wilson J.L.T. (1996) in *Blackwells Dictionary of Neuropsychology*. edited by Beaumont J.G., Kenealy P.M. and Rogers M.J.C., Blackwell Publishers, Massachusetts, USA.

96. Yang X.F., Wang S.Y., Zhao R.C., Ao S.Q., Xu L.C. and Wang X.R. (2000) Biomed. Environ. Sci. 13:19.

97. Stohs S.J., Bagchi D., Hasson E. and Bagchi M. (2000) J. Environ. Pathol. Toxicol. Oncol. 19:201.

98. Sigel H. and Sigel A. (1993) in *Metal ions in Biological Systems* edited by Sigel H. and Sigel A., Vol. 29 Marcel Dekker New York.

99. Thayer J.S. (1993) in *Metal ions in Biological Systems* edited by Sigel H. and Sigel A., Vol. 29 Marcel Dekker New York.

100. Krishnamurthy S. (1992) J. Chem. Educ. 69:347.

101. McAlphine D. and Shukuro A. (1958) Lancet 2:629.

102. Bakir F., Damluji S.F., Amin-Zaki L., Mortadha M., Khalidi A., Al-Rawi N.Y., Tikriti S., Dhahri H.I., Clarkson T. W., Smith J.C., and Doherty R.A. (1973) Science 181:230.

103. Bakir F., Rustin H, Tikriti S., Al-Damluji S.F and Shihristani H (1980) Post Grad. Med. J. 56:1.

104. Mellon E.K. and Stock A. (1977) J. Chem. Educ. 54:211.

105. Olivieri G., Brack C., Müller-Spahn , Stähelin H.B., Hermann M., Renard P., Brockhaus M. and Hock C. (2000) Journal of Neurochemistry 74:231.

106. Perl D.P. and Good P.F. (1991) in *Aging and Alzheimer's Disease* edited by Growdon J.H., Corkin S., and Ritter-Walker E. and Wurtman R., Vol. 640, New York Academy of Science, New York, Pg.8.

107. Reed D.M. and Brody J.A. (1975) Am. J. Epi. 101:287.

108. Garruto R.M. (1991) Neuro. Toxicology 12:347.

109. De Boni U. and Crapper DR. (1978) Nature 271:566.

110. Szutowicz A., Tomaszewicz M., Jankowska A., Madziar B and Bielarczyk H. (2000) Metabolic Brain Disease 15:29.

111. Marques H.M. (1991) J. Inorganic Biochemistry 41:187.

112. Florence T.M. (1991) in *Trace Elements, Micronutrients and Free Radicals* edited by Dreosti I.E. Humana Press, New Jersey, Pg. 171.

113. Rowley D.A. and Halliwell B. (1983) Arch. Biochim. Biophys. 225:279.

114. Yoshida Y., Tsuchiya J. and Niki E. (1994) Biochim. Biophys. Acta 1200:85.

115. Dexter D.T., Carayon A. and Javoy-Agid F. (1991) Brain 114:1953.

116. Halliwell B. and Gutteridge J.M.C. (1984) Biochem. J. 219:1

117. Halliwell B. and Gutteridge J.M.C. (1985) Mol. Aspects Med. 8:89.

118. Hartard C., Weisner B., Dieu C., Kunze K. (1993) J. Neurol. 241:101.

119. White A.R., Bush A.J., Beyreuther K., Masters C.L. and Cappai R (1999) J. Neurochem. 72:2092.

120. Multhaup G., Schlicksupp A., Hesse L., Beher D., Ruppert T., Masters C.L. and Beyreuther K. (1996) Science 271:1406.

121. Horning M.S., Blakemore L.J.and Trombely P.Q. (2000) Brain Research. 852:56.

122. White A.R., Multhaup G., Maher F., Bellingham S., Camakains J., Zheng H., Bush A.I., Beyreuther K., Masters C.L. and Cappi R. (1999) J. of Neuroscience. 19:9170.

123. White A.R., Reyes R., Mercer J.F.B., Camakains J., Zheng H., Bush A.I., Multhaup G., Beyreuther K., Masters C.L. and Cappi R. (1999) Brain research. 842:439.

124. Sloviter R.S. (1985) Brain Research 330:150.

125. Frederickson C.J., Hernandez M.D. and McGinty J.F. (1989) Brain Research 480:317.

126. Tonder N., Johansen F.F. and Fredrickson C.J. (1990) Neurosci. Lett. 109:247.

127. Koh J.Y., Suh S.W. and Choi D.W. (1996) Science 272:1013.

128. Suh S.W., Chen J.W., Motamedi M., Bell B., Listiak K., Pons N.F., Danscher G. and Fredrick C.J. (2000) Brain Research 852:268.

129. Weis J.H., Sensi S.L. and Koh J.Y. (2000) Trends in Pharmacological Sciences. 21:395.

130. Ebadi M. (1991) in *Methods in Enzymology*, edited by Riordan J.F and Vallee B.L, Academic Press, New York, vol. 205.

131. Limson J.L. (1998) PhD Thesis, Rhodes University, Grahamstown.

132. Manev H., Kharlamov E. and Cagnoli C.M. (1997) Exp. Neurol. 146:171.

133. Satter R. J., Charlton M.P., Hafner M. and Tymianski M. (1998) Neurochem 71:2349.

134. Sculptoreanu A., Abramovici H., Abdullah A.A., Bibikova A., Panet-Raymond V., Frankel D., Schipper H.M., Pinsky L., Trifiro M.A. (2000) Mol Cell Biochem. 203:23.

135. Paschen W. (2000) Brain Res. Bull., 53:409.

136. Coppen A., Shaw D.M. and Farrell J.P. (1963) Lancet 1:79.

137. Coppen A., Shaw D.M., Mallenson A. and Constain R. (1966) Br. Med. J. 1:71

138. Skene D. (1979) Masters Thesis, Rhodes University. Grahamstown.

139. Resnick L.M., Barbagallo M., Dominguez L.J., Veniero J.M., Nicholson J.P., Gupta R.K. (2001) Hypertension 38:709.

140. Lerche H., Jurkat-Rott K., Lehmann-Horn F. (2001) Am. J. Med. Genet. 106:146.

141. Shaw D.M., Frigel D., Camps F.E. and White E. (1969) Br. J. Psychiat. 115:69.

142. Ullucci P.A. (2000) in *Encyclopedia of Analytical Chemistry: Applications, Theory and Instrumentation* edited by Meyers R.A., John Wiley and Sons, West Sussex, UK.

143. Baastrup P.C. and Schou M. (1967) Arch. Gen. Psychiat. 16:162.

144. Forrest J.N. (1975) New Engl. J. of Med. 292:317.

145. Knapp S. and Mandell A.J. (1973) Science 180:645.

146. Dawes P.M. and Vizi E.S. (1973) Br. J. Pharmacol. 48:225.

147. Vizi E.S (1975) in *Lithium Research and Therapy* edited by Johnson F.N. Academic Press, London 391.

148. Gottesfeld Z., Samuel D. and Icekson I. (1973) Experentia 29:68.

149. *Encyclopaedia of Chemical Technology*, 3rd edition, vol.11, editors: Grayson M. and Eckroth D., John Wiley and Sons.Publishers, Toronto, (1980) Pg. 972.

150. Pudderphatt R.J. (1978) in *The Chemistry of Gold*, monograph 16, 1st edition, edited by Clark R.J. H., Elsevier Scientific Publishing Company, Amsterdam.

151. Prakash K.M.M.S., Probahakar L.D. and Venkata Reddy D. (1986) Analyst 111:1301.

152. Cannell R. (1992) in *Techniques used in Bioproduct Analysis* edited by Tooting A.M.J. Butterworth-Heinemann Ltd. Oxford. 171.

153. Salisbury C.D.C., Chan W., Saschenbrecker P.W. (1991) J. Assoc. Off. Anal. Chem. 74:587.

154. Zasadowski K., Markiewicz M. and Buszko M. (1993) Polish J. of Env. Studies. 2:39.

155. Salisbury C.D.C. and Chan W. (1985) J. Assoc. Off. Anal. Chem. 68:218.

156. Versieck J. (1988) in *Methods in Enzymology* Vol 158. Part (A) edited by Riordan J.F. and Vallee B.L. Academic Press, New York.

157. Groenewald T. (1969) Analytical Chemistry. 41:1012.

158. Barefoot R.R. and van Loon J.C. (1996) Anal. Chim. Acta 334:5.

159. de Llano J.J.M. and Andreu E.J., Knecht E. (1996) Analytical Biochemistry 243:210.

160. Wang J. (1994) in *Analytical Electrochemistry* 1st edition VCH Publishers Inc., U.K.

161. Locatelli C. (1997) Electroanalysis 13:1014.

162. Brett C.M.A. and Brett A.M.O. (1993) in *Electrochemistry: Principles, Methods and Applications*, Oxford University Press Inc. U.S.A.

163. Kissenger P.T, Preddy C.R. Sharp R.E. and Heineman W.R., (1996) in *Laboratory Techniques in Electroanalytical Chemistry*, 2nd edition, edited by Kissenger P.T and Heineman W.R., Marcel Dekker Inc., New York.

164. Kissenger P.T. (1996) in *Laboratory techniques in Electroanalytical Chemistry*, 2nd edition, edited by Kissenger P.T and Heineman W.R., Marcel Dekker Inc., New York.

165. Killard A.J., Sequeria M., Diamond D. and Smyth M.R. (2000) in *Encyclopedia of Analytical Chemistry: Applications, Theory and Instrumentation* edited by Meyers R.A., John Wiley and Sons, West Sussex, UK.

166. Bard A.J. and Faulkner L.R. (1980) in *Electrochemical Methods: Fundamentals and Applications*. John Wiley and Sons, New York.

167. Brainina Kh. Z., (1995) Anal. Chim. Acta. 305:140.

168. Hawridge F.M. (1996) in *Laboratory Techniques in Electroanalytical Chemistry* 2nd edition, edited by Kissenger P.T. and Heineman W.R., Marcel Dekker Inc. New York.

169. Dryhurst G. and McAllister D.L. (1996) in *Laboratory Techniques in Electroanalytical Chemistry* 2nd edition, edited by Kissenger P.T. and Heineman W.R., Marcel Dekker Inc. New York.

170. Vallee B.L. (1991) in *Methods in Enzymology* Vol 205. edited by Riordan J.F. and Vallee B.L. Academic Press, New York.

171. Wang J. (1996) in *Laboratory techniques in Electroanalytical Chemistry*, 2nd edition, edited by Kissenger P.T and Heineman W.R., Marcel Dekker Inc., New York.

172. Limson J. and Nyokong T. (1997) Anal. Chim. Acta. 344:87.

173. Petrovic S.C. and Dewald H.D. (1997) Anal. Chim. Acta. 357:33.

174. Kissenger P.T. and Ridgway T.H. (1996) in *Laboratory Techniques in Electroanalytical Chemistry*, 2nd edition, edited by Kissenger P.T and Heineman W.R., Marcel Dekker Inc., New York.

175. Ramaley L. and Krause M.S. (Jr.) (1969) Anal. Chem. 41:1362.

176. Turner J.A., Christie J.H., Vokovic M. and Osteryoung R.A. (1997) Anal. Chem. 49:1899.

177. O`Dea J.J., Osteryoung J. and Osteryoung R.A. (1981) Anal. Chem. 53:695.

178. Comba P. and Hambley T.W. (1995) in *Molecular Modeling of Inorganic Compounds*, 1st edition, VCH Publishers, New York.

179. Gordon D.B. (1996) in *Practical Biochemistry: Principles and Techniques*, 4th edition, edited by Wilson K. and Walker J. Cambridge University Press, U.K.

180. Vogel A.I. (1994) in *Vogel's Textbook of Practical Organic Chemistry*, 5th edition edited by Furniss B.S., Hannaford A.J, Smith P.W.G and Tactchell A.R. Longman Group, U.K.

181. Leslie M.R. (1980) PhD Thesis, Rhodes University, Grahamstown, South Africa.

182. Alpert N.L., Keisser W.E. and Szymandi K.A., IR: (1970) in *Theory and Practice of Infrared spectroscopy*, 2nd edition, Plenum Press, NewYork.

183. Reiter R.J. (1993) Experientia 49:654.

184. Pufulete M. (1997) Chemistry in Britain Nov.:31.

185. Daya S. (1999) Spec. Med. 21:528.

186. Reiter R.J., Guerrero J.M., Garcia J.J. and Acuna-Castrovieg D. (1998) Ann. N. Y. Acad. Sci. 854:410.

187. Rich A., Farrugia G. and Rae J.L. (1999) Am. J. Physiol. 276:923.

188. Petit L., Guardiola B., Delagrange P., Jockers R. and Strosberg A.D. (1998) Therapie 53:421.

189. Pavlidis M., Greenwood L., Paalavuo M., Molsa H. and Laitinen J.T. (1999) Gen. Comp. Endocrinol. 113:240.

190. Geary G.G., Duckles S.P. and Krause D.N. (1998) Br. J. Pharmacol. 123:1533.

191. Peschke E., Peschke D., Hammer T. and Csernus V. (1997) J. Pineal Research 23:156.

192. Southgate G.S. (1998) PhD Thesis, Rhodes University, Grahamstown, South Africa.

193. Zhang Q.Z. and Zhang J.T. (1999) Chung Kuo Li Hsueh Pao. 20:206.

194. Hirafuji M., Kawahara F., Ebihara T., Nezu A., Tanimura A. and Minamani M. (1999) Eur. J Pharmacol. 380:163.

195. Herness M.S. and Chen Y. (2000). J. Membr. Biol. 173:127.

196. Lauber J.K. and Vriend J. (1989) Gen. Comp. Endocrinol. 76: 414.

197. Pablos M.I., Santaolaya M.J., Agapito M.T. and Recio J.M. (1994) Neurosci. Lett. 174:55.

198. Limson J., Nyokong T. and Daya S. (1998) J. Pineal Research 24:15.

199. Wang J. (1989) in *Electroanalytical Chemistry* edit Bard A.J., Wiley, New York, 16:1.

200. Zoulis N.E., Nikolelis D.P. and Efstathiou C.E. (1990) Analyst 115:291.

201. Wang J. Lu J. and Yarnitzky C. (1993) Anal. Chim. Acta 280:61.

202. Zhang Z. Q., Chen S.-Z., Lin H.-M. and Zhang H. (1993) Anal. Chim. Acta, 272:227.

203. Radi A. and Bekhiet G.E. (1998) Bioelectrochemistry and Bioenegetics 45:275.

204. Beal M.F., Mazurek M.F., Ellison D.W., Kowall N.W., Solomon P.R., Pendlebury W.W. (1989) Neuroscience 29:339.

205. Richter J.A., Perry E.K., and Tomlinson B.E. (1980) Life Science 26:1683.

206. Ehmann W.D., Markesbury W.R., Alauddin M., Hossian T.I.M., and Brubaker E.H. (1986) Neurotoxicology 7:197.

207. Thompson C.M., Markesbery W.R., Ehmann,W.D., Mao Y.X., and Vance D.E. (1988) J. Neurotoxicology 9:1.

208. Hock C., Drasch G., Golombowski S., Muller-Spahn F., Willershausen-Zonnchen B., Schwartz P., Hock U., Growdon J.H., and Nitsch R.M. (1998) J. Neural Trasnm. 105:59.

209. Wenstrup D., Ehmann W.D., Markesbury W.R. (1990) Brain Res. 533:125.

210. Cullen M.R., Robins J.M., and Eskenazi B. (1983) Medicine 62:221.

211. Goldstein G.W., Ashbury A.K., and Diamond I. (1974) Arch. Neurol. 31:382.

212. Silbergeld E.K. (1992) FASEB J. 6:3201.

213. Yoshida S. (2001) Brain Res. 892:102.

214. Weis J.H., Sensi S.L. and Koh J.Y. (2000) TiPS. 21:395.

215. Heron P., Cousins K., Boyd C. and Daya S. (2001) Life Science 68:1575.

216. Grunewald T. and Beal M.F. (1999) Ann. NY Acad. Sci. 893:203.

217. Berman S.B. and Hastings T.G. (1999) J. Neurochem. 73:1127.

218. Lack B., Duncan J. and Nyokong T. (1999) Anal. Chim. Acta 385:393.

219. Galwey A.K. and Brown M.E. (1999) in *The Thermal Decomposition of Ionic Solids*. Elsevier Publishers, Amsterdam.

220. Nakamoto K. and McCarthy P.J. (1968) in *Spectroscopy and the Structure of Metal Chelate Compounds*. John Wiley and Sons, New York.

221. Pouchert C.J. (1975) in *The Aldrich Library of Infrared Spectra* 2nd edit., Aldrich Company Press Inc.

222. Bellamy L.J. and Branch R.F. (1954) J. Chem. Soc. 4487.

223. Chung D.D.L. (2000) in *Encyclopedia of Analytical Chemistry: Applications, Theory and Instrumentation* edited by Meyers R.A., John Wiley and Sons, West Sussex, UK.

224. Matlaba P., Daya S. and Nyokong T. (2000) Pharm. Pharmacol. Commun. 6:201.

225. Watson C.M., Dwyer D.J., Andle J.C., Bruce A.E. and Bruce M.R. (1999) Anal. Chem. 71:3181.

226. Bonfil Y., Brand M. and Kirowa-Eisner E. (2000) Anal. Chim. Acta. 424:65.

227. Yao H. and Ramelow G.J. (1998) Talanta 45:1139.

228. Ghoneim M.M., Hassanein A.M., Hammam E. and Beltagi A.M. (2000) Fresenius J. Anal. Chem. 367:378.

229. Reiter R.J., Tan D., Kim S.J., Manchester L.C., Garcia J.J., Cabera J.C., El-Sokkary G., and Rouivier-Garay V. (1999) Mech. Ageing Dev. 110:157.

230. Skaper S.D., Floreani M., Ceccon M., Facci L., Giusti P. (1999) Ann. N. Y. Acad. Sci. 890:107.

231. Willis G.L. and Armstrong S.M. (1999) Physiol Behav. 66:785.

232. Miguez J.M., Martin F.J. and Aldegunde M. (1997) Neurochem. Res. 22:87.

233. Beskonakli E., Palaoglu S., Renda N., Kulacoglu S., Turhan T. and Taskin Y. (2000) J. Clin. Neurosci. 7:320.

234. Reiter R.J., Chen L-D., Poeggler B.H., Barlow-Walden L., Seweryneck E. and Melchiorri D. (1996) in *Handbook of Antioxidants* edited by Cadenas E and Packer L. Marcel Dekker, New York.

235. Earl C.J. (1961) in *Wilson's Disease-Some Current Concepts* edited by Walshe J.M. and Cummings J.N., Blackwell Scientific, Oxford.

236. Thompson R.H.S. (1961) in *Regional Neurochemistry* edited by Kety S.S. and Elkes J. Pergamon Press, New York.

237. Wong P.Y. and Fritze K. (1969) J. Neurochem. 16:1231.

238. Uitti R.J., Rajput A.H., Rozdilsky B., Bickis M., Wollin T. and Yuen W.K. (1989) Can. J Neurol. Sci. 16:310.

239. Finkelstein Y., Markowitz M.E. and Rosen J.F. (1998) Brain Res. Rev. 27:168.

240. Center for Disease Control (1991) *Preventing Lead Poisoning in Young Children.* U.S. DHHS, Public Health Services, Centre for Disease Control, Atlanta Georgia.

241. Agency for Toxic Substances and Disease Registery (1988) *The Nature and Extent of Lead Poisoning in Children in the USA*: A report to congress. Agency for Toxic Substances, Atlanta Georgia.

242. Kumar R., Agarwal A.K., and Seth P.K. (1996) Toxicol. Lett. 89:65.

243. Gupta A., Gupta A., Murthy R.C., Thakur S.R., Dubey M.P., Chandra S.V. (1990) Biochem. Int. 21:97.

244. Constant M.G. and van den Berg J. (1991) Anal. Chim. Acta. 250:265.

245. Hoffman R.A. and Reiter R.J. (1974) Anat. Rec. 153:19.

246. Skoog D.A., Holler F.J. and West D.M (eds.) (1992) in *Fundamentals of Analytical Chemistry*. 6th edition. Saunders College Publishers, San Diego.

247. Jaenicke S., Sabarathinam R.M., Fleet B. and Gunasingham H. (1998) Talanta 45:703.

248. Daniele S., Bragato C., Baldo M.A., Wang J. and Lu J. (2000) Analyst 125:731.

249. Zar J.H. (1974) in *Biostatistical Analysis* 1st edition. Prentice Hall, New Jersey.

250. Hasan F., Cookman G.R. Keane G.J. Bannigan J.G. King W.B. Regan C.M. (1989) Neurotoxicol. Teratol. 11:433.

251. Vašàk M. and Hasler D. (2000) Current Opinion in Chemical Biology 4:177.

252. Awad A., Govitrapong P., Hama Y., Hegazy M. and Ebadi M. (1989) J. Neural Transm. 76:129.

253. Rodella L., Rezzani R., Lanzi R and Bianchi R. (2001) Brain Res. 889:229.

254. Colomina M.T., Sanchez D.J., Sanchez-Turet M. and Domingo J.L. (1999) Neuropsychobiology 40:142.

255. Golub M.S., Han B., Keen C.L. (1996) Biol. Trace Elem. Res. 55:241.

256. Platt B., Fiddler G., Riedel G., Henderson Z. (2001) Brain Res. Bull 55:257.

257. Lal B., Gupta A., Murthy R.C., Ali M.M. and Chandra S.V. (1993) Indian J Exp. Biol. 31:30.

258. Landsberg J.P., McDonald B., and Watt F. (1992) Nature 360:65.

259. Hodgeson A.N. and Bernard R.T.F. (1992) in *An Introduction to Histological Techniques*, Rhodes University, Grahamstown. South Africa.

260. Freeman W.H. (1967) in *An Atlas of Histology* 2nd edition Heinemann Educational Books Ltd, Oxford.

261. Bauer J.D., Ackerman P.G. and Toro G. (1974) in *Clinical Laboratory Methods.* The C.V. Mosby Company, St Louis.

262. Brenner S.R. and Yoon K.W. (1994) Neurosci. Lett. 178:260.

263. Campbell A.K. (1985) in *Intracellular Calcium its Universal Role as Regulator.* John Wiley and Sons, New York Pg. 427.

264. Christoffersen G.R.J. and Johansen E.S. (1976) Anal. Chim. Acta. 81:191.

265. Brown H.M., Pemberton J.P. and Owen J.D. (1976) Anal. Chim. Acta. 85:261.

266. Oehme M., Kessler M. and Simon W. (1976) Chimia. 30:204.

267. Tsien R.Y. and Rink T.J. (1981) J. Neurosci. Method. 4:73.

268. Amman D. (1986) in *Ion Selective Microelectrodes: Principles, Design and Application.* Springer-Verlag, Berlin.

269. Lanter F., Steiner R.A., Amman D and Simon W. (1982) Anal. Chim. Acta. 135:51.

270. Durst R.A. (1978) in *Ion-selective Electrodes in Analytical Chemistry.* Vol. 1. Edited by H. Freiser. Plenum Press, New York.

271. Tsien R.Y. (1981) Nature 290:527.

272. Brennan M.B. (1999) Chemical and Engineering News. Dec.:91.

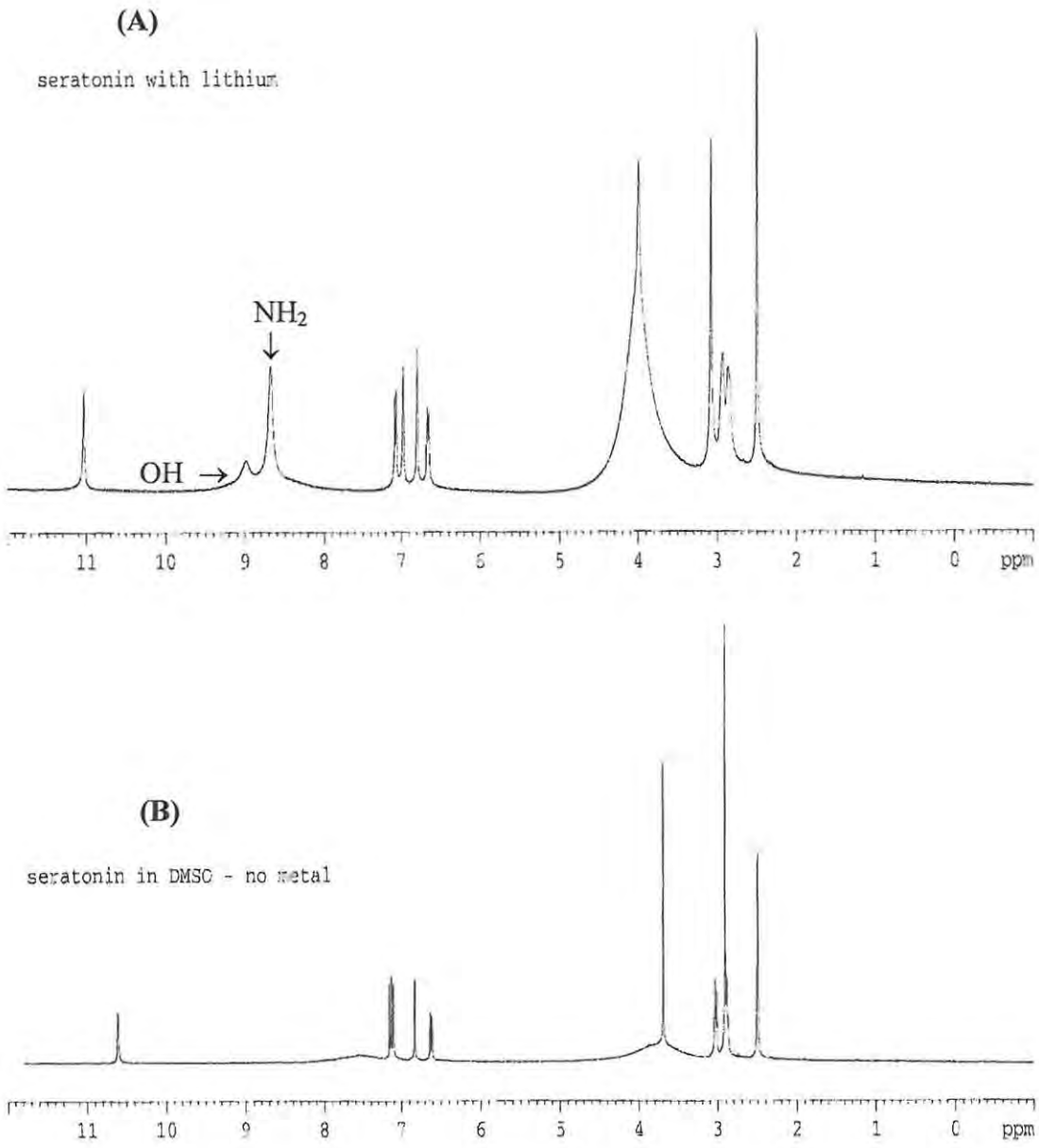

Appendix 1: NMR data for serotonin in the presence (A) and absence (B) of Li^+.

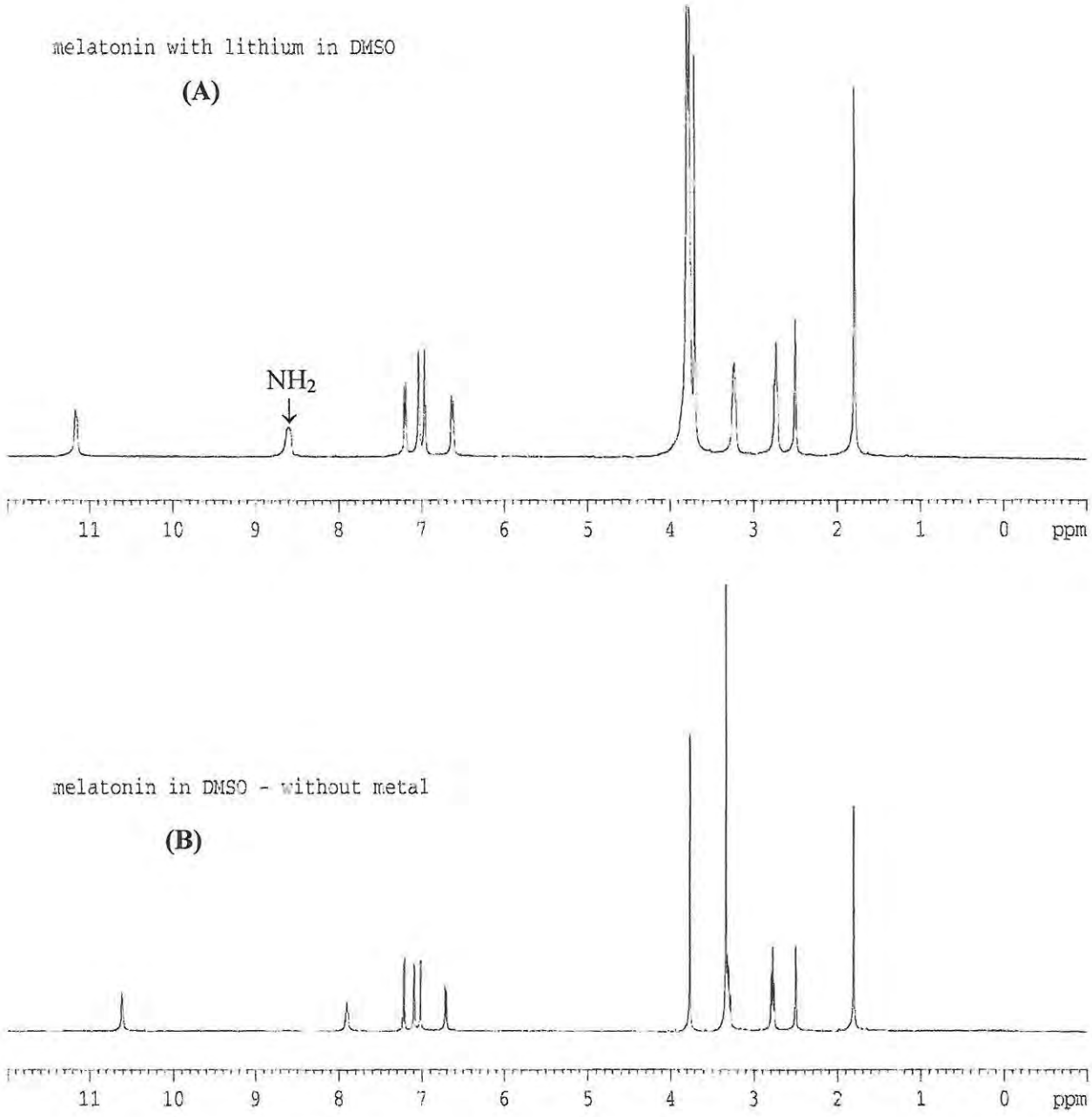

Appendix 2: NMR data for melatonin in the presence (A) and absence (B) of Li^+.